

**2D QSAR, DESIGN, *IN SILICO* STUDIES, SYNTHESIS AND
ANTIBACTERIAL EVALUATION OF MANNICH BASES OF 1, 3, 4-
THIADIAZOLE-BENZIMIDAZOLE DERIVATIVES**

Dissertation submitted to

THE TAMIL NADU Dr M.G.R MEDICAL UNIVERSITY

CHENNAI – 600032

In partial fulfilment of the requirements for the award of the Degree of

MASTER OF PHARMACY

IN

BRANCH-II PHARMACEUTICAL CHEMISTRY

Submitted by,

**PADMA.K
261915007**

Under the Guidance of

Dr. N. RAMALAKSHMI, M.Pharm., Ph.D.,

Professor and Head, Department Of Pharmaceutical Chemistry



**DEPARTMENT OF PHARMACEUTICAL CHEMISTRY C.L. BAID METHA
COLLEGE OF PHARMACY THORAIPAKKAM,
CHENNAI-600097.
OCTOBER2021**



Srinivasan.R
Chairman

K.K. Selvan
Executive Trustee

Dr. Grace Rathnam
Principal

Dr. Grace Rathnam, M.Pharm; Ph.D;

C.L.Baid Metha College of Pharmacy,

Thoraipakkam, Chennai-97.

CERTIFICATE

This is to certify that the project entitled “**2D QSAR, DESIGN, *IN SILICO* STUDIES, SYNTHESIS AND ANTIBACTERIAL EVALUATION OF MANNICH BASES OF 1, 3, 4 - THIADIAZOLE-BENZIMIDAZOLE DERIVATIVES**” was submitted by **PADMA.K (261915007)** in partial fulfilment for the award of the degree of **Master of Pharmacy** under the supervision of Dr. N. Ramalakshmi M.pharm; Ph.D., Head and Professor, Department of Pharmaceutical Chemistry, during the academic year 2020–2021.

Date:

Place: Chennai

Dr. Grace Rathnam,
M.Pharm; Ph.D;

Principal,

C.L.Baid Metha College of Pharmacy,
Thoraipakkam, Chennai-97.



Srinivasan.R
Chairman

K.K. Selvan
Executive Trustee

Dr. Grace Rathnam
Principal

Dr.N.Ramalakshmi, M.Pharm; Ph.D;

Professor & Head,

Department Of Pharmaceutical Chemistry,

CERTIFICATE

This is to certify that the project entitled “**2D QSAR, DESIGN, *IN SILICO* STUDIES, SYNTHESIS AND ANTIBACTERIAL EVALUATION OF MANNICH BASES OF 1, 3, 4-THIADIAZOLE-BENZIMIDAZOLE DERIVATIVES**” was submitted by **PADMA.K (261915007)** in partial fulfillment for the award of the degree of **Master of Pharmacy** during the academic year 2020–2021 under my guidance.

Date:

Place: Chennai

Dr.N.Ramalakshmi, M.Pharm; Ph.D;

Professor & Head,
Department Of Pharmaceutical Chemistry,

C.L. Baid Metha College of Pharmacy,

Chennai-97.

DECLARATION

The thesis entitled, “**2D QSAR, DESIGN, *IN SILICO* STUDIES, SYNTHESIS AND ANTIBACTERIAL EVALUATION OF MANNICH BASES OF 1, 3, 4-THIADIAZOLE-BENZIMIDAZOLE DERIVATIVES**” was carried out by me in C.L.Baid Metha College of Pharmacy, PADMA. K hereby declare that this dissertation work has been originally carried out by me during the academic year 2020-2021. The work embodied in this thesis is original and is not submitted in part or full for any other degree of this or any other university.

Date:
Place: Chennai

PADMA. K
(261915007)

Department of Pharmaceutical
Chemistry

ACKNOWLEDGEMENT

First and foremost, I would like to thank God Almighty for giving me the strength, knowledge, ability and opportunity to undertake this research study and to persevere and complete it satisfactorily. Without his blessings, this achievement would not have been possible.

I express my sincere gratitude to my guide, **Dr. N. RAMALAKSHMI M.Pharm., Ph.D.**, HOD, Department of Pharmaceutical Chemistry, C.L. Baid Metha College of Pharmacy, Chennai who gave inspiration and guidance at every stage of my dissertation work, her valuable suggestion and discussion have enabled me to execute the present work successfully.

I sincerely thank **Dr. GRACE RATHNAM, M. Pharm, Ph.D., Principal**, C.L. Baid Metha College of Pharmacy, Chennai, for providing the necessary facilities for my project work.

I sincerely thank our Chief Librarian, **Mrs. RAJALAKSHMI**, for providing necessary reference material for my project work.

I owe special thanks to **Mr. Srinivasan and Mrs. Shanthi**, Stores in-charge, C.L. Baid Metha College of Pharmacy, Chennai, for their timely supply of all necessary chemicals and reagents required for the completion of my project work.

I am thankful to **Mrs. MUTHULAKSHMI**, Lab attender, Department of Pharmaceutical Chemistry, C.L. Baid Metha College of Pharmacy, Chennai, for providing clean and sophisticated environment during the work period.

I am thankful to **Mr. GANESH BAHADUR**, Chief Security, C.L. Baid Metha College of Pharmacy, Chennai, for providing an uninterrupted service at the college campus during the work period.

The acknowledgement would be incomplete if I did not mention my **Family, Friends** and **Well Wishers** for their moral support and encouragement in completing this project work successful.

Place: Chennai

PADMA. K
(261915007)

Date:

Department of Pharmaceutical Chemistry

CONTENTS

S.No.	PARTICULARS	PAGE NO.
1	INTRODUCTION	1
	1.1 2-Amino 1,3,4- Thiadiazole	4
	1.2 Benzimidazole	5
	1.3 Mannich Base	6
	1.4 <i>Escherichia coli</i> (<i>E.coli</i>)	7
	1.5 Heptosyltransferase-I (WaaC)	9
	1.6 Docking	12
2	REVIEW OF LITERATURE	14
3	AIM AND OBJECTIVE	19
4	PLAN OF THE STUDY	21
5	MATERIALS AND METHODS	23
	5.1 2D QSAR model	23
	5.2 Design Of Compounds	25
	5.3 <i>In Silico</i> Screening of Designed Compounds	28
	5.4 Docking	33
	5.5 Synthesis	36
	5.6 Characterization	38
	5.7 Biological Evaluation	40

S.No.	PARTICULARS	PAGE NO.
	RESULTS AND DISCUSSION	42
6	6.1 2D QSAR model	43
	6.2 Design of Compounds	56
	6.3 <i>In Silico</i> Screening of Designed Compounds	64
	6.4 Docking	85
	6.5 Synthesis	91
	6.6 Characterisation	92
	6.7 Biological Evaluation	104
7	CONCLUSION	109
8	BIBLIOGRAPHY	110

LIST OF FIGURES

FIGURE NO.	TITLE	PAGE NO.
1	Structure of LPS	9
2	Hep I Inhibition mechanism	11
3	Crystallographic structure of Hep I with ligand	34
4	Steps in Docking	35
5	Synthetic scheme	37
6	Scatter Plot of Dataset compound	51
7	LMO scatter plot	51
8	Y-Scramble graph	51
9	Williams Plot	51
10	Superimposed image of Co-crystallized ligand and its re-docking pose	87
11	2D and 3D interactions of Streptomycin and ADP	87
12	3D interaction of 3e, 3g and 3j	88
13	3D interaction of 3n and 3y	89
14	2D interaction of best 5 compounds	90
15	Antibacterial effects of samples (3e, 3g, 3j, 3n, and 3y) against <i>E.coli</i>	106

LIST OF TABLES

TABLE NO.	TITLE	PAGE NO.
1	Structure of original dataset compounds with experimental and predicted MIC against <i>e.coli</i>	45
2	Descriptor correlation matrix of the best model	44
3	Predicted MIC values of original dataset using model 2	53
4	Internal and external validation parameters of model 1 and 2	54
5	Structure of designed molecules with its predicted activity	56
6	Molinspiration results	66
7	Bioactivity Score	68
8	SwissADME results	70
9	Drug filters results from swissADME	72
10	PreADME/Tox results	75
11	ProToxII results	82
12	Binding affinities of designed compounds with interacting residues	86
13	Antibacterial activity results	105

ABBREVIATIONS

IC50 – 50% inhibition concentration

MIC – Minimum inhibitory concentration

NMR – Nuclear Magnetic Resonance

MS – Mass Spectrometry

m.p. – Melting point

IR – Infrared

E.coli – *Escherichia coli*

QSAR – Quantitative structure-activity relationship

LMO – Leave More Out

LOO – Leave One Out

PDB – Protein Data Bank

Hep I – Heptosyltransferase-I

BZD - Benzimidazole

INTRODUCTION

**2D QSAR, DESIGN, *IN SILICO* STUDIES, SYNTHESIS
AND ANTIBACTERIAL EVALUATION OF MANNICH
BASES OF 1, 3, 4-THIADIAZOLE-BENZIMIDAZOLE
DERIVATIVES**

1. INTRODUCTION

Medicinal chemistry is a discipline that encloses the design, development, and synthesis of pharmaceutical drugs. Medicinal/Pharmaceutical chemistry deals with the discovery, design, development and both pharmacological and analytical characterization of drug substances. The use of plants, minerals, and animal parts as medicines has been recorded since the most ancient civilizations. With the evolution of the knowledge the means for drug discovery also evolved. New molecules with potential pharmaceutical interest, 'hits', are natural products, or compounds generated by computational chemistry, or compounds from a screening of chemical libraries, from combinatorial chemistry, and from pharmaceutical biotechnology. The "hit" compound is improved for its pharmacologic, pharmacodynamic and pharmacokinetic properties by chemical or functional group modifications, transforming it into a lead compound. A lead compound should have a known structure and a known mechanism of action. The lead compound is further optimized to be a drug candidate that is safe to use in human clinical trials.

Thus, Medicinal chemistry is the field of pharmaceutical sciences which applies the principles of chemistry and biology to certain of knowledge leading to the introduction of new therapeutic agents.

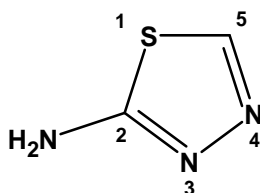
Medicinal chemistry covers three critical steps



Heterocyclic compounds are carbocyclic compounds with at least one atom other than carbon atom (N, S, and O) forming a part of the ring system.

1.1 2-AMINO 1, 3, 4- THIADIAZOLE

1, 3, 4 Thiadiazole is a heterocyclic ring with nitrogen at 3 and 4 position and sulphur at 1 position. 1, 3, 4 thiadiazole is an important scaffold known to be associated with several biological activities including antimicrobial [1, 2], antituberculosis, antiviral [3], analgesic, antidepressant [4] and anxiolytic inhibitors. 2-amino-1, 3, 4-thiadiazole moiety may be an excellent scaffold for future pharmacologically active 1, 3, 4-thiadiazole derivatives.



Molecular Formula: C₂H₃N₃S

Formula Weight: 101.13032

Composition: C (23.75%) H (2.99%) N (41.55%) S (31.71%)

Molar Refractivity: 25.05 ± 0.3 cm³

Molar Volume: 67.6 ± 3.0 cm³

Parachor: 204.5 ± 4.0 cm³

Index of Refraction: 1.662 ± 0.02

Surface Tension: 83.6 ± 3.0 dyne/cm

Density: 1.495 ± 0.06 g/cm³

Dielectric Constant: Not available

Polarizability: 9.93 ± 0.5 10⁻²⁴cm³

RDBE: 3

Monoisotopic Mass: 101.004767 Da

Nominal Mass: 101 Da

Average Mass: 101.1303 Da

M+: 101.004219 Da

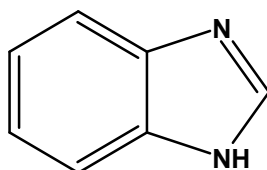
M-: 101.005316 Da

[M+H]⁺: 102.012044 Da

[M+H]⁻: 102.013141 Da

1.2. BENZIMIDAZOLE

Nitrogen-containing heterocycles have been widely used and investigated by the researchers resulting in the design and discovery of newer chemical entities. Benzimidazole is one such often used nitrogen containing heterocycle. Its unique structural features and electron-rich nature enable it to bind to several biologically important targets, resulting in a wide range of activities [5–7]. It has a bicyclic structure composed of a benzene ring fused with an imidazole ring. Benzimidazole core containing compounds have been reported in several biological studies including antimicrobial, [8] anticancer, [9] anti-oxidant, [10] antiprotozoal, [11] antiviral, [12] antihypertensive, [13] antidiabetic, [14] antiallergic, [15] activities etc.



Molecular Formula: $C_7H_6N_2$

Formula Weight: 118.13594

Composition: C (71.17%) H (5.12%) N (23.71%)

Molar Refractivity: $36.61 \pm 0.3 \text{ cm}^3$

Molar Volume: $95.0 \pm 3.0 \text{ cm}^3$

Parachor: $264.8 \pm 4.0 \text{ cm}^3$

Index of Refraction: 1.696 ± 0.02

Surface Tension: $60.1 \pm 3.0 \text{ dyne/cm}$

Density: $1.242 \pm 0.06 \text{ g/cm}^3$

Dielectric Constant: Not available

Polarizability: $14.51 \pm 0.5 \cdot 10^{-24} \text{ cm}^3$

RDBE: 6

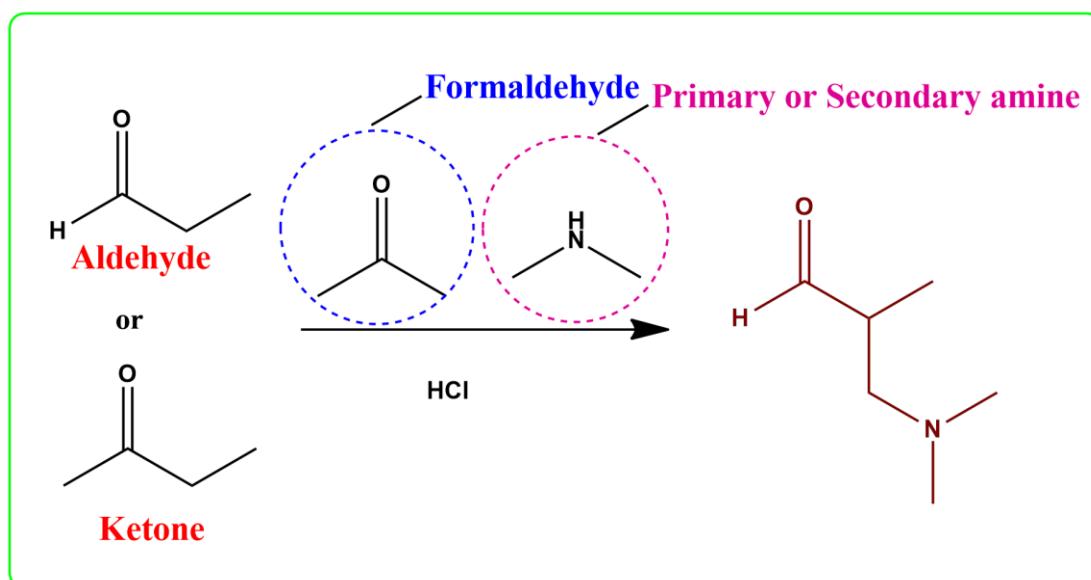
Monoisotopic Mass: 118.053098 Da

Nominal Mass: 118 Da

Average Mass: 118.1359 Da

1.3. MANNICH BASES:

Mannich bases, beta-amino ketones carrying compounds, are the end products of Mannich reaction [16, 17]. Mannich reaction is a carbon-carbon bond forming nucleophilic addition reaction and is a key step in synthesis of a wide variety of natural products, pharmaceuticals, and so forth. Mannich reaction is a nucleophilic addition reaction which involves the condensation of a compound with active hydrogen(s) with an amine (primary or secondary) and formaldehyde (any aldehyde) [18]. Mannich bases act as important pharmacophores or bioactive leads which are further used for synthesis of various potential agents of high medicinal value which possess amino alkyl chain [19]. Mannich bases are known to possess potent activities like antibacterial, anti-inflammatory, anticancer, antifilarial, antifungal, anticonvulsant, anthelmintic, antitubercular, analgesic, anti-HIV, antimalarial, antipsychotic, antiviral activities.



1.4. *Escherichia coli* (*E.coli*)

In humans, *E. coli* is the dominant anaerobe that exists in the colon. It belongs to the family *Enterobacteriaceae* and genus *Escherichia* [20, 21]. Most of the bacteria falls in this category are gram-negative bacilli (motile). Typical mucosal pathogens can be said to follow one or more of four strategies for infection: (i) colonization, (ii) evasion of host defenses, (iii) reproduction, and (iv) Host destruction. The dissemination of pathogenic *E. coli* infections can involve only mucosal surfaces or can reach throughout the body. From inherently pathogenic *E. coli* strains, there are three general clinical syndromes: urinary tract infection (UTI), sepsis/meningitis, and enteric/diarrhea. There are three groups of *E.coli* strains in humans: commensal, extraintestinal, and gastrointestinal [22]. *E. coli* strains vary in their mechanism by which they cause diarrhea, but many are known to act as intestinal pathogens [23].

During the past few years, we have seen an increase in antimicrobial resistance on a global scale. Compared to previous assumptions, the epidemic is spreading faster. Multidrug-resistant bacteria like superbugs are endemic in many places around the world. Approximately 80 percent of UTIs are caused by *Escherichia coli* [24, 25]. The use of beta-lactam antibiotics alone or in combination with fluoroquinolones seems to increase *E. coli* resistance in UTI, especially to these groups of antibiotics [26, 27]. Depending on the bacteria, antibiotic resistance can be acquired, intrinsic, or adaptive. A bacterium's intrinsic properties determine its inherent resistance. As the name suggests, acquired resistance occurs when an organism acquires a resistance mechanism from an exogenous source (horizontal gene transfer) or by mutation of its DNA. A specific environmental signal (e.g., stress, growth state, pH, ions concentration, nutrient conditions, sub-inhibitory levels of antibiotics) can cause adaptive resistance to one or more antibiotics [28].

Mechanism of antibiotic resistance

The most common causes of antibiotic resistance are

- Destruction or modification of antibiotics,

- Target alteration (target substitution, target mutation, target site enzymatic effect, target site protection, target overproduction, target bypass), and
- Reduce antibiotic accumulation via decreased permeability or increased efflux.

Due to their high resistance rates, trimethoprim-sulfamethoxazole and ciprofloxacin cannot be used as empiric treatment for UTIs in many areas. The quinolones are synthetic antimicrobials have excellent activity against *Escherichia coli* and other Gram-negative bacteria in human and veterinary medicine alike. These drugs share the same mechanism of action: inhibition of DNA Gyrase and Topoisomerase IV enzymes. The use of fluoroquinolone antibiotics is becoming less effective against *Escherichia coli* that cause community-acquired urinary tract infections (COMA-UTI) because of its prevailing resistance [29].

1.5. HEPTOSYLTRANSFERASE-I (Hep-I OR WaaC)

Since antibiotic resistance is on the rise, treatment for Gram-negative bacterial infections has grown to be challenging [30]. It is particularly complicated to develop antibiotics for these organisms due to their outer membrane (OM) which serves as a permeability barrier and prevents compounds from entering the bacterial cell [31]. Gram-negative bacteria have an asymmetric outer membrane (OM) that protects it from their external environment and an inner membrane (IM) that surrounds their cytoplasm [32]. OM consists of Lipopolysaccharide (LPS), Phospholipids, OM proteins, and lipoproteins. LPS (complex amphipathic molecule) and protein components play a vital role in survival and virulence of these bacterium.

LPS is an essential endotoxin for gram-negative bacteria to survive. Approximately 75% of OM is filled with LPS and it's also felt to be effective barrier against detergents and hydrophobic antibiotics as it is found on primary zone of contact between bacteria and environment. Structure of LPS is given in **Figure 1**.

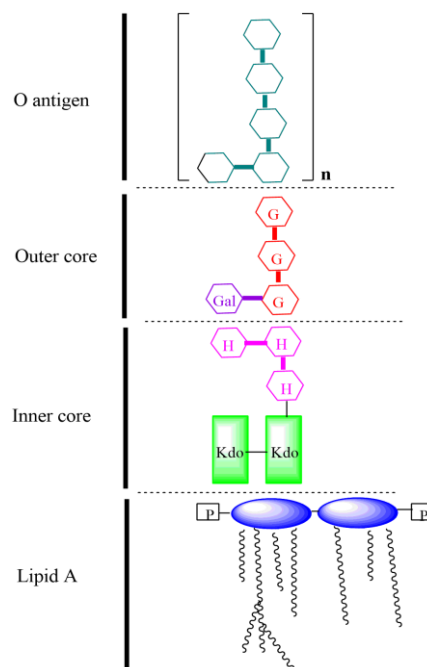


Figure 1. Structure of LPS

Lipid A consists of fatty acids with glucosamine disaccharides. Oligosaccharide core is made of 3-deoxy-D-manno-oct-2-ulosonic acid (Kdo) and hexose molecules in its outer core plus two units of heptose in the inner core. And O antigen is made repeated units of oligosaccharides [33].

The first core sugar attached to lipid A is kdo. This Kdo-lipid A or deep-rough LPS is the minimal structural requirement for the growth of gram-negative bacteria [34].

E.coli LPS possesses a conserved inner OS core-lipid-A structure composed of Hep₃-Kdo₂-lipid A with Hep I and Hep II residues phosphorylated at position 4'[35].

Hep enzymes belongs to Glycosyltransferase family, it helps in transfer of sugar from activated donor (UDP, GDP/ADP) to another molecule. Addition first heptose moiety to Kdo-lipid-A molecule is catalyzed by Hep I/WaaC enzyme. This addition leads to biosynthesis of LPS [36].

Presence of heptose and its phosphorylation is essential for viability of *E.coli*. All Waa genes are involved in synthesis of inner core region of LPS, among them WaaP, WaaY, and WaaQ are located in central operon of Waa locus on chromosome of *E.coli*.

Addition of first heptose to Kdo₂-lipid A molecule is catalyzed by Hep I or WaaC enzyme. When there is an absence of heptose, protein content in outer membrane gets reduced which ultimately increase sensitivity of bacteria to hydrophobic antibiotics. Therefore, inhibiting heptose transfer to Kdo₂-lipid A will indirectly influence bacterial sensitivity by hindering formation of main element LPS. So, this enzyme could be taken as best target against gram-negative bacteria. Hep I inhibition is shown in **Figure 2** [37].

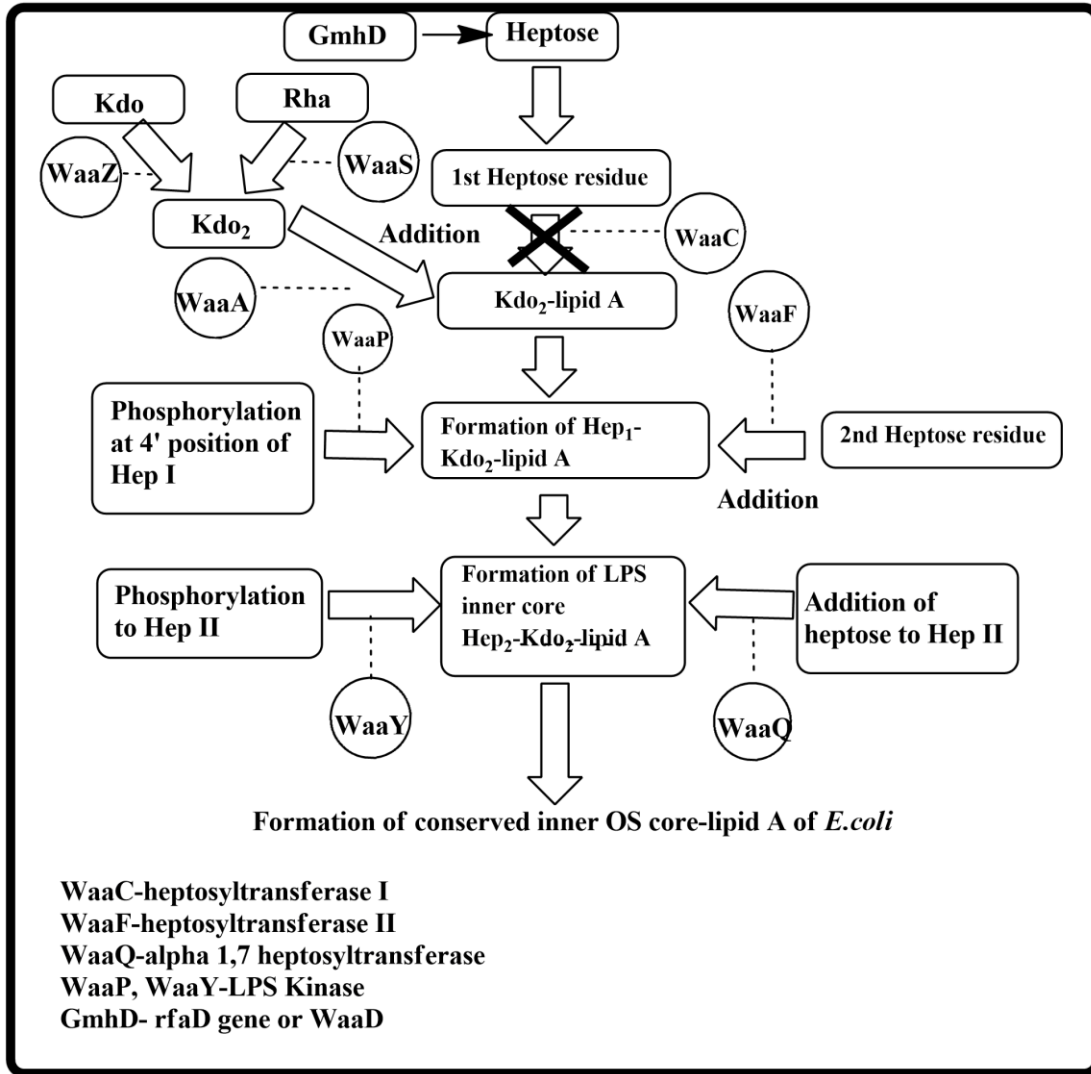


Figure 2.Hep I/ WaaC inhibition mechanism.

1.6. DOCKING

Docking is a procedural method to predict the preferred orientation of one molecule to another when bound forming a stable complex.

Docking is important in Drug designing which is used for calculating the binding alignment of small molecular drugs or inhibitors to their protein targets and can predict affinity and activity of complex formed.

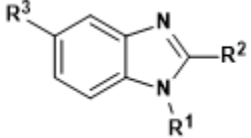
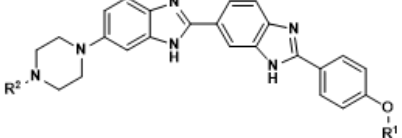
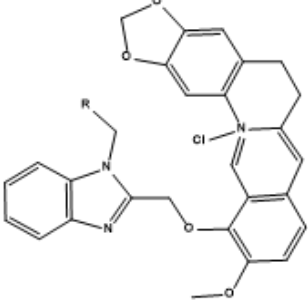
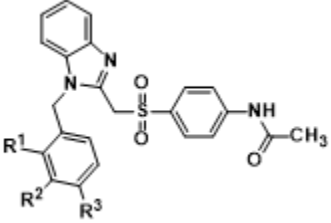
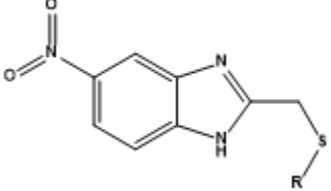
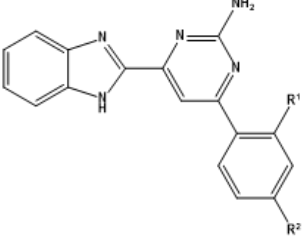
Molecular docking is an attractive scaffold to understand drug biomolecular interactions for the rational drug design and discovery, as well as in the mechanistic study by placing a molecule (ligand) into the preferred binding site of the target specific region of the DNA/protein (receptor) mainly in a non-covalent fashion to form a stable complex of potential efficacy and more specificity. The information obtained from the docking technique can be used to suggest the binding energy, free energy and stability of complexes. At present, docking technique is utilized to predict the tentative binding parameters of ligand-receptor complex beforehand.

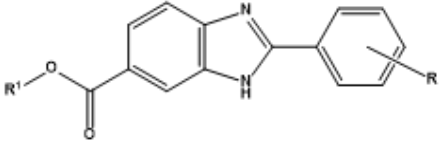
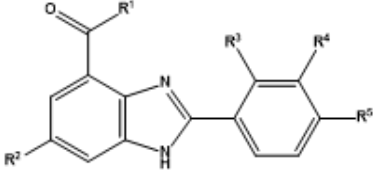
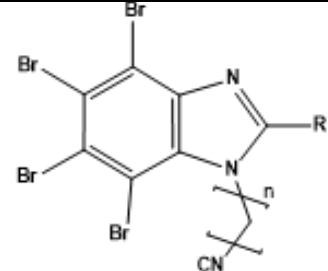
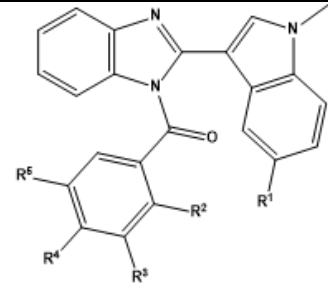
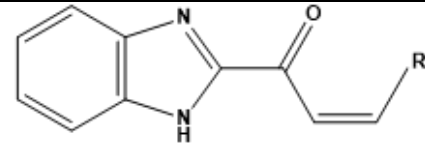
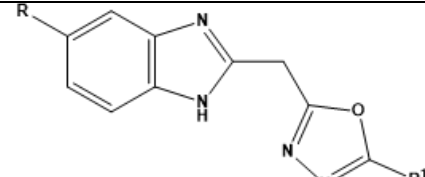
The main objective of molecular docking is to attain ligand-receptor complex with optimized conformation and with the intention of possessing less binding free energy.

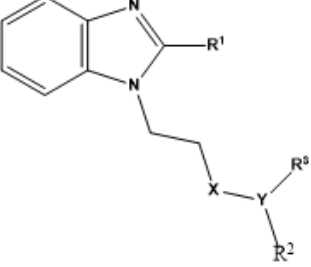
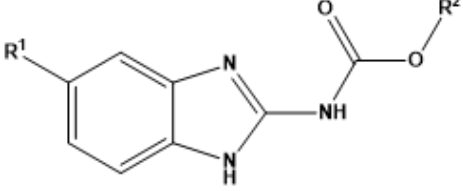
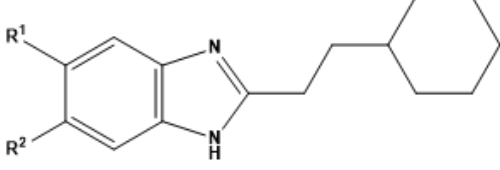
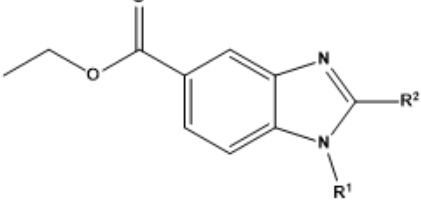
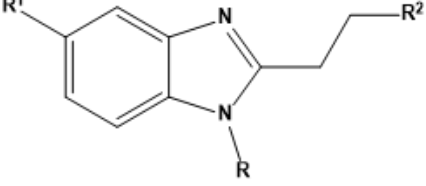
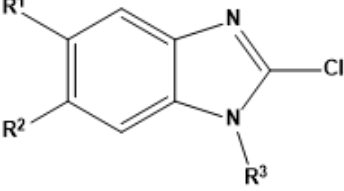
Molecular docking can demonstrate the feasibility of any biochemical reaction as it is carried out before experimental part of any investigation. There are some areas, where molecular docking has revolutionized the findings. In particular, interaction between small molecules (ligand) and protein target (may be an enzyme) may predict the activation or inhibition of enzyme. Such type of information may provide a raw material for the rational drug designing. Some of the major applications of molecular docking are Lead optimization, Hit identifications, Drug-DNA interaction.

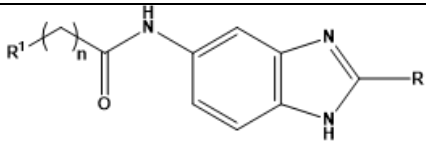
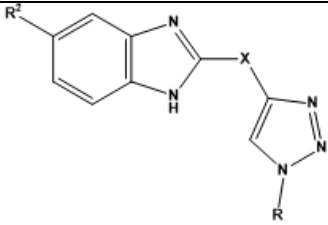
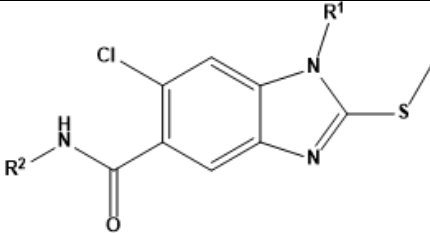
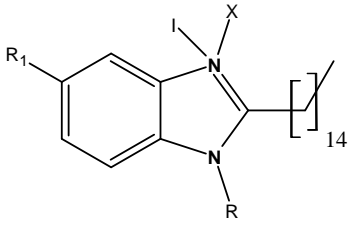
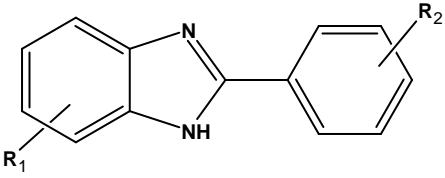
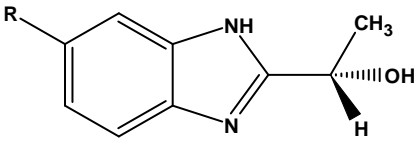
REVIEW OF LITERATURE

2. REVIEW OF LITERATURE

Structures	References	Reported activities
	Fatmah A. S. Alasmary <i>et al.</i> [38]	Antibacterial and Antifungal
	N.T. Chandrika <i>et al.</i> [39]	Antifungal activity
	Jeyakkumar P <i>et al.</i> [40]	Antimicrobial activity
	H.-Z. Zhang <i>et al.</i> [41]	Antimicrobial activity
	N.S. El-Gohary <i>et al.</i> [42]	Antimicrobial activity
	Han-Bo Liu <i>et al.</i> [43]	Antimicrobial activity

Structures	References	Reported activities
	C. Karthikeyan <i>et al.</i> [44]	Antiproliferative activity
	IskandarAbdullah <i>et al.</i> [45]	Anticancer activity
	EdytaŁukowska-Chojnacka <i>et al.</i> [46]	Anticancer and pro-apoptotic activity
	Y.-T. Wang <i>et al.</i> [47]	Anticancer and Antiproliferative activity
	L. Wu <i>et al.</i> [48]	Antitumor activity
	MdJawaid Akhtar <i>et al.</i> [49]	Antitumor activity

Structures	References	Reported activities
	T. Ma <i>et al.</i> [50]	Anticancer activity
	Jae Eun Cheong <i>et al.</i> [51]	Anticancer activity
	K. Gobiset <i>et al.</i> [52]	Antimycobacterial activity
	Y.K. Yoon <i>et al.</i> [53]	Antimycobacterial activity
	Y. Luo <i>et al.</i> [54]	Antiviral activity
	Ritika Srivastava <i>et al.</i> [55]	Antiviral activity

Structures	References	Reported activities
	Y. Li <i>et al.</i> [56]	Anticancer activity
	A. Bistrović <i>et al.</i> [57]	Antiproliferative activity
	Paulina Flores-Carrillo <i>et al.</i> [58]	Antiprotozoal activity
	M. Tonelli <i>et al.</i> [59]	Antiprotozoal activity
	Nerea Escala <i>et al.</i> [60]	Antiprotozoal activity
	H. Amanet <i>et al.</i> [61]	Anti-urease activity

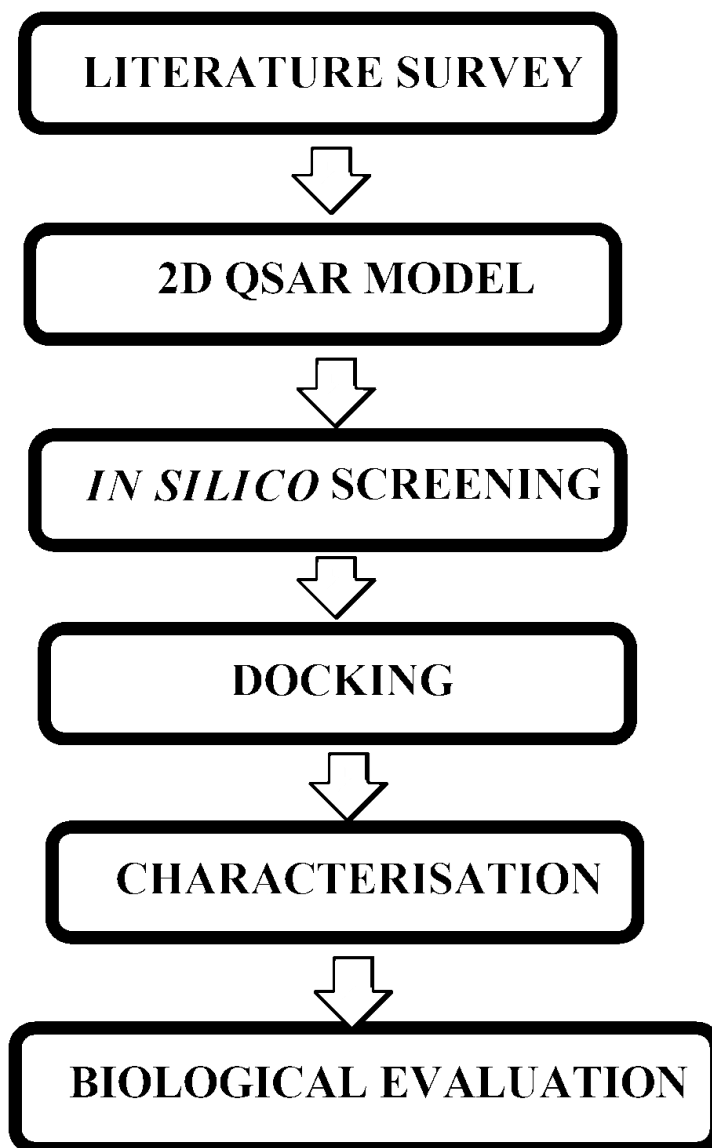
AIM AND OBJECTIVE

3. AIM AND OBJECTIVE

As more microbial strains are becoming resistant to antimicrobial agents, there is a pressing need to synthesize more effective antibiotics than currently available. To design using available *insilico*softwares-SwissADME, Molinspiration, Pre ADMET, ProTox II, and AutoDockVina, followed by characterization and biological evaluation of novel antibacterial derivative against antibiotic resistant E.coli strains.

PLAN OF THE STUDY

4. PLAN OF THE STUDY



MATERIALS AND METHODS

5. MATERIALS AND METHODS

5.1. 2D-QSAR MODEL:

In this study, a reported series of 35 substituted benzimidazole derivatives with antibacterial activity against *E.coli* was used to study 2D QSAR model [62-65]. The structures and biological activity of the above mentioned derivatives are shown in Table 1. The biological activities of the derivatives expressed in terms of MIC (μM , maximal inhibitory concentration) is converted to logarithmic pMIC and it is taken as dependent variable in 2D-QSAR model. The structure of the compounds was built with ACD/Chemsketch Freeware and saved in .mol file format. The molecular descriptors for the studied compound were calculated using Padel-descriptor 2.21 software.

QSAR studies were carried out using QSARINS software. The Genetic algorithm (GA) and multiple linear regression (MLR) methods were used in QSARINS [66] to construct QSAR models using experimental biological activities and molecular descriptors. In order to obtain significant model, the descriptors with constant, semi-constant (80%) values and pair-wise correlation more than 0.85, were excluded. And the remaining descriptors were used as input for model development. The data was spitted according to a random percentage method where, approximately 20% compounds were retained in test set (6) and remaining 80% (29) compounds were used for model development. Parameters such as: all subset until 1, genetic iteration: 10000 with maximum of 5 variables were chosen and other parameters were set as default. The applicability domain [67] of QSAR model was used to verify the prediction reliability, to identify the problematic compounds and to predict the compounds with acceptable activity that falls within this domain. The leverage approach allows the determination of the position of new chemical in the QSAR model, i.e., whether a new chemical will lie within the structural model domain or outside of it. Furthermore, the leverage approach along with the William plot is used to determine the applicability in all QSAR models. To construct the William plot, the leverage h_i for each chemical compound, in which QSAR model was used to predict its activity, was calculated according to the following equation:

$$H_i = x_i^T (X^T X)^{-1} x_i$$

Where x_i is the descriptor vector of the considered compound and X is the descriptor matrix derived from the training set descriptor values and the warning leverage (h^*) was determined as

$$h^* = 3(p+1)/n$$

Where n is the number of training compounds, p is the number of predictor variables. The defined applicability domain (AD) was then visualized via a Williams plot, the plot of the standardized residual versus the leverage values (h). A compound with $h_i > h^*$ seriously influences the regression performance and may be excluded from the applicability domain, but it doesn't appear to be an outlier because its standardized residual may be small. Moreover, a value of 3 for standardized residuals is commonly used as a cut-off value for accepting predictions, because points that lie within ± 3 standardized residual from the mean cover 99% of the normally distributed data.

QSAR validation:

Validation is done to evaluate the predictive ability of the obtained QSAR model. There are two types of validation methods such as internal and external validation. Internal validation is carried out using Leave one out (LOO) method. The best model was selected on the basis of various statistical parameters, such as a square of the correlation coefficient (r^2), and the quality of each model was estimated from the cross-validated squared correlation coefficient (rcv^2).

Leave one out cross-validation: [68]

Leave one out cross-validation (LOO CV) is one of the most effective methods for validation of a model with a small training dataset.

Leave-one-out cross validation technique was employed to determine the predictive power of the model. This was evaluated by using this mathematical expression;

$$Q^2_{cv} = 1 - \frac{\sum (Y_{pred} - Y_{exp})^2}{\sum (Y_{exp} - Y_{training})^2}$$

Where Y_{pred} , Y_{exp} and $Y_{training}$ represents the experimental, the predicted and mean values of experimental activity of training set compounds

External validation (r^2_{cv}):

For external validation, the activity of each molecule in the test set was predicted using the model developed by the training set. The regression coefficient (r^2_{cv}) value is calculated as follows.

$$r^2_{cv} = 1 - \frac{\sum (Y_{pred}(test) - Y(test))^2}{\sum (Y(test) - Y(training))^2}$$

Where r^2_{cv} refers cross validated regression coefficient, Y_{test} and Y_{pred} are observed and predicted activity of the molecule in the test set, respectively, and $Y(training)$ is the average activity of all molecules in the training set. Both, summations are over all molecules in the test set.

5.2. DESIGN OF COMPOUNDS:

35 compounds were designed using Chemsketch software and physicochemical properties were calculated for all compounds.

Molar refractivity

Molar refractivity, A , is a measure of the total polarizability of a mole of a substance and is dependent on the temperature, the index of refraction, and the pressure.

The molar refractivity is defined as

$$A = \frac{4\pi N_A \alpha}{3}$$

Where $N_A \approx 6.0221023$ is the Avogadro constant and α is the mean polarizability of the molecule.

Molar Volume

The molar volume, symbol V_m , is the volume occupied by one mole of a substance (chemical element or chemical compound) at a given temperature and pressure. It is equal to the molar mass (M) divided by the mass density (ρ). It has the SI unit cubic meters per mole (m^3/mol), although it is more practical to use the units cubic decimetres per mole (dm^3/mol) for gases and cubic centimeters per mole (cm^3/mol) for liquids and solids. The molar volume of a substance can be found by measuring its molar mass and density then applying the relation

$$V_m = M/\rho$$

Index of refraction

The refractive index or index of refraction of a material is a dimensionless number that describes how light propagates through that medium.

It is defined as $n = c/v$

Where, c is the speed of light in vacuum and v is the phase velocity of light in the medium.

Surface Tension

Surface tension is the elastic force of a fluid surface which makes it acquire the least surface area possible. Surface tension has the dimension of force per unit length, or of energy per unit area.

Polarizability

Polarizability is the ability to form instantaneous dipoles. It is a property of matter. Polarizabilities determine the dynamical response of a bound system to external fields and provide insight into a molecule's internal structure. In a solid, polarizability is defined as the dipole moment per unit volume of the crystal cell.

Parachor

It is an empirical constant for a liquid that relates the surface tension to the molecular volume and that may be used for a comparison of molecular volumes under conditions such that the liquids have the same surface tension and for determinations of partial structure of compounds by adding values obtained for constituent atoms and structural features called also molar parachor, molecular parachor.

Parachor is a quantity defined according to the formula:

$$P = \sqrt[4]{\gamma} M / d$$

Where: $\sqrt[4]{\gamma}$ is the fourth root of surface tension M is the molar mass, D is the density.

Density

The density, or more precisely, the volumetric mass density, of a substance is its mass per unit volume.

$$\rho = m/V$$

Dielectric constant

Substances have capacity to produce dipoles in another molecule. Dielectric constant is a measure of this capacity and it is a physical property. It is affected by both the attractive forces that exist between atoms and also molecules. It is denoted by ϵ .

5.3. *IN SILICO* SCREENING OF DESIGNED COMPOUNDS

In silico is an expression meaning "performed on computer or via computer simulation" in reference to biological experiments. When lead molecules have been identified, they have to be optimized in terms of potency, selectivity, pharmacokinetics (i.e.) absorption, distribution, metabolism and excretion (ADME) and toxicology before they can become candidates for drug development. *In silico* approaches to predict pharmacokinetic parameters (ADME) were pioneered by Lipinski *et al.* By studying the physicochemical properties of >2000 drugs from the WDI (World Drug Index, Derwent Information, London), which can be assumed to have entered Phase II human clinical trials (and therefore must possess drug-like properties), the so-called 'rule-of five' was derived to predict oral bioavailability (intestinal absorption) of a compound that can be considered as the major goal of drug development.

The ADME properties of the designed compounds were evaluated using Swiss ADME and PreADMET online softwares. Toxicity of all the designed compounds was evaluated by using ProTox II software.

SwissADME

Lipinski's rule of five

Lipinski's rule of five also known as the Pfizer's rule of five or simply the rule of five (RO5) is a rule of thumb to evaluate drug likeness or determine if a chemical compound with a certain pharmacological or biological activity has chemical properties and physical properties that would make it a likely orally active drug in humans.

The rule

Lipinski's rule states that, in general, an orally active drug has no more than one violation of the following criteria:

- No more than 5 hydrogen bond donors (the total number of nitrogen–hydrogen and oxygen–hydrogen bonds)
- No more than 10 hydrogen bond acceptors (all nitrogen or oxygen atoms)

- A molecular mass less than 500 daltons
- An octanol-water partition coefficient log P not greater than 5

Ghose Filter

This filter defines drug-likeness constraints as follows:

- Calculated log P is between -0.4 and 5.6
- Molecular weight is between 160 and 480
- Molar refractivity is between 40 and 130
- The total number of atoms is between 20 and 70.

Veber Filter

The molecules fitting to these two properties have a high probability of good oral bioavailability.

- Rotatable bond: max. 12
- Polar Surface Area: max. 140Å²

Egan Rule

Predicts good or bad oral bioavailability.

- $0 \geq \text{TPSA} \leq 132$
- $-1 \geq \log P \leq 6$.

Molar Refractivity

It is a measure of the total polarizability of a mole of a substance and is dependent on the temperature, the index of refraction, and the pressure.

The molar refractivity is defined as

$$A = \frac{4\pi}{3} N_A \alpha$$

Where $N_A = 6.022 \times 10^{23}$ is the Avogadro constant and α is the mean polarizability of a molecule

Polar surface area (PSA) or topological polar surface area (TPSA)

It is a measure of apparent polarity of a molecule is defined as the surface sum overall polar atoms, primarily oxygen and nitrogen, also including their attached hydrogen atoms. PSA is a commonly used for the optimization of a drug's ability to permeate cells. Molecules with a polar surface area of greater than 140 angstroms squared tend to be poor at permeating cell membranes.

For molecules to penetrate the blood–brain barrier (and thus act on receptors in the central nervous system), a PSA less than 90 angstroms squared is usually needed.

Topological PSA (TPSA, fast 2D calculation).

ADME Guideline

- $TPSA < 140 \text{ \AA}^2$ good intestinal absorption.
- $TPSA < 70 \text{ \AA}^2$ good brain penetration.

Lipophilicity

Lipophilicity is the ability of a molecule to mix with an oily phase rather than with water, is usually measured as partition coefficient, P , between the two phases and is often expressed as $\log P$. Lipophilicity has also been found to affect a number of pharmacokinetic parameters: higher lipophilicity ($\log P > 5$) gives, in general, lower solubility, higher permeability in the gastrointestinal tract, across the blood–brain barrier and other tissue membranes, higher affinity to metabolizing enzymes and efflux pumps, and higher protein binding. Low lipophilicity can also negatively impact permeability and potency and thus results in low BA and efficacy.

Partition coefficient, P

It is defined as a particular ratio of the concentrations of a solute between the two solvents (a biphasic of liquid phases), specifically for un-ionized solutes, and the logarithm of the ratio is thus $\log P$. When one of the solvents is water and the other

is a non-polar solvent, then the log P value is a measure of lipophilicity or hydrophobicity.

- $\log P_{\text{oct/wat}} = \log \frac{[\text{solute}]_{\text{unionized octanol}}}{[\text{solute}]_{\text{unionized water}}}$
- $\log P_{\text{oct/wat}} = \log \frac{C_{\text{O}}}{C_{\text{W}}}$

Lipophilicity not only impacts solubility but also influences permeability, potency, selectivity, absorption, distribution, metabolism, and excretion (ADME) properties and toxicity. A desired logP value (octanol-water partition coefficient) is no more than 5.

Water Solubility

Water solubility is a measure of the amount of chemical substance that can dissolve in water at a specific temperature. Solubility is common physicochemical parameter for drug discovery compounds. Determination of the aqueous solubility of the drug candidate is an important analysis as it reflects the bioavailability of the compound.

Log S

The aqueous solubility of a compound significantly affects its absorption and distribution characteristics. Typically, a low solubility goes along with a bad absorption and therefore the general aim is to avoid poorly soluble compounds.

- Log S value is a unit stripped logarithm (base10) of the solubility measured in mol/liter.
- Log S value should be greater than -4.

Rotatable Bonds

The bioavailability of a drug like molecule is related with its rotatable bond number. Less than seven rotatable bonds are essential for good bioavailability. Many highly potent molecules carried more than 10 rotatable bonds and still administered through oral route.

- Hydrogen bond acceptors and donors

- 12 or fewer H-bond donors and acceptors will have a high probability of good oral bioavailability.

PreADMET Drug-Likeliness

Drug likeness is a qualitative concept used in drug design for how "druglike" a substance is with respect to factors like bioavailability. It is estimated from the molecular structure before the substance is even synthesized and tested. The most well-known rule relating the chemical structures to their biological activities is Lipinski's rule and it is called the 'rule of five'. Another well-known rule is the Lead-like rule. PreADMET contains drug- likeness prediction module based on these rules.

ADME Prediction

Numerous in vitro methods have been used in the drug selection process for assessing the intestinal absorption of drug candidates. Among them, Caco2-cell model and MDCK (Madin-Darby canine kidney) cell model has been recommended as a reliable in vitro model for the prediction of oral drug absorption. In absorption, this module provides prediction models for in vitro Caco2-cell and MDCK cell assay. Additionally, *insilico* HIA

(human intestinal absorption) model and skin permeability model can predict and identify potential drug for oral delivery and transdermal delivery.

In distribution, BBB (blood brain barrier) penetration can give information of therapeutic drug in the central nervous system (CNS), plasma protein binding model in its disposition and efficacy. In order to build these QSAR models, genetic functional approximation is used to select relevant descriptors from all 2D descriptors that calculated by Topomol module, followed by Resilient back-propagation (Rprop) neural network to develop successful nonlinear model.

Toxicity prediction

Insilico toxicity prediction will have more and more importance in early drug discovery since 30% of drug candidates fail owing to these issues.

ProTox II

ProTox II, a virtual lab for the prediction of toxicities of small molecules. The prediction of compound toxicities is an important part of the drug design development process. Computational toxicity estimations are not only faster than the determination of toxic doses in animals, but can also help to reduce the amount of animal experiments.

ProTox II incorporates molecular similarity, fragment propensities, most frequent features and (fragment similarity based CLUSTER cross-validation) machine-learning, based a total of 33 models for the prediction of various toxicity endpoints such as acute toxicity, hepatotoxicity, cytotoxicity, carcinogenicity, mutagenicity, immunotoxicity, adverse outcomes (Tox21) pathways and toxicity targets.

Toxic doses and Toxicity classes

Toxic doses are often given as LD50 values in mg/kg body weight. The LD50 is the median lethal dose meaning the dose at which 50% of test subjects die upon exposure to a compound.

Toxicity classes are defined according to the globally harmonized system of classification of labelling of chemicals (GHS). LD50 values are given in [mg/kg]:

- ✓ Class I: fatal if swallowed ($LD50 \leq 5$)
- ✓ Class II: fatal if swallowed ($5 < LD50 \leq 50$)
- ✓ Class III: toxic if swallowed ($50 < LD50 \leq 300$)
- ✓ Class IV: harmful if swallowed ($300 < LD50 \leq 2000$)
- ✓ Class V: may be harmful if swallowed ($2000 < LD50 \leq 5000$)
- ✓ Class VI: non-toxic ($LD50 > 5000$)

5.4. DOCKING

Docking is a technique for predicting the preferred orientation and affinity of a ligand in a protein's binding site. Knowledge of the preferred orientation in turn may be used to predict the strength of association or binding affinity between two molecules using, for example, scoring functions.

In this study, AutodockVina in AutoDock Tools is used to perform docking studies. Docking studies were performed with the active site of *E.coli* Heptosyltransferase Hep I or WaaC (PDB ID: 2H1F) [69].

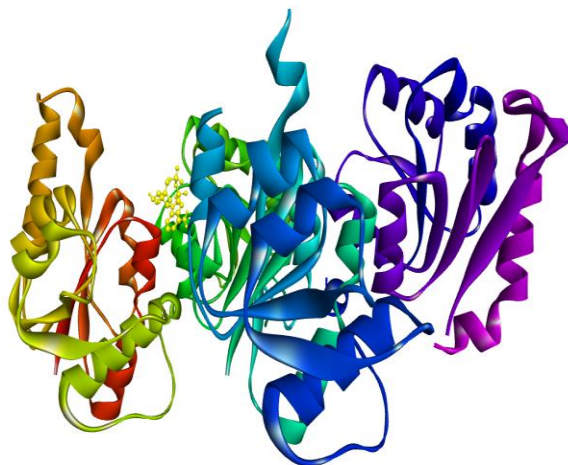


Figure 3. Crystallographic structure of Heptosyltransferase-I (2H1F) with ligand.

The following steps are pictographically explained in Figure 4.

Protein Preparation

Protein 2H1F was downloaded from RCSB and prepared for docking study by removing water molecules, ligands if available. Polar hydrogen's, Kollman charges were added and AD4 type atoms are assigned to the protein. Then protein was converted to .pdbqt format by choosing it as macromolecule.

Ligand Preparation

Similarly ligands were prepared by adding Gasteiger charges, the torsion tree was defined by choosing the root; the number of rotatable bonds was identified and saved in PDBQT format.

Grid parameter

These parameters were set to cover the entire 3-dimensional active site of the enzyme. Grid spacing was set to 1.00 Å. Center grid box values were set to x = 12.030, y =

40.723, and $z = 51.748$. The number of gridpoints along the x, y, and z dimensions was set as 108 X 68 X 66.

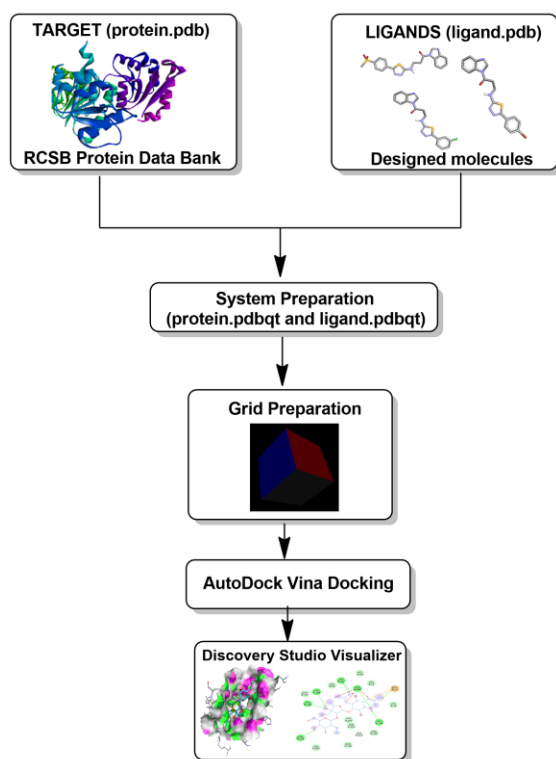


Figure 4.Steps in Docking

Running AutoDockVina

The AutoDockVina was executed by autodockvina and vina split executable file. All required format files are ready to run autodockvina. Results was obtained by writing commands “vina.exe –config config.txt –log log.txt” and splitting docking poses from output file using command “vina_split.exe –input output.pdbqt”.The results were analyzed; ranked based on their binding energies; saved in PDBQT format; the lowest bindingenergy complex was saved in PDB format for further analysis.

Visualizing interactions

Discovery Studio 3.5 from Biovia is used to visualize and study the 2-dimensional, 3-dimensional, and surface annotationof ligand interaction with the protein.

Docking Validation

Scoring functions and docking programs can be validated by a number of ways. The most common one is pose selection; this redocks compounds into a target's active site with a known conformation and orientation, usually from a crystal structure. The redocked complex was then superimposed on to the reference co-crystallized complex using Biovia Discovery Studio. These were done to validate the docking procedure to ensure the validation of docking.

5.5. SYNTHESIS:

General procedure for synthesis

Synthesis of 1-acetyl Benzimidazole

Benzimidazole is formed when O-phenylenediamine is heated with organic acid i.e. formic acid (HCOOH) in presence of strong alkali sodium hydroxide (NaOH), it gives benzimidazole. To 27g of O-phenylenediamine, 17.5g of formic acid was added in a round bottom flask and heated at 100° for 2h, cooled and 10% sodium hydroxide was added slowly with constant stirring of flask till the mixture became alkaline to litmus paper. The crude benzimidazole was filtered off the pump and washed again with 25mL of cold water, drained well and once again washed with water. The crude product was dissolved in 400 mL of boiling water and 2g of decoloring carbon was added and digested for 15mins, filtered rapidly at the pump through a preheated Buchner funnel and flask, the filtrate was cooled to about 10°, benzimidazole was filtered off, washed with 25mL of cold water and dried at 100°, the yield of benzimidazole was 25g (85%) and m.p. 171-172°

Acetylation of benzimidazole

Dissolve 0.5g of amine (benzimidazole) in 2M Hydrochloric acid, and add a little of crushed ice. Introduce a solution of 5g of hydrated sodium acetate in 25mL of water, followed by 5mL of acetic anhydride. Shake the mixture in the cold until the smell of acetic anhydride disappears. Collect the solid acetyl derivative, and recrystallise it from water or dilute ethanol.

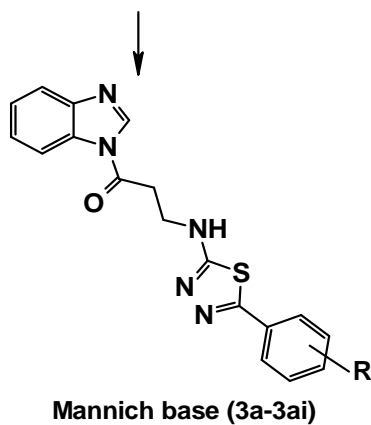
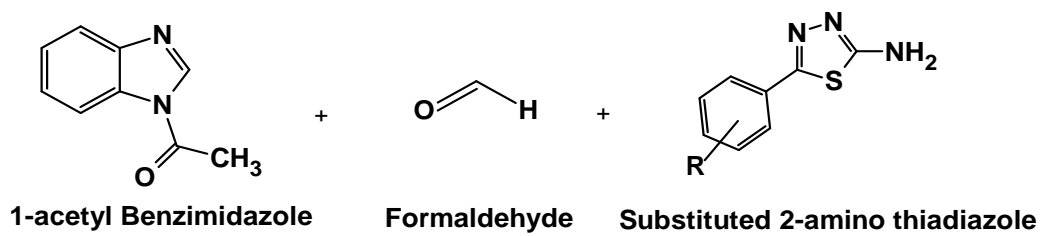
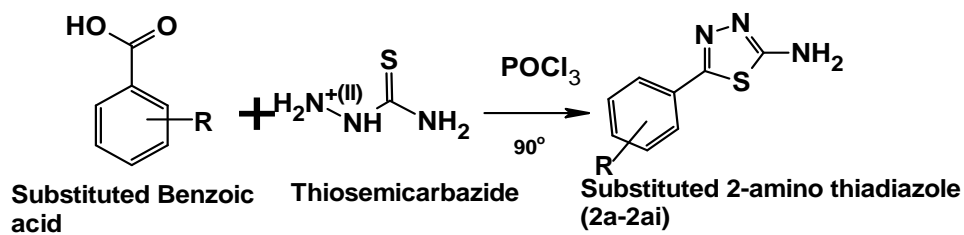
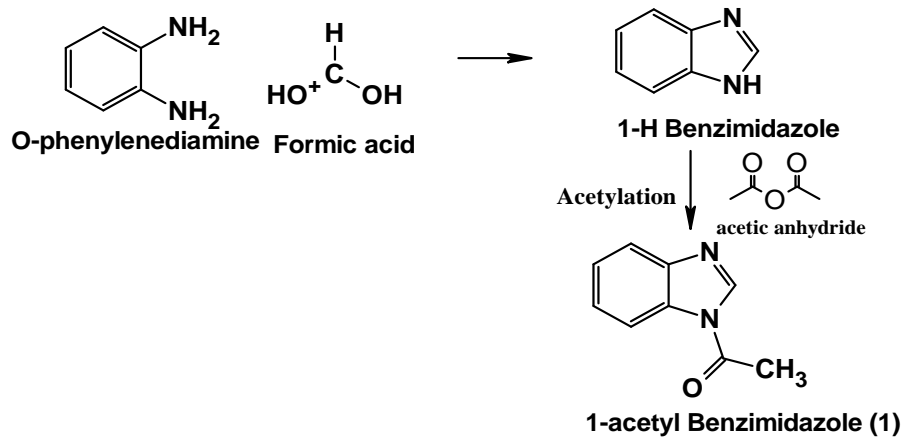


Figure 5.Synthetic scheme

Synthesis of 5-substituted 1, 3, 4-thiadiazol-2-amine

Respective carboxylic acids (0.1mol) and thiosemicarbazide (0.1mol) in phosphorous oxychloride (30mL) were refluxed gently for 30min and cooled followed by careful addition of water (90 mL). The separated solid was filtered and suspended in water and basified with aqueous potassium hydroxide followed by filtration, drying, and crystallization from mixture of DMF and ethanol (9 : 1) to obtain colourless solid with 65% yield.

Synthesis of Mannich base

In a solution of 1-acetyl benzimidazole (0.01 mol, 1.6g,) in ethanol (10mL), were added formaldehyde (0.11 mole, 1 ml) and appropriate amines(step 2 products) (0.11 mol). The mixture was heated in microwave at the power of 300 watts for 10 min. The mixture was kept overnight in refrigeration. The product thus obtained was filtered and recrystallized using aqueous ethanol to yield pure products.

5.6. CHARACTERIZATION:

All the synthesized compounds were characterized by using FT-IR, ¹H- NMR, and MASS Spectroscopy.

Infrared Spectroscopy

The infrared spectroscopy is one of the most powerful analytical techniques, this offers the possibility of chemical identification. The most important advantages of infrared spectroscopy over the other usual methods of structural analysis are that it provides useful information about the functional groups present in the molecule quickly. The technique is based upon the simple fact that a chemical substance shows marked selectable absorption in the infrared region. After absorbing IR radiations the molecules of a chemical compound exhibit small vibrations, giving rise to closely packed absorption bands called as IR absorption spectrum which may extend over a wide wavelength range. Various bands will be present in IR spectrum which corresponds to the characteristic functional groups and bonds present in a chemical substance. Thus an IR spectrum of a chemical compound is a fingerprint for its identification.

Nuclear Magnetic Resonance Spectroscopy

It is the branch of spectroscopy in which radiofrequency waves induces transitions between magnetic energy levels of nuclei of a molecule. The magnetic energy levels are created by keeping nuclei in a magnetic field. Without the magnetic field the spin states of nuclei are degenerated i.e., possess the same energy and the energy level transition is not possible. The energy level transition is possible with the application of external magnetic field which requires different R_f radiation to put them into resonance. This is a measurable phenomenon. It is a powerful tool for the investigation of nuclei structure. ^1H NMR and ^{13}C NMR Spectras of the prepared derivatives were done by using 400-MHz and 500-MHz

Bruker spectrometer using internal standard as tetra methyl silane. ^1H and ^{13}C NMR Spectral were taken with dimethyl sulphoxide (DMSO) as a solvent and the data of chemical shift were shown as delta values related to trimethylsilane (TM) in ppm.

Mass spectroscopy

Mass spectrometer performs three essential functions. First, it subjects molecules to bombardment by a stream of more amounts of energy electrons, converting some of the molecules to ions, which are then accelerated in a field of electric. Second, the ions which are accelerated are divided according to their ratios of mass to charge in an electric or magnetic field. Finally the ions that have particular mass-to-charge ratio are detected by a device which can count the number of ions striking it. The detector's output is amplified and fed to a recorder. The trace from the recorder is a mass spectrum a graph of particles detected as a function of mass-to-charge ratio. The Mass spectra of the synthesized compounds were taken using Agilent spectrometer.

5.7 BIOLOGICAL EVALUATION OF ANTIBACTERIAL ACTIVITY

DETERMINATION OF ZONE OF INHIBITION BY AGAR WELL DIFFUSION METHOD

The antimicrobials present in the given sample were allowed to diffuse out into the medium and interact in a plate freshly seeded with the test organisms. The resulting zones of inhibition will be uniformly circular as there will be a confluent lawn of growth. The diameter of zone of inhibition can be measured in millimetres [70].

MATERIALS REQUIRED

(*E.coli*- 443) was purchased from MTCC, Chandihar, India. Nutrient Agar medium, Nutrient broth, Gentamicin antibiotic solution was purchased from Himedia, India. Test samples, petri-plates, test tubes, beakers conical flasks were from Borosil, India. Spirit lamp, double distilled water.

a. Nutrient Agar Medium

The medium was prepared by dissolving 2.8 g of the commercially available Nutrient Agar Medium (HiMedia) in 100ml of distilled water. The dissolved medium was autoclaved at 15 lbs pressure at 121°C for 15 minutes. The autoclaved medium was mixed well and poured onto 100mm petriplates (25-30ml/plate) while still molten.

b. Nutrient broth

Nutrient broth was prepared by dissolving 2.8 g of commercially available nutrient medium (HiMedia) in 100ml distilled water and boiled to dissolve the medium completely. The medium was dispensed as desired and sterilized by autoclaving at 15 lbs pressure (121°C) for 15 minutes.

PROCEDURE

Petri plates containing 20 ml nutrient agar medium were seeded with 24 hr culture of bacterial strains were adjusted to 0.5 OD value according to McFarland standard, (*E.coli*- 443)Wells were cut and concentration of sample 3j, 3y and 3g (500, 250, 100 and 50 µg/ml) was added. The plates were then incubated at 37°C for 24 hours. The antibacterial activity was assayed by measuring the diameter of the inhibition zone formed around the wells [71].Gentamicin antibiotic was used as a positive control. The values were calculated using Graph Pad Prism 6.0 software (USA).

EVALUATION AGAINST QUINOLONE RESISTANT *E.COLI*

Escherichia coli ATCC 25922 is used for evaluating antibacterial activity via zone of inhibition. *E.coli* ATCC 25922quinolone resistant recommended CLSI control strain used worldwide for antimicrobial susceptibility testing (including quinolones).

Among the synthesized compounds, **3y** with high potency on *E.coli*- 443 is tested against the quinolone resistant strain of *E. coli* ATCC 25922.

RESULTS AND DISCUSSION

6. RESULTS AND DISCUSSION

6.1. 2-D QSAR analysis

2D-QSAR models were generated to determine the effect of structural features benzimidazole as antibacterial agents. The best model was selected based on statistical parameters such as observed squared correlation coefficient ($r^2 > 0.6$), which is a relative measure of the quality of fit. The cross leave one out squared correlation coefficient (q^2) should be high for predicting the goodness of the QSAR model, and the difference between q^2 and r^2 should not be more than 0.3. The standard error of estimate (SEE < 0.3) represents an absolute measure of prediction accuracy.

Initially input data was split into 29 training set and 6 prediction or test set. 498 descriptors were totally excluded from the input data and only remaining 482 variables were used as independent variable.

The linear correlation between experimental biological activities (pMIC) as a dependent variable and 2D descriptors as independent variables is expressed in the 2D-QSAR model is given below,

Model 1

$$\text{pMIC} = -7.6187 + 0.0078 (\text{ATSC3i}) + 2.4025 (\text{MATS1s}) - 1.1174 (\text{GATS8i}) + 0.0163 (\text{VE3_DzZ}) - 4.7697 (\text{BCUTc-1I})$$

$$n_{\text{tr}} = 29, n_{\text{pred}} = 6, R^2 = 0.8191, R^2_{\text{adj}} = 0.7798, R^2 - R^2_{\text{adj}} = 0.0393, \text{LOF} = 0.0191, \\ \text{RMSE}_{\text{tr}} = 0.0905, \text{MAE}_{\text{tr}} = 0.0670, \text{RSS}_{\text{tr}} = 0.2378, \text{CCC}_{\text{tr}} = 0.9006, s = 0.1017, F = 20.8295.$$

This model showed up three outliers, two from training set (compound 2, 5) and one from prediction set (compound 29) in William's plot, with less fit external validation parameters. After removing these outliers, the best fit model without any outliers was obtained.

Model 2

$$pMIC = -6.4805 - 0.7737 (\text{AATSC6s}) + 1.4548 (\text{MATS1c}) + 0.6389 (\text{GATS5i}) \\ + 0.1074 (\text{C1SP2}) - 0.03 (\text{ZMIC2})$$

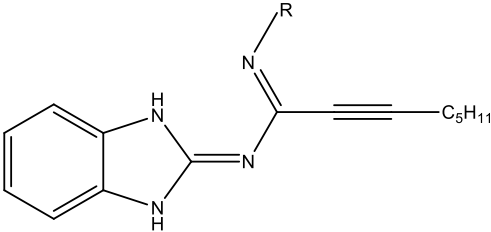
$n_{tr} = 27$, $n_{pred} = 5$, $R^2 = 0.8641$, $R^2_{adj} = 0.8301$, $R^2 - R^2_{adj} = 0.0340$, $LOF = 0.0148$,
 $RMSE_{tr} = 0.0749$, $MAE_{tr} = 0.0632$, $RSS_{tr} = 0.1460$, $CCC_{tr} = 0.9271$, $s = 0.0854$, $F = 25.4374$.

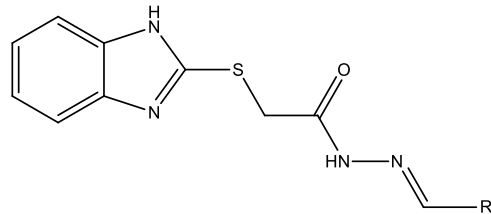
Fitting criteria and internal validation values for model 2 is good. Compared to previous model, it shows slight improvements in external validation parameter values, without any outliers in the William's plot. The descriptor correlation matrix of model 2 was given in **Table 2**. Experimental and predicted activities of original dataset compounds are given **Table 1**.

Table 2. Descriptor correlation matrix for the best model.

	AATSC6s	MATS1c	GATS5i	C1SP2	ZMIC2
AATSC6s	1				
MATS1c	0.4183	1			
GATS5i	0.0641	-0.5104	1		
C1SP2	-0.1516	0.1685	-0.3951	1	
ZMIC2	-0.1052	-0.0615	0.1007	-0.0415	1

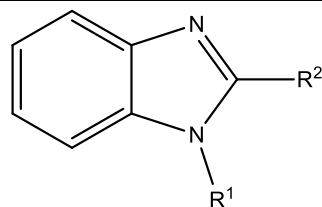
Table 1. Structures of dataset compounds with experimental and predicted MIC against *E.coli*

			
Compounds	R	MICmM <i>E.coli</i>	pMIC
1	-C ₆ H ₅ NO ₂	0.021	-7.68
2	-C ₆ H ₅ OH	0.09	-7.05
3	-2-pyridine	0.024	-7.62
4	-p-C ₆ H ₅ COOH	0.021	-7.68
5	-3-hydroxybenzenesulfonic acid	0.019	-7.72
6	-2(trifluoromethoxy)benzene	0.019	-7.72



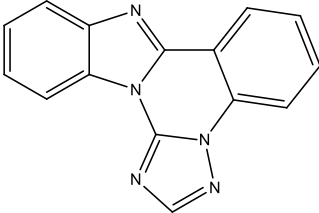
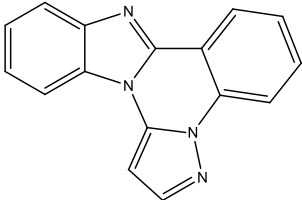
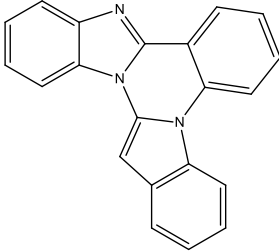
Compounds	R	MIC mM	pMIC
7	-2-anisole	0.073	-7.14
8	-3-anisole	0.037	-7.43
9	-4-anisole	0.037	-7.43
10	-2,4 dimethoxybenzene	0.067	-7.17
11	-3,4,5 trimethoxybenzene	0.062	-7.21
12	-4-Hydroxybenzene	0.037	-7.43
13	-2-chlorobenzene	0.036	-7.44
14	-4-Chlorobenzene	0.036	-7.44
15	-4-Fluorobenzene	0.038	-7.42

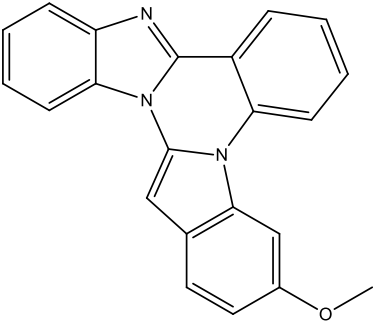
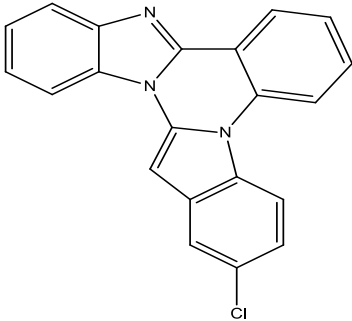
16	-4-Bromobenzene	0.032	-7.49
17	-4-Nitrobenzene	0.035	-7.46
18	-3-methoxyphenol	0.035	-7.46
19	-3-ethoxyphenol	0.067	-7.17
20	- Benzaldehyde	0.037	-7.43
21	-styrene	0.037	-7.43
22	-2-Hydroxybenzene	0.038	-7.42
23	-N,N-dimethylaniline	0.035	-7.46
24	-N,N-diethylaniline	0.033	-7.48
25	-naphthalen-1-ol	0.033	-7.48
26	-2-furan	0.042	-7.38



Compounds	R ¹	R ²	MIC mM	pMIC
27	-4-methylamino phenyl ethanone	-H	0.024	-7.63
28	-H	0	0.047	-7.33
29	-H	- succinic acid	0.027	-7.57

Compounds	Structure	MIC mM	pMIC
30		0.031	-7.51

31		0.015	-7.81
32		0.062	-7.21
33		0.013	-7.89

34		0.047	-7.32
35		0.012	-7.93

In **Figure 6**, the scatter plot depicts the experimental versus calculated antibacterial activities of benzimidazole derivatives against *E.coli*, showing that predicted values are closer to experimental values.

Since the model parameters were within the LMO parameters in **Figure 7**, the model was robust and stable. This Y-scramble plot in **Figure 8** shows that the final model correlation coefficients are much higher than those after endpoint scrambling.

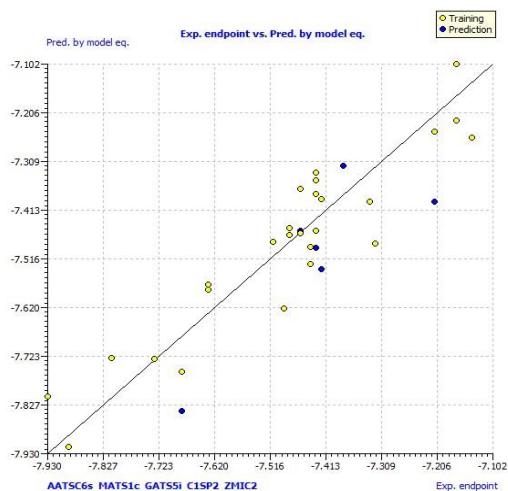


Figure 6. Scatter plot of dataset compounds

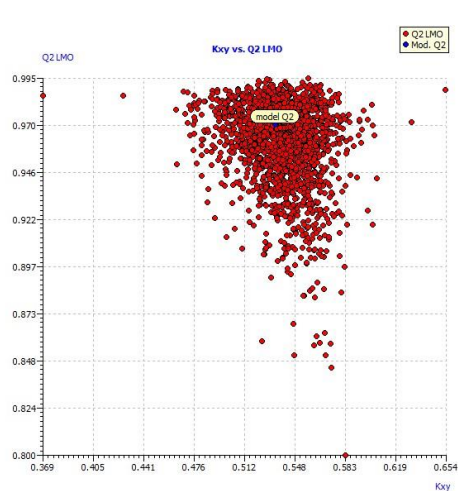


Figure 7. The LMO Scatter plot.

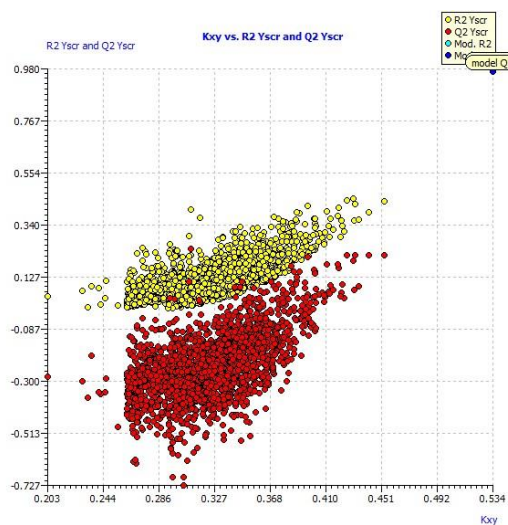


Figure 8. Y-scramble plot.

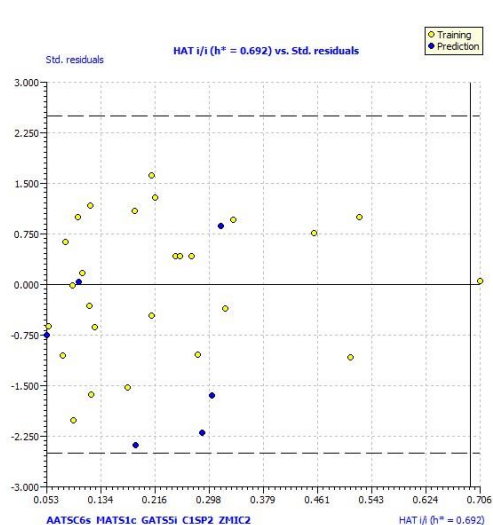


Figure 9. William's plot of the best model.

William's plot used to express the model's applicability domain. From William's plot (**Figure 9**) it reveals that one molecule is present near the line and remaining all molecules are found inside the applicability domain with leverage values lower than the warning h^* of 0.692. The Q2-F1, Q2-F2, and Q2-F3 values are above 0.7 and good CCC (concordance correlation coefficient) value.

According to all these results, the best model obtained wasn't by chance, and there's a connection between benzimidazole analog structure and an activity against *E. coli*.

AATSC6s is the average centered Broto-Moreau autocorrelation - lag 6 / weighted by I-state. This descriptor showed negative contribution (-6.4805) to the model which means its increase will decrease the activity of the compound. MATS1c is the Moran autocorrelation - lag 1 / weighted by charges, it showed positive contribution (1.4548) to the model. GATS5i is the Geary autocorrelation - lag 5 / weighted by first ionization potential. This descriptor showing positive contribution (0.6389) to the model. Therefore, increase in GATS5i, increases the activity of the compound.

C1SP2 (PaDELCarbonTypesDescriptor) is the doubly bound carbon bound to one other carbon which showed a positive contribution on activity (0.1074). ZMIC2 (Information Content Descriptor) is the Z-modified information content index (neighborhood symmetry of 2-order) showing a negative contribution (-0.03) to the model.

From the correlation, it is clear that there is inverse relationship between AATSC6s, ZMIC2 descriptors and biological activities values. The direct relationship was found between MATS1c, GATS5i, C1SP2 descriptors and biological activity. The model 2 equation is more acceptable due to high R^2 , Q^2 values and low error values such as s, RMSE, MAE parameters. Based on the final model 2, pMIC values for all compounds were calculated and shown in **Table 3**. And the internal and external parameters are shown in **Table 4**.

Table 3. pMIC values of original dataset predicted by the best model equation.

Name	AATSC6s	MATS1c	GATS5i	C1SP2	ZMIC2	PredpMIC	ExppMIC	Residual
c_01	0.075384	-0.65525	0.985961	1	36.04458	-7.836092128	-7.68	0.156092
c_02	-0.03812	-0.71924	0.99697	1	33.39192	-7.75474769	-7.05	0.704748
c_03	-0.03476	-0.82606	1.062346	3	30.85545	-7.580089728	-7.63	-0.04991
c_04	0.075556	-0.75586	1.007292	2	32.43232	-7.753189604	-7.68	0.07319
c_05	-0.05227	-0.70365	1.019033	1	33.37846	-7.706629042	-7.74	-0.03337
c_06	-0.50405	-0.8483	1.042907	1	39.14449	-7.725252341	-7.73	-0.00475
c_07	-0.01094	-0.46611	0.986254	2	31.72052	-7.256828121	-7.14	0.116828
c_08	0.068567	-0.47265	0.855967	2	29.59108	-7.347217033	-7.43	-0.08278
c_09	0.10539	-0.47627	0.879387	2	29.93078	-7.376204244	-7.43	-0.0538
c_10	-0.09648	-0.41959	0.990003	2	31.06559	-7.100928816	-7.17	-0.06907
c_11	-0.02302	-0.39366	0.86586	2	37.46554	-7.391353164	-7.21	0.181353
c_12	0.04187	-0.55162	0.853139	2	29.92691	-7.453322145	-7.43	0.023322
c_13	-0.00972	-0.52286	0.885006	2	34.51044	-7.488717654	-7.44	0.048718
c_14	0.030331	-0.53956	0.861182	2	33.35305	-7.524497595	-7.44	0.084498
c_15	0.039321	-0.52407	0.765549	2	32.20418	-7.535557239	-7.42	0.115557
c_16	0.029153	-0.54375	0.842823	2	35.93801	-7.618968862	-7.49	0.128969
c_17	0.032519	-0.48634	0.837134	2	33.03385	-7.454559567	-7.46	-0.00544
c_18	0.116791	-0.49375	0.861592	2	28.02068	-7.364516014	-7.46	-0.09548
c_19	-0.02464	-0.50519	0.935234	2	27.83428	-7.219090435	-7.17	0.04909
c_20	0.027739	-0.46504	0.810312	3	33.07476	-7.330833044	-7.43	-0.09917
c_21	-0.03775	-0.54383	0.927342	2	35.16418	-7.490098297	-7.43	0.060098
c_22	-0.11745	-0.54188	0.827304	2	31.75232	-7.387164044	-7.42	-0.03284

c_23	0.126686	-0.46583	0.885466	2	32.77993	-7.459083912	-7.46	-0.00092
c_24	0.109142	-0.48353	0.93177	2	33.51764	-7.46380408	-7.48	-0.0162
c_25	-0.00698	-0.53779	1.042361	2	35.69814	-7.447661125	-7.48	-0.03234
c_26	0.179303	-0.50984	0.827973	3	26.90364	-7.316852355	-7.38	-0.06315
c_27	0.199371	-0.47006	0.963412	0	28.86509	-7.56902194	-7.63	-0.06098
c_28	0.029167	-0.71985	0.982564	1	19.26266	-7.393023958	-7.33	0.063024
c_29	-0.77756	-0.65485	0.719567	3	27.31072	-6.868959523	-7.57	-0.70104
c_30	-0.11306	-0.74084	1.006135	3	32.37902	-7.477153288	-7.51	-0.03285
c_31	-0.1353	-0.68484	0.986074	1	36.28958	-7.723407131	-7.81	-0.08659
c_32	-0.08187	-0.47674	0.918558	3	34.70981	-7.242939844	-7.21	0.03294
c_33	-0.02329	-0.6277	0.875764	2	43.72041	-7.912946492	-7.89	0.022946
c_34	-0.01148	-0.48141	0.904669	2	36.74825	-7.481628677	-7.32	0.161629
c_35	-0.02372	-0.60191	0.891636	2	41.73247	-7.805307499	-7.93	-0.12469

Table 4. Internal and external validation parameter of Model 1 and 2.

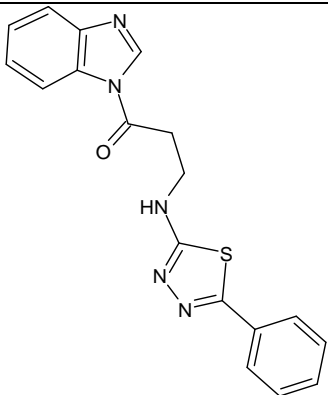
Parameters	Model 1	Model 2
Internal validation		
Q2loo	0.744	0.7811
R2-Q2loo	0.0747	0.083
RMSE cv	0.1076	0.0951
MAE cv	0.0827	0.0819
PRESS cv	0.336	0.2351
CCC cv	0.8562	0.883
Q2LMO	0.7046	0.9667
R2Yscr	0.1794	0.1198

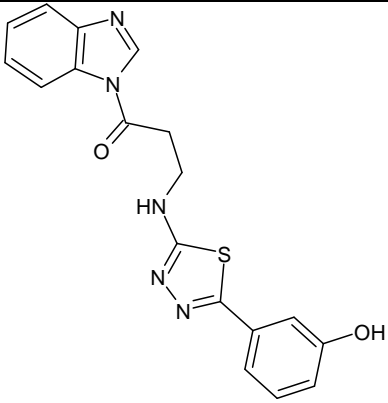
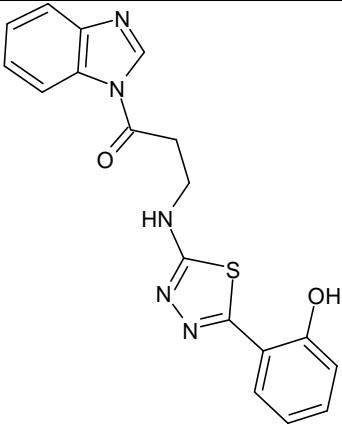
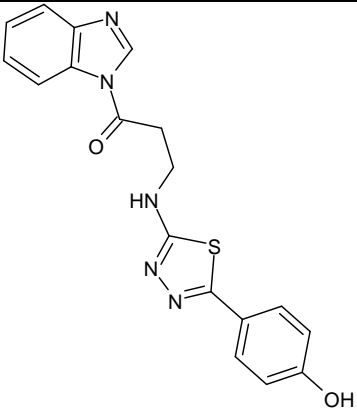
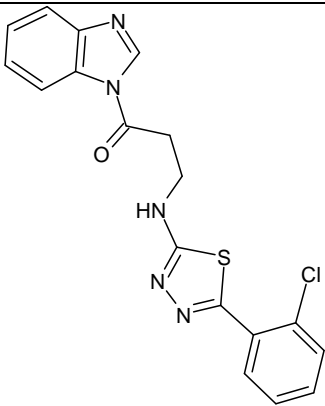
Q2Yscr	-0.3956	-0.2309
RMSE AV Yscr	0.1925	0.2616
External validation		
RMSE ext	0.2952	0.048
MAE ext	0.2147	0.0335
PRESS ext	0.5227	0.0184
R2ext	0.6268	0.9551
Q2-F1	0.3908	0.9551
Q2-F2	0.3034	0.9544
Q2-F3	0.6785	0.9704
CCC ex	0.7433	0.9762
r2m aver.	0.6003	0.9150
r2m delta	0.2358	0.0450

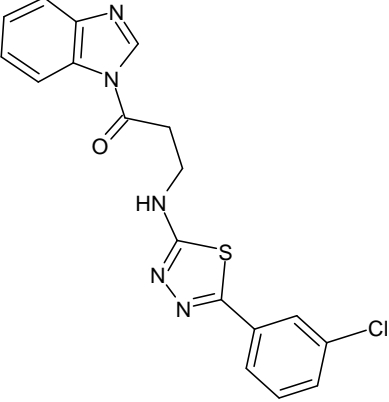
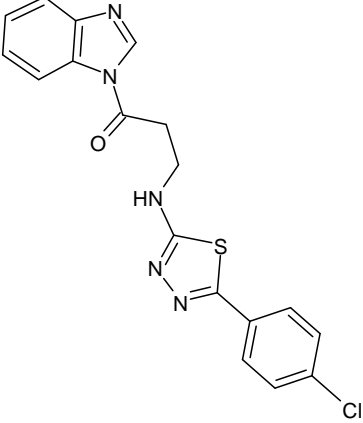
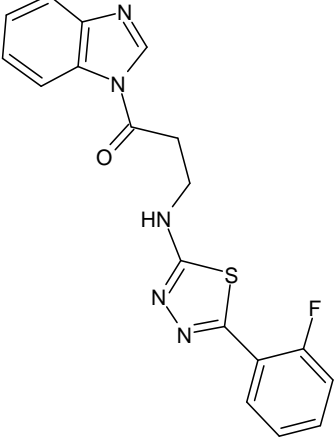
6.2. DESIGN OF COMPOUNDS

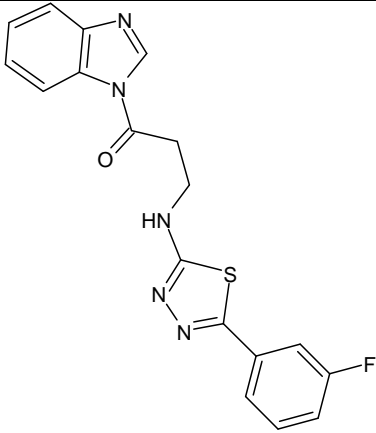
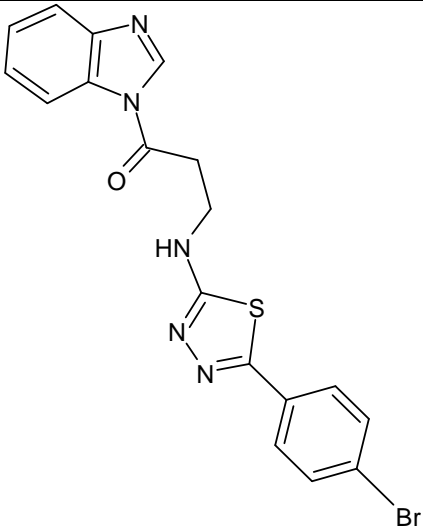
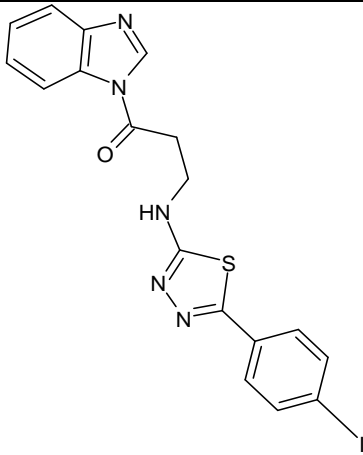
35 compounds were designed using Chemskech software and physicochemical properties were calculated for all compounds. The designed compounds and their predicted pMIC using model 2 was given in **Table 5**.

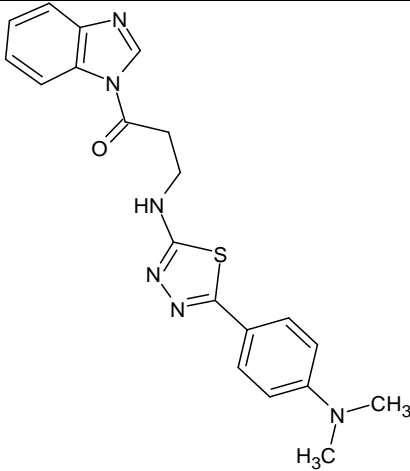
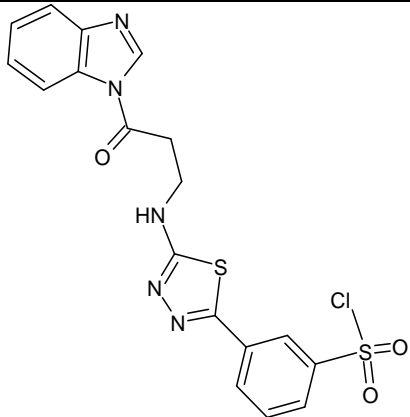
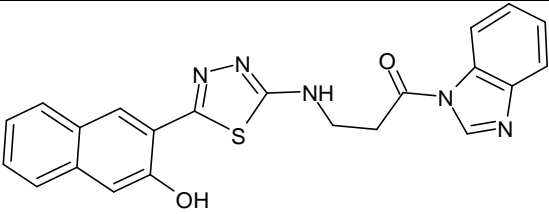
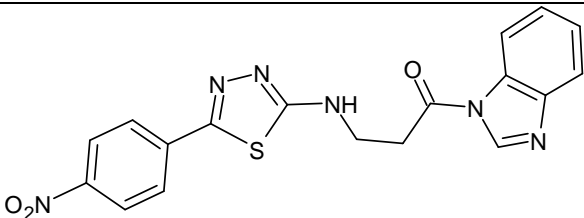
Table 5. Designed molecules with their predicted activity using model 2.

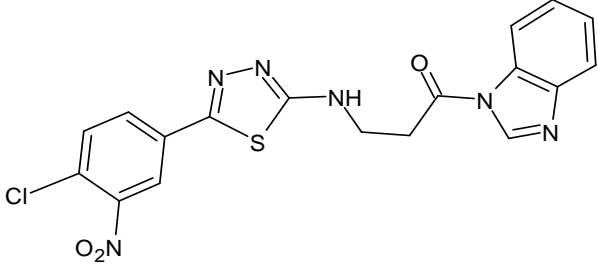
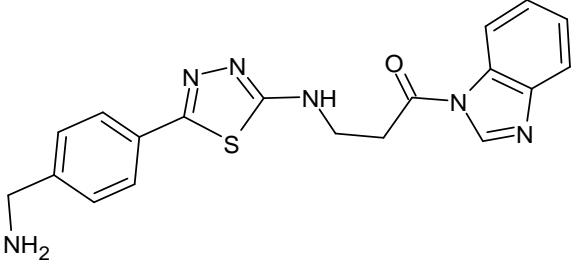
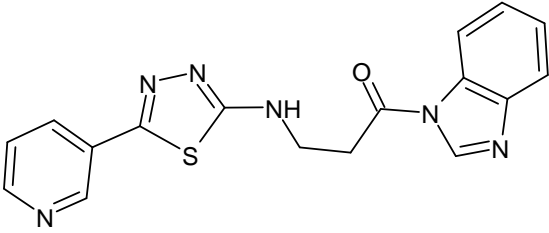
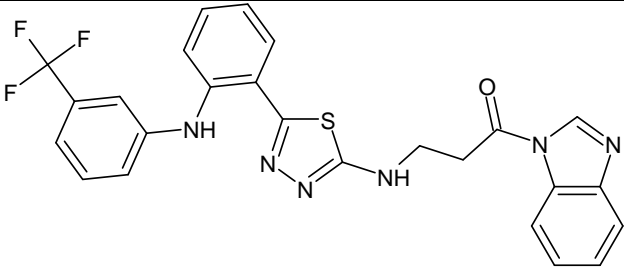
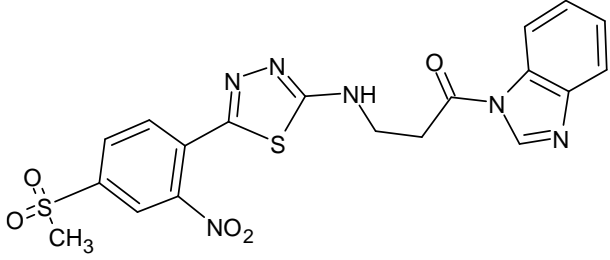
S.No	COMPOUNDS	STRUCTURE	pKi
1	3a		-7.4296

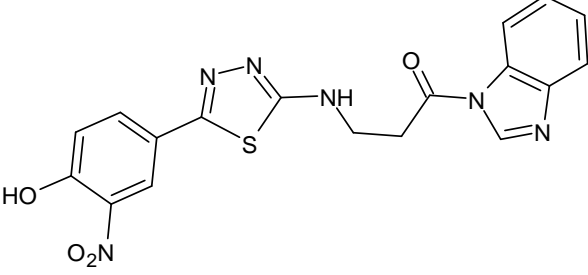
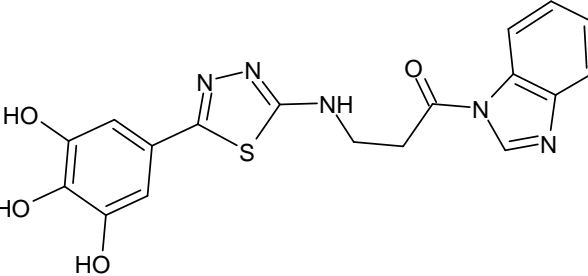
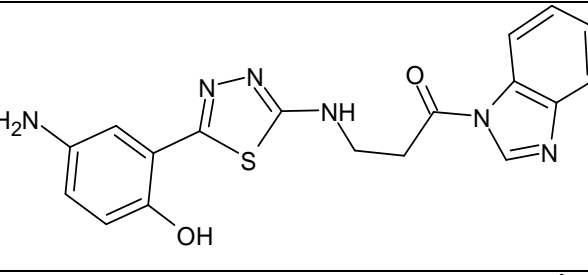
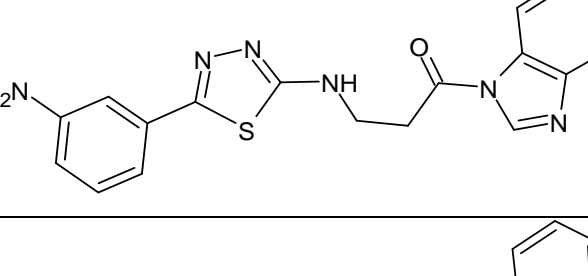
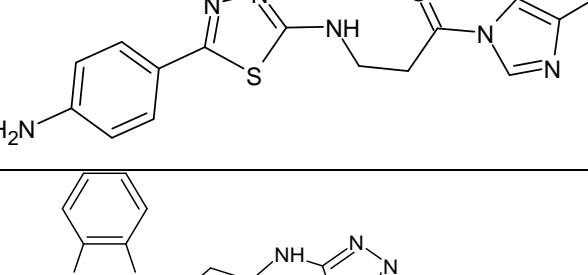
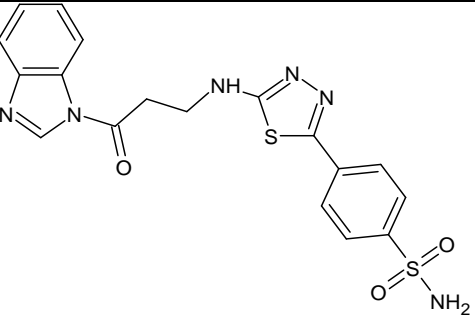
2	3b		-7.2835
3	3c		-7.3130
4	3d		-7.2398
5	3e		-7.3592

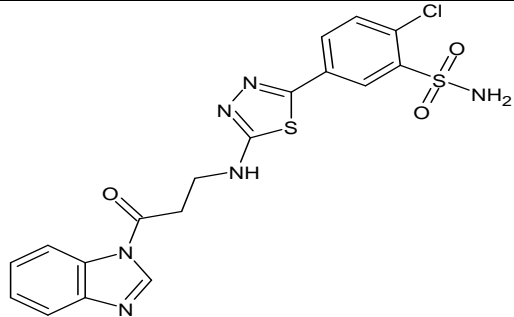
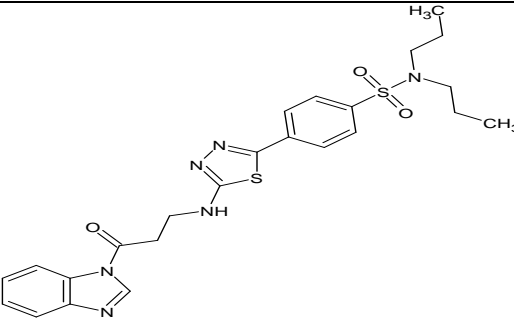
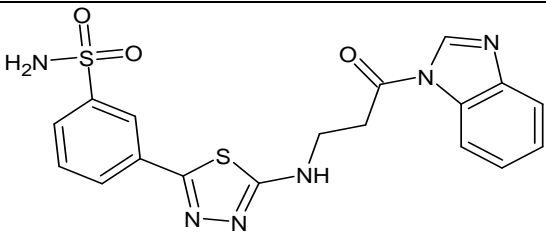
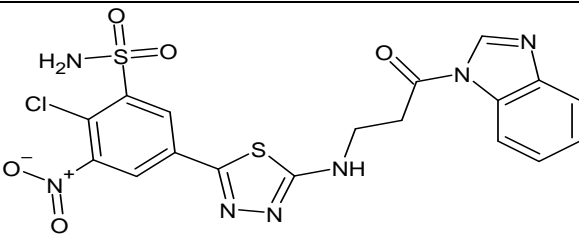
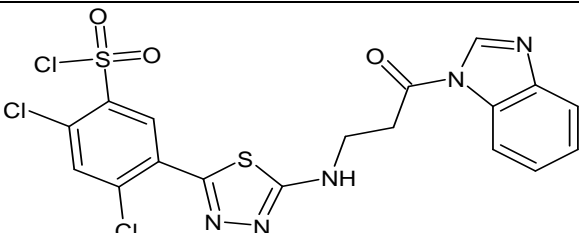
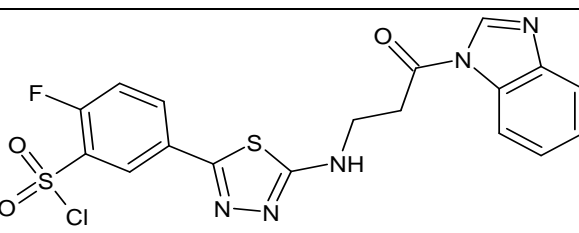
6	3f		-7.3517
7	3g		-7.3494
8	3h		-7.4115

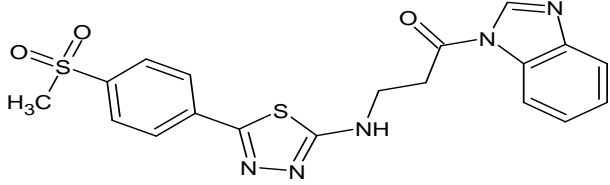
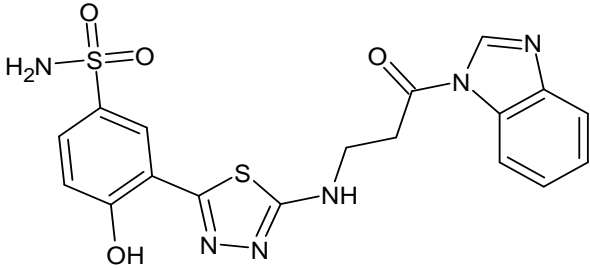
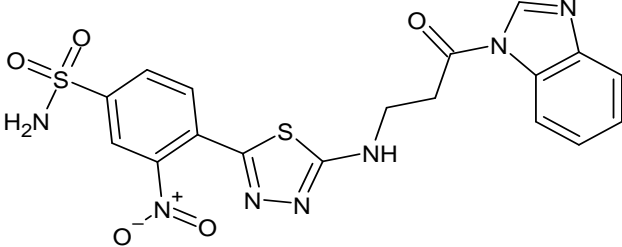
9	3i		-7.4159
10	3j		-7.4412
11	3k		-7.5600

12	3l		-7.3445
13	3m		-7.2424
14	3n		-7.3859
15	3o		-7.2657

16	3p		-7.0151
17	3q		-7.3148
18	3r		-6.9373
19	3s		-7.6483
20	3t		-8.0238

21	3u		-6.9788
22	3v		-7.4326
23	3w		-7.1644
24	3x		-7.3417
25	3y		-7.3501
26	3z		-7.5276

27	3aa		-7.2265
28	3ab		-7.3419
29	3ac		-7.3047
30	3ad		-7.9045
31	3ae		-7.2871
32	3af		-7.1662

33	3ag		-7.3767
34	3ah		-7.8244
35	3ai		-8.3594

6.3. *IN SILICO* SCREENING OF DESIGNED COMPOUNDS

- The molecular properties were calculated using Molinspiration and tabulated in **Table 6**.
- Molinspiration software was used to evaluate molecular properties such as miLogP, no. of rotatable bonds, molecular weight and volume of designed compounds and its results were tabulated (table). No violations were reported with the designed compounds.
- The bioactivity scores of the synthesized complexes were calculated for different parameters such as binding to G protein-coupled receptor (GPCR) ligand and nuclear receptor ligand, ion channel modulation, kinase inhibition, protease inhibition, and enzyme activity inhibition. The bioactivity score is given in **Table 7**. If the bioactivity score is more than 0.0, then the complex is active; if it is between -5.0 and 0.0, then the complex is moderately active, and if the bioactivity score is less than -5.0, then it is inactive. The synthesized compounds

were found to be moderately bioactive (<0) towards all the enzyme considered for the study.

The Pharmacokinetic properties such as TPSA, No. of H-bond acceptor/donor, Molar refractivity, logP, Bioavailability score, GI absorption, of the designed compound were evaluated using SWISS ADME and software and their results were tabulated (**Table 8, 9**).

- TPSA has been used as descriptor for characterizing absorption and passive transportation properties through biological membranes, allowing a good prediction of transport of candidate drugs in the intestines and through the blood-brain barrier. Compounds with TPSA values within the range 140 \AA^2 have good intestinal absorption. TPSA (Total Polar Surface Area) of our designed compounds were found to be in the range of 100-215 \AA^2 . Except the molecules 3m, 3o, 3p, 3t-w, 3z, 3aa-ai remaining was expected to possess good intestinal absorption.
- Lipophilicity (logP) plays an important role in the absorption, distribution, metabolism, excretion, and toxic effects of a drug. LogP of the designed compounds was found to be in the range of 1-5. So there is a strong lipophilic character of the molecule plays a major role in producing the antimicrobial effect.
- Molar refractivity is related, not only to the volume of the molecules but also to the London dispersive forces that act in the drug-receptor interaction. All the designed compounds were within the normal range of 40-130 $\text{ J mol}^{-1} \text{ K}^{-1}$. The majority of compounds have bioavailability score of **0.55** which indicates a good pharmacokinetic property.
- Antibacterial agents generally possess greater number of hydrogen bond acceptors. All the designed compounds have hydrogen bond donors in the range of 1-4 and 4-9 hydrogen bond acceptors. This obeys Lipinski rule of five. Molecular weight of the most designed compounds was around 500 daltons except, 3s, 3ab, 3ad, and 3ae.
- CaCo^2 is primarily used as a model of the intestinal epithelial barrier. It is used to predict *in vivo* absorption of the drugs. All the synthesized compounds are found

to be with high absorption predicted permeability of $>10 \times 10^{-6}$ cm/s and good Human Intestinal Absorption (HIA).

- Cytochrome P450 enzymes are essential for the metabolism of many medications. Knowledge of the most important drugs metabolized by cytochrome P450 enzymes, as well as the most potent inhibiting and inducing drugs, can help minimize the possibility of adverse drug reactions and interactions. From synthesized compounds 3n, 3y are 2C9 inhibitor and most of the designed compounds are weakly CYP3A4 substrate.
- Toxicity of all the designed compounds were evaluated by using two softwares ProTox II and Pre ADMET and its results were tabulated (**Table 10 and 11**). According to Pre ADMET toxicity study- all the synthesized compounds was found to be non-mutagenic, non-carcinogenic with medium risk of hERG inhibition.
- Protox II results shows predicted LD50 mg/kg of class 5 for the synthesized compounds without any toxicity.

Table 6. MOLINSPIRATION RESULTS

Compound	milogP	TPSA	N atoms	Molecular weight	Number of violations	num. rotatable bonds	volume
3a	3.76	72.71	25	349.42	0	5	299.45
3b	3.26	92.94	26	365.42	0	5	307.47
3c	3.5	92.94	26	365.42	0	5	307.47
3d	3.28	92.94	26	365.42	0	5	307.47
3e	4.39	72.71	26	383.86	0	5	312.99
3f	4.42	72.71	26	383.86	0	5	312.99
3g	4.44	72.71	26	383.86	0	5	312.99

3h	3.88	72.71	26	367.41	0	5	304.38
3i	3.9	72.71	26	367.41	0	5	304.38
3j	4.57	72.71	26	428.31	0	5	317.34
3k	4.85	72.71	26	475.31	0	5	323.44
3l	3.87	75.95	28	392.49	0	6	345.36
3m	3.63	106.85	29	447.93	0	6	344.42
3n	4.66	92.94	30	415.48	0	5	351.46
3o	3.72	118.53	28	394.42	0	6	322.79
3p	4.33	118.53	29	428.86	0	6	336.32
3q	2.95	98.73	27	378.46	0	6	327.54
3r	2.69	85.6	25	350.41	0	5	295.3
3s	6.58	84.73	36	508.53	2	8	414.56
3t	2.52	152.67	32	472.51	1	7	370.78
3u	3.43	138.76	29	410.42	0	6	330.8
3v	2.5	133.39	28	397.42	0	5	323.5
3w	2.55	118.96	27	380.43	0	5	318.76
3x	2.89	98.73	26	364.43	0	5	310.74
3y	2.84	98.73	26	364.43	0	5	310.74
3z	2.46	132.87	29	428.50	0	6	342.17
3aa	3.06	132.87	30	462.94	0	6	355.71
3ab	4.83	110.09	35	512.66	1	11	444.00
3ac	2.43	132.87	29	428.50	0	6	342.17
3ad	2.95	178.70	33	507.94	2	7	379.04

3ae	4.86	106.85	31	516.82	1	6	371.49
3af	3.74	106.85	30	465.92	0	6	349.35
3ag	2.63	106.85	29	427.51	0	6	347.44
3ah	2.17	153.10	30	444.50	0	6	350.19
3ai	2.34	178.70	32	473.50	1	7	365.51

Table 7. BIOACTIVITY SCORE

Compound	GPCR ligand	Ion channel modulator	Kinase inhibitor	Nuclear receptor ligand	Protease inhibitor	Enzyme inhibitor
3a	-0.11	-0.86	0.16	-0.42	-0.43	-0.09
3b	-0.07	-0.79	0.21	-0.27	-0.42	-0.02
3c	-0.09	-0.9	0.17	-0.35	-0.5	-0.12
3d	-0.06	-0.79	0.19	-0.28	-0.4	-0.03
3e	-0.12	-0.9	0.15	-0.43	-0.5	-0.11
3f	-0.11	-0.85	0.14	-0.41	-0.47	-0.11
3g	-0.11	-0.84	0.13	-0.43	-0.46	-0.12
3h	-0.1	-0.85	0.19	-0.47	-0.48	-0.1
3i	-0.07	-0.83	0.2	-0.35	-0.42	-0.09
3j	-0.2	-0.9	0.11	-0.52	-0.53	-0.15
3k	-0.1	-0.83	0.16	-0.39	-0.48	-0.14
3l	-0.1	-0.8	0.17	-0.38	-0.42	-0.1
3m	0.09	-0.88	0.09	-0.38	-0.33	-0.06
3n	-0.04	-0.74	0.24	-0.26	-0.41	-0.04
3o	-0.24	-0.83	0.01	-0.48	-0.52	-0.19
3p	-0.23	-0.82	0.01	-0.57	-0.59	-0.2
3q	0	-0.71	0.26	-0.55	-0.18	0.02
3r	-0.03	-0.84	0.33	-0.43	-0.39	-0.01

3s	-0.07	-0.63	0.27	-0.26	-0.3	0.01
3t	-0.3	-0.91	-0.07	-0.5	-0.39	-0.04
3u	-0.23	-0.98	0.03	-0.4	-0.55	-0.14
3v	-0.09	-0.74	0.2	-0.32	-0.4	0
3w	-0.06	-0.83	0.26	-0.41	-0.42	-0.03
3x	-0.07	-0.79	0.27	-0.47	-0.34	0.01
3y	-0.07	-0.78	0.25	-0.47	-0.34	-0.01
3z	-0.18	-0.84	0.11	-0.57	-0.23	0.03
3aa	-0.17	-0.9	0.09	-0.54	-0.27	0.02
3ab	-0.12	-0.85	-0.09	-0.41	-0.25	-0.13
3ac	-0.17	-0.93	0.11	-0.55	-0.21	0.05
3ad	-0.27	-0.83	-0.04	-0.65	-0.34	-0.06
3ae	0.04	-0.87	0.08	-0.37	-0.39	-0.08
3af	0.06	-0.89	0.12	-0.35	-0.36	-0.07
3ag	-0.11	-0.9	0.12	-0.3	-0.22	0.06
3ah	-0.16	-0.96	0.1	-0.5	-0.28	0.02
3ai	-0.35	-0.85	-0.07	-0.75	-0.4	-0.06

Table 8. SWISS ADME RESULTS

Compd. code.	Formula	Molecular weight (g/mol)	Fraction Csp3	Number rotatable bonds	Number H bond acceptors	Number H bond donors	Molar refractivity	TPSA (Å)	Log P _{o/w}	Log S
3a	C18H15N5OS	349.41	0.11	6	4	1	98.76	100.94	3.14	-4.68
3b	C18H15N5O2S	365.41	0.11	6	5	2	100.78	121.17	2.75	-4.53
3c	C18H15N5O2S	365.41	0.11	6	5	2	100.78	121.17	2.83	-4.53
3d	C18H15N5O2S	365.41	0.11	6	5	2	100.78	121.17	2.83	-4.53
3e	C18H14ClN5OS	383.85	0.11	6	4	1	103.77	100.94	3.64	-5.26
3f	C18H14ClN5OS	383.85	0.11	6	4	1	103.77	100.94	3.65	-5.26
3g	C18H14ClN5OS	383.85	0.11	6	4	1	103.77	100.94	3.67	-5.26
3h	C18H14FN5OS	367.40	0.11	6	5	1	98.72	100.94	3.45	-4.83
3i	C18H14FN5OS	367.40	0.11	6	5	1	98.72	100.94	3.44	-4.83
3j	C18H14BrN5OS	428.31	0.11	6	5	1	106.46	100.94	3.72	-5.58
3k	C18H14IN5OS	475.31	0.11	6	5	1	111.48	100.94	3.78	-5.85
3l	C20H20N6OS	392.48	0.20	7	4	1	112.97	104.18	3.20	-4.89

3m	C18H14CIN5O3S2	447.92	0.11	7	6	1	111.84	143.46	3.28	-5.15
3n	C22H17N5O2S	415.47	0.09	6	5	2	118.29	121.17	3.72	-5.65
3o	C18H14N6O3S	394.41	0.11	7	6	1	107.58	146.76	2.65	-4.71
3p	C18H13CIN6O3S	428.85	0.11	7	6	1	112.59	146.76	3.15	-5.31
3q	C19H18N6OS	378.45	0.16	7	5	2	106.43	126.96	2.65	-4.02
3r	C17H14N6OS	350.40	0.12	6	5	1	96.56	113.83	2.42	-4.01
3s	C25H19F3N6O3S	508.52	0.12	9	7	2	133.31	112.97	5.35	-6.93
3t	C219H16N6O5S2	472.50	0.16	8	8	1	120.68	189.28	2.16	-4.59
3u	C18H14N6O4S	410.41	0.11	7	7	2	109.61	166.99	2.28	-4.92
3v	C18H15N5O4S	397.41	0.11	6	7	4	104.83	161.63	2.01	-4.24
3w	C18H16N6O2S	380.42	0.11	6	5	3	105.19	147.19	2.36	-4.17
3x	C18H16N6OS	364.42	0.11	6	4	2	103.16	126.96	2.66	-4.31
3y	C18H16N6OS	364.42	0.11	6	4	2	103.16	126.96	2.63	-4.31
3z	C18H16N6O3S2	428.49	0.11	7	7	2	109.75	169.48	2.08	-4.11
3aa	C18H15CIN6O3S2	462.93	0.11	7	7	2	114.76	169.48	2.57	-4.71

3ab	C24H28N6O3S2	512.65	0.33	12	7	1	138.79	146.70	4.02	-5.71
3ac	C18H16N6O3S2	428.49	0.11	7	7	2	109.75	169.48	2.01	-4.11
3ad	C18H14ClN7O5S2	507.93	0.11	8	9	2	123.59	215.30	1.84	-4.77
3ae	C18H12Cl3N5O3S2	516.81	0.11	7	6	1	121.86	143.46	4.19	-6.34
3af	C18H13ClFN5O3S2	465.91	0.11	7	7	1	111.80	143.46	3.43	-5.31
3ag	C19H17N5O3S2	427.50	0.16	7	6	1	111.85	143.46	2.89	-4.53
3ah	C18H16N6O4S2	444.49	0.11	7	8	3	111.78	189.71	1.79	-3.97
3ai	C18H15N7O5S2	473.49	0.11	8	9	2	118.58	215.30	1.34	-4.17

Table 9. Drug filters results from Swiss ADME

Cmpd No.	Lipinski	Ghose	Veber	Egan	Muegge	Bioavailability score	GI absorption	BBB permeation	P-gp substrate	Log K_P cm/s	Synthetic accessibility score
3a	Yes	Yes	Yes	Yes	Yes	0.55	High	No	No	-5.64	3.06
3b	Yes	Yes	Yes	Yes	Yes	0.55	High	No	No	-5.99	3.06

3c	Yes	Yes	Yes	Yes	Yes	0.55	High	No	No	-5.99	3.1
3d	Yes	Yes	Yes	Yes	Yes	0.55	High	No	No	-5.99	3.08
3e	Yes	Yes	Yes	Yes	Yes	0.55	High	No	No	-5.41	3.15
3f	Yes	Yes	Yes	Yes	Yes	0.55	High	No	No	-5.41	3.08
3g	Yes	Yes	Yes	Yes	Yes	0.55	High	No	No	-5.41	3.06
3h	Yes	Yes	Yes	Yes	Yes	0.55	High	No	No	-5.68	3.08
3i	Yes	Yes	Yes	Yes	Yes	0.55	High	No	No	-5.68	3.07
3j	Yes	Yes	Yes	Yes	Yes	0.55	High	No	No	-5.63	3.09
3k	Yes	Yes	Yes	Yes	Yes	0.55	High	No	No	-5.95	3.2
3l	Yes	Yes	Yes	Yes	Yes	0.55	High	No	No	-5.82	3.32
3m	Yes	Yes	No	No	Yes	0.55	Low	No	No	-6.23	3.3
3n	Yes	Yes	Yes	Yes	Yes	0.55	High	No	No	-5.41	3.32
3o	Yes	Yes	No	No	Yes	0.55	Low	No	No	-6.04	3.18
3p	Yes	Yes	No	No	Yes	0.55	Low	No	No	-5.81	3.25
3q	Yes	Yes	Yes	Yes	Yes	0.55	High	No	Yes	-6.63	3.2
3r	Yes	Yes	Yes	Yes	Yes	0.55	High	No	No	-6.41	3.07
3s	No	No	Yes	No	No	0.17	Low	No	No	-4.89	3.86
3t	Yes	Yes	No	No	No	0.55	Low	No	No	-7.06	3.65

3u	Yes	Yes	No	No	No	0.55	Low	No	No	-6	3.29
3v	Yes	Yes	No	No	No	0.55	Low	No	No	-6.69	3.17
3w	Yes	Yes	No	No	Yes	0.55	Low	No	No	-6.57	3.21
3x	Yes	Yes	Yes	Yes	Yes	0.55	High	No	No	-6.22	3.17
3y	Yes	Yes	Yes	Yes	Yes	0.55	High	No	No	-6.22	3.13
3z	Yes	Yes	No	No	No	0.55	Low	No	No	-7.15	3.28
3aa	Yes	Yes	No	No	No	0.55	Low	No	Yes	-6.91	3.34
3ab	Yes	No	No	No	Yes	0.55	Low	No	No	-5.98	3.97
3ac	Yes	Yes	No	No	No	0.55	Low	No	No	-7.15	3.34
3ad	No	No	No	No	No	0.17	Low	No	No	-7.3	3.57
3ae	Yes	No	No	No	No	0.55	Low	No	No	-5.76	3.43
3af	Yes	Yes	No	No	Yes	0.55	Low	No	No	-6.27	3.34
3ag	Yes	Yes	No	No	Yes	0.55	Low	No	No	-6.66	3.29
3ah	Yes	Yes	No	No	Yes	0.55	Low	No	No	-7.5	3.39
3ai	Yes	Yes	No	No	No	0.55	Low	No	No	-7.54	3.63

Table 10. Pre ADME/Tox Results

ADME Result

Compounds	Caco2	CYP inhibition				CYP substrate		HIA	MDCK
		2C19	2C9	2D6	3A4	2D6	3A4		
3a	22.6207	Non	Non	Non	Non	Non	Weakly	97.569243	0.727687
3b	3.01806	Non	Inhibitor	Non	Non	Inhibitor	Non	95.971294	0.858247
3c	3.01671	Non	Inhibitor	Non	Non	Inhibitor	Non	95.969618	1.07916
3d	3.31426	Non	Inhibitor	Non	Non	Inhibitor	Non	95.971321	1.30533
3e	29.3595	Non	Non	Non	Non	Non	Weakly	97.038357	0.169652
3f	29.3595	Non	Non	Non	Non	Non	Weakly	97.038357	0.170431
3g	32.4144	Non	Non	Non	Non	Non	Weakly	97.038357	0.233158
3h	21.911	Non	Non	Non	Non	Non	Weakly	97.560834	0.379314
3i	21.911	Non	Non	Non	Non	Non	Weakly	97.560834	0.320304
3j	25.3878	Non	Non	Non	Non	Non	Weakly	96.880215	0.0257726
3k	24.5671	Non	Non	Non	Non	Non	Weakly	97.923394	0.323377

3l	32.7051	Non	Non	Non	Non	Non	Weakly	97.456597	0.317284
3m	4.72144	Non	Inhibitor	Non	Non	Non	Weakly	98.916435	0.318393
3n	19.9437	Non	Inhibitor	Non	Non	Inhibitor	Weakly	95.766217	0.215524
3o	0.6186	Non	Inhibitor	Non	Non	Non	Weakly	93.917297	0.883753
3p	2.24253	Non	Inhibitor	Non	Non	Non	Weakly	96.89409	0.299803
3q	2.81784	Non	Inhibitor	Non	Substrate	Non	Weakly	96.889445	5.37924
3r	12.4378	Non	Non	Non	Non	Non	Substrate	98.056441	12.6896
3s	18.7684	Non	Inhibitor	Non	Non	Non	Weakly	95.981831	0.0484831
3t	0.407953	Non	Inhibitor	Non	Non	Non	Weakly	89.399421	0.466323
3u	0.452036	Non	Inhibitor	Non	Non	Inhibitor	Weakly	86.312868	1.56162
3v	1.24473	Non	Inhibitor	Non	Non	Inhibitor	Non	85.719112	0.556657
3w	1.30403	Non	Inhibitor	Non	Non	Inhibitor	Weakly	93.152179	4.99203
3x	2.09136	Non	Inhibitor	Non	Non	Non	Weakly	96.698511	2.79432
3y	21.4207	Non	Inhibitor	Non	Non	Non	Weakly	96.698535	4.09999
3z	0.422142	Non	Inhibitor	Non	Non	Non	Non	94.635126	3.76345

3aa	0.42893	Non	Inhibitor	Non	Non	Non	Weakly	96.708762	0.294144
3ab	21.6045	Non	Inhibitor	Non	Non	Non	Substrate	98.979568	0.104343
3ac	0.418368	Non	Inhibitor	Non	Non	Non	Weakly	94.635126	3.49108
3ad	0.38671	Non	Inhibitor	Non	Non	Non	Weakly	85.253401	0.13165
3ae	7.29327	Non	Inhibitor	Non	Non	Non	Weakly	97.758873	0.0251649
3af	5.95018	Non	Inhibitor	Non	Non	Non	Weakly	98.917583	0.264058
3ag	3.27565	Non	Inhibitor	Non	Non	Non	Weakly	98.501632	0.812871
3ah	0.376834	Non	Inhibitor	Non	Non	Inhibitor	Weakly	88.589187	4.03104
3ai	0.37462	Non	Inhibitor	Non	Non	Inhibitor	Weakly	76.98416	2.78916

Drug-likeness Result

Compounds	CMC like Rule	Lead-like Rule	MDDR like Rule	WDI like Rule
3a	Qualified	Violated	Mid-structure	In 90% cutoff
3b	Qualified	Violated	Mid-structure	In 90% cutoff
3c	Qualified	Violated	Mid-structure	In 90% cutoff

3d	Qualified	Violated	Mid-structure	In 90% cutoff
3e	Qualified	Violated	Mid-structure	In 90% cutoff
3f	Qualified	Violated	Mid-structure	Out of 90% cutoff
3g	Qualified	Violated	Mid-structure	Out of 90% cutoff
3h	Qualified	Violated	Mid-structure	In 90% cutoff
3i	Qualified	Violated	Mid-structure	In 90% cutoff
3j	Qualified	Violated	Mid-structure	Out of 90% cutoff
3k	Qualified	Violated	Mid-structure	Out of 90% cutoff
3l	Qualified	Violated	Mid-structure	Out of 90% cutoff
3m	Qualified	Violated	Mid-structure	Out of 90% cutoff
3n	Qualified	Violated	Mid-structure	In 90% cutoff
3o	Qualified	Violated	Mid-structure	Out of 90% cutoff
3p	Qualified	Violated	Mid-structure	Out of 90% cutoff
3q	Qualified	Violated	Mid-structure	Out of 90% cutoff
3r	Qualified	Violated	Mid-structure	In 90% cutoff
3s	Not qualified	Violated	Mid-structure	Out of 90% cutoff

3t	Qualified	Violated	Mid-structure	Out of 90% cutoff
3u	Qualified	Violated	Mid-structure	In 90% cutoff
3v	Qualified	Violated	Mid-structure	In 90% cutoff
3w	Qualified	Violated	Mid-structure	In 90% cutoff
3x	Qualified	Violated	Mid-structure	In 90% cutoff
3y	Qualified	Violated	Mid-structure	In 90% cutoff
3z	Qualified	Violated	Mid-structure	Out of 90% cutoff
3aa	Qualified	Violated	Mid-structure	Out of 90% cutoff
3ab	Not qualified	Violated	drug-like	Out of 90% cutoff
3ac	Qualified	Violated	Mid-structure	Out of 90% cutoff
3ad	Qualified	Violated	Mid-structure	Out of 90% cutoff
3ae	Not qualified	Violated	Mid-structure	Out of 90% cutoff
3af	Qualified	Violated	Mid-structure	Out of 90% cutoff
3ag	Qualified	Violated	Mid-structure	Out of 90% cutoff
3ah	Qualified	Violated	Mid-structure	Out of 90% cutoff
3ai	Qualified	Violated	Mid-structure	Out of 90% cutoff

Toxicity Result

Compounds	Ames test	Carcino Mouse	Carcino Rat	hERG inhibition
3a	mutagen	negative	negative	medium risk
3b	mutagen	negative	negative	high risk
3c	mutagen	negative	negative	high risk
3d	mutagen	negative	negative	medium risk
3e	Non-mutagen	negative	negative	medium risk
3f	mutagen	negative	negative	medium risk
3g	Non-mutagen	negative	negative	medium risk
3h	mutagen	negative	positive	medium risk
3i	mutagen	negative	positive	medium risk
3j	Non-mutagen	negative	negative	medium risk
3k	Non-mutagen	negative	positive	medium risk
3l	mutagen	negative	negative	medium risk

3m	mutagen	negative	negative	low risk
3n	Non-mutagen	negative	negative	medium risk
3o	mutagen	negative	positive	medium risk
3p	mutagen	negative	positive	medium risk
3q	non-mutagen	negative	negative	medium risk
3r	mutagen	negative	negative	medium risk
3s	non-mutagen	negative	negative	high risk
3t	mutagen	negative	negative	low risk
3u	mutagen	negative	positive	high risk
3v	mutagen	negative	negative	high risk
3w	mutagen	negative	negative	high risk
3x	mutagen	negative	negative	high risk
3y	Non-mutagen	negative	negative	medium risk
3z	Non-mutagen	negative	negative	ambiguous
3aa	Non-mutagen	negative	negative	ambiguous
3ab	Non-mutagen	negative	negative	low risk

3ac	Non-mutagen	negative	negative	ambiguous
3ad	mutagen	negative	negative	ambiguous
3ae	Non-mutagen	negative	negative	low risk
3af	Non-mutagen	negative	negative	low risk
3ag	Non-mutagen	negative	negative	low risk
3ah	Non-mutagen	negative	negative	ambiguous
3ai	mutagen	negative	negative	ambiguous

Table 11. PROTOX II RESULTS

Compound No	Predicted LD50 mg/kg	Predicted toxicity class	Carcinogenicity	Immunotoxicity	Mutagenicity	Cytotoxicity
3a	1000	4	Active	Inactive	Inactive	Inactive
3b	1100	4	Active	Inactive	Inactive	Inactive
3c	500	4	Active	Inactive	Inactive	Inactive
3d	1000	4	Active	Inactive	Inactive	Inactive

3e	2300	5	Inactive	Inactive	Inactive	Inactive
3f	1000	4	Inactive	Inactive	Inactive	Inactive
3g	2600	5	Inactive	Inactive	Inactive	Inactive
3h	1000	4	Inactive	Inactive	Inactive	Inactive
3i	1000	4	Inactive	Inactive	Inactive	Inactive
3j	2900	5	Inactive	Inactive	Inactive	Inactive
3k	1000	4	Inactive	Inactive	Inactive	Inactive
3l	1000	4	Inactive	Inactive	Inactive	Inactive
3m	1500	4	Inactive	Inactive	Inactive	Inactive
3n	2200	5	Inactive	Inactive	Inactive	Inactive
3o	1000	4	Active	Inactive	Active	Inactive
3p	1000	4	Active	Active	Active	Inactive
3q	1000	4	Active	Inactive	Inactive	Inactive
3r	1000	4	Active	Inactive	Inactive	Inactive
3s	1000	4	Active	Active	Inactive	Inactive
3t	1500	4	Active	Active	Active	Inactive

3u	1000	4	Active	Active	Active	Inactive
3v	1000	4	Inactive	Inactive	Inactive	Inactive
3w	500	4	Active	Active	Inactive	Inactive
3x	1000	4	Active	Inactive	Inactive	Inactive
3y	3000	5	Inactive	Inactive	Inactive	Inactive
3z	1500	4	Inactive	Inactive	Inactive	Active
3aa	1500	4	Inactive	Inactive	Inactive	Inactive
3ab	1500	4	Inactive	Inactive	Inactive	Inactive
3ac	1500	4	Inactive	Inactive	Inactive	Active
3ad	1500	4	Inactive	Active	Active	Inactive
3ae	1500	4	Inactive	Active	Inactive	Inactive
3af	1500	4	Inactive	Inactive	Inactive	Inactive
3ag	1500	4	Inactive	Inactive	Inactive	Inactive
3ah	1500	4	Inactive	Inactive	Inactive	Inactive
3ai	1500	4	Active	Active	Active	Inactive

6.4. DOCKING RESULTS

By *insilico* docking, the target conformation and orientation of the ligand and target (enzyme or receptor) are predicted. It is a two-step process; first, information about the different conformations of ligands in the active site of proteins is collected, and then, based on the score function for each orientation, these conformations are ranked in order of binding affinity. In addition to scanning the entire target protein for binding sites, Blind Docking also optimizes the conformation of ligands. The PDB structure used for docking is WaaC/ Hep I pdb id: 2H1F.

In order to verify docking, the co-crystalline ADP was re-docked on the active surface. **Figure 10.** shows the superimposed structure of HEP I crystallized with ADP and its re-docking position with HEP I. As shown in figure 10, the molecule ADP goes to the same site as its crystal structure and is almost overlapping it. **Table 12** provides binding energy and residues that interact with each compound according to its best pose. Interestingly, molecule 3e with binding affinity of has hydrogen bond interaction with Ala77 and Asn302, π -charge interactions with Ala84, Ile287, Leu286 and Pro56 residues and the -8.3 kcal/mol. Similarly, the molecule 3g, 3j, 3n and 3y have a good interaction with residues and having binding affinity -8.1 kcal/mol, -8.2 kcal/mol, -8.6kcal/mol, and -8.6 kcal/mol respectively. The molecule 3g showed hydrogen bond interaction with Asn302, Pro56 from two aza groups in thiadiazole ring and N-1 group of Benzimidazole respectively. The residues Ala77, Pro281, and Asn302 formed hydrogen bond with anaza group, amino group in thiadiazole, and carbonyl group respectively, in the molecule 3j. Totally five hydrogen bond interactions were seen molecule 3n with amino acid residues Arg61, Glu39, Glu303, Gln306 and Gly301. And Three Hydrogen bonds were formed to same residue- Arg298, with two nitrogen groups of thiadiazole and carbonyl group. Pi-sulfur interaction was also seen in molecule 3y with Phe315 to thio group.

Apart from these all the analysed molecules showed corresponding vanderwaals interactions. Finally, the standard drug streptomycin of binding affinity showed six hydrogen bond interaction with aminoacids Ser46, Arg298, Val296, Glu245, His168, Glu318. In both molecule 3y and streptomycin, the residue Arg298 behaves similarly by

forming H-bond, suggesting inhibition of LPS synthesis. The 3D and 2D interaction plot of compound 3e, 3g, 3j, 3n, and 3y were shown in **Figure. 12, 13 and 14.**

Table 12. Binding affinities with interacting residues

Compounds	Binding affinity Kcal/mol	Interacting residues (distance in Å) H-bond interaction
3e	-8.3	Asn302 (2.07), Ala77 (2.18)
3g	-8.1	Pro56 (2.63), Asn302 (2.52, 2.70)
3j	-8.2	Asn302 (2.09), Ala77 (2.34), and Pro281 (2.55)
3n	-8.6	Gln306 (2.05), Arg61 (3.05), Gly301 (2.58), Glu303 (2.00), and Glu39 (2.66)
3y	-8.6	Arg298 (2.43, 1.91 and 1.94)
Streptomycin	-8.4	Arg298 (2.41, 2.96), His168 (2.23), Glu245 (2.29), Glu318 (2.63), Ser46 (2.72, 2.41) Val296 (2.44) and Glu52 (2.15)
Validation	-7.4	Lys192 (2.45), Met11 (2.15), Thr262 (2.20), Gly263 (2.23, 2.76), Leu264 (2.40) and Asp261 (2.53)

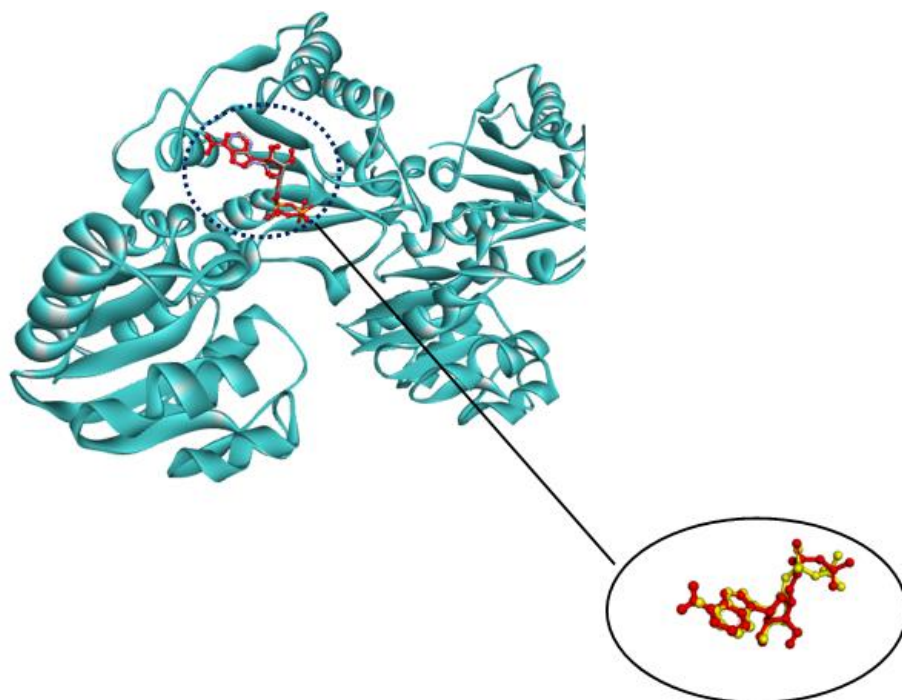
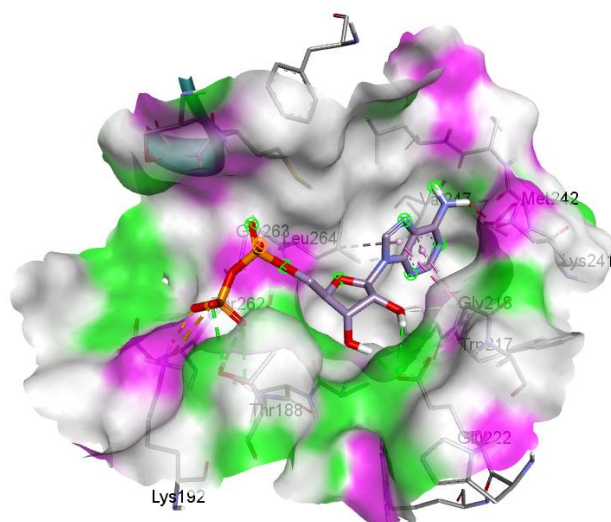


Figure 10. The superimposed image of co-crystallized ligand ADP (yellow) and redocking pose of ADP (red) with HEP I.

(A)



(B)

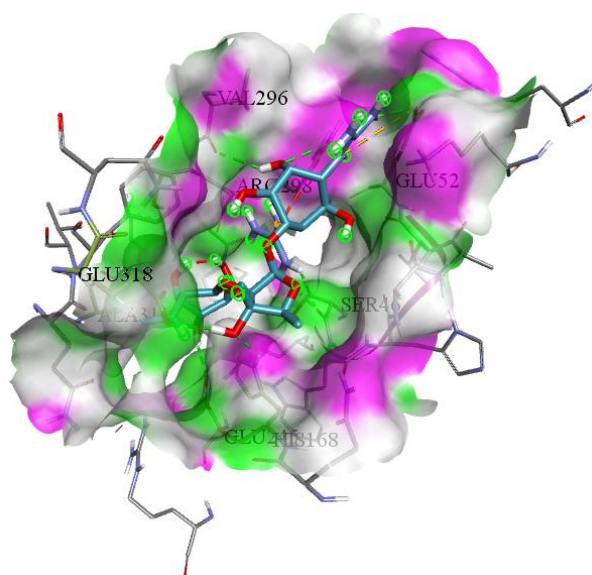


Figure 11. 3D interaction of co-crystallized ligand (A) and Streptomycin (B)

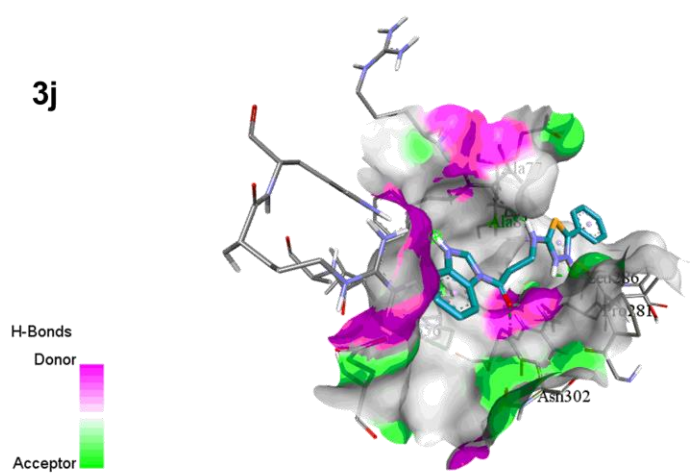
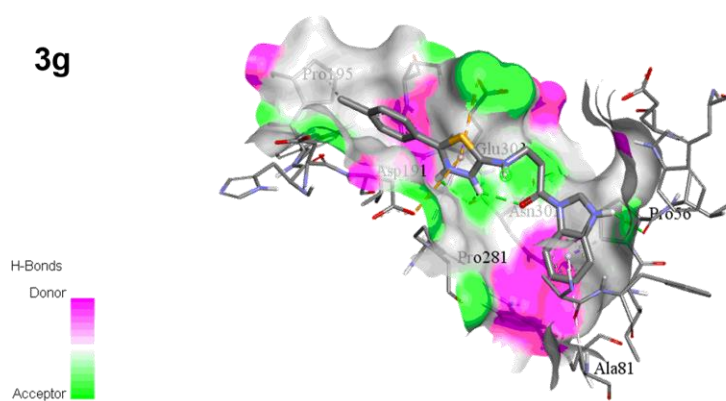
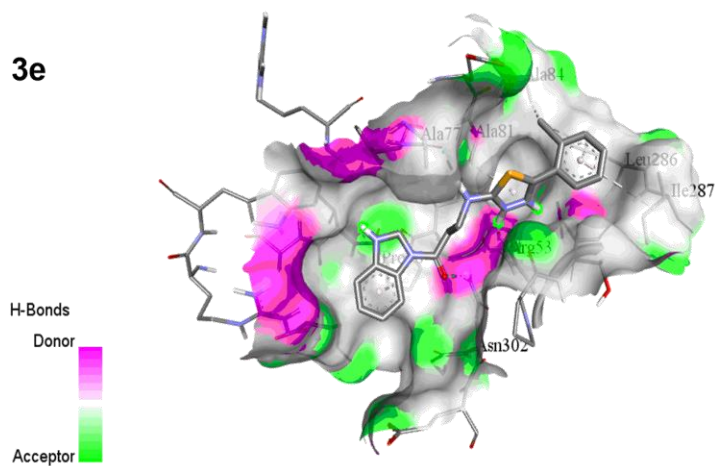


Figure 12. 3D interactions of compounds 3e, 3g and 3j.

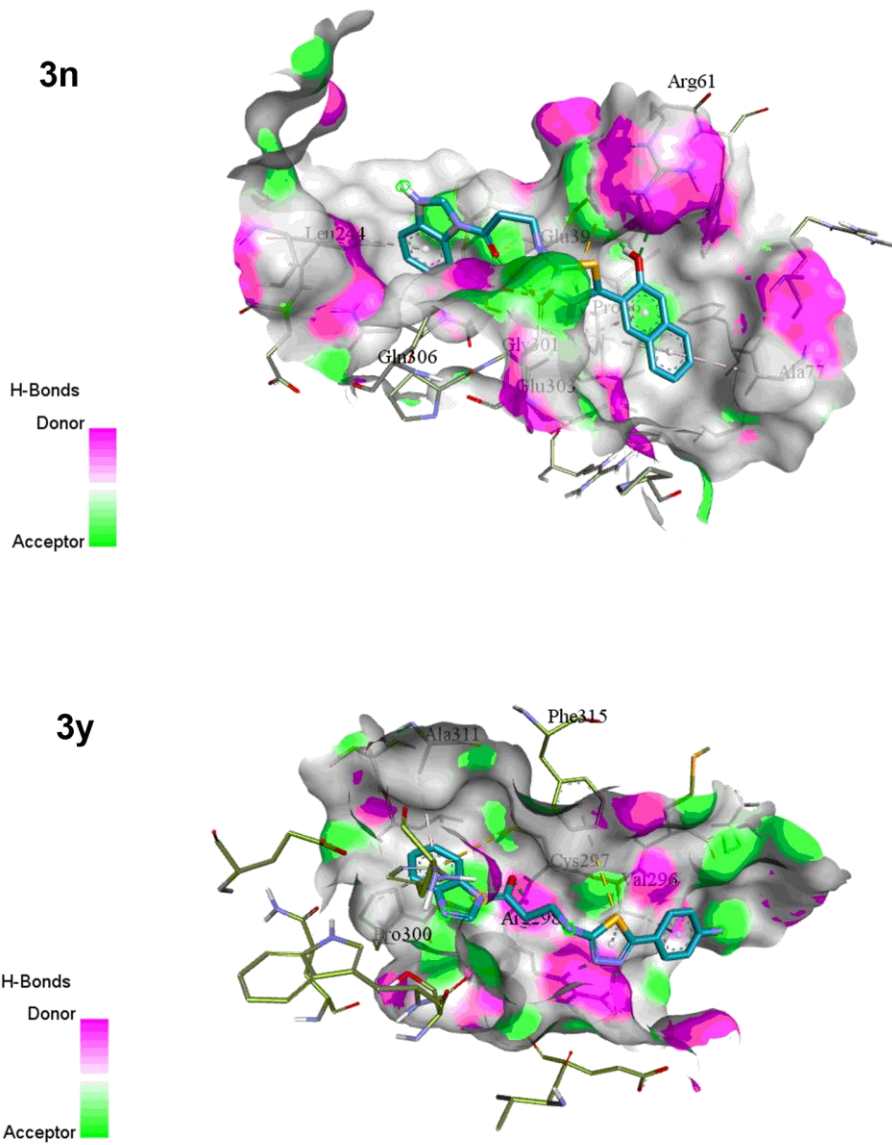


Figure 13. 3D interactions of compounds 3n, 3y.

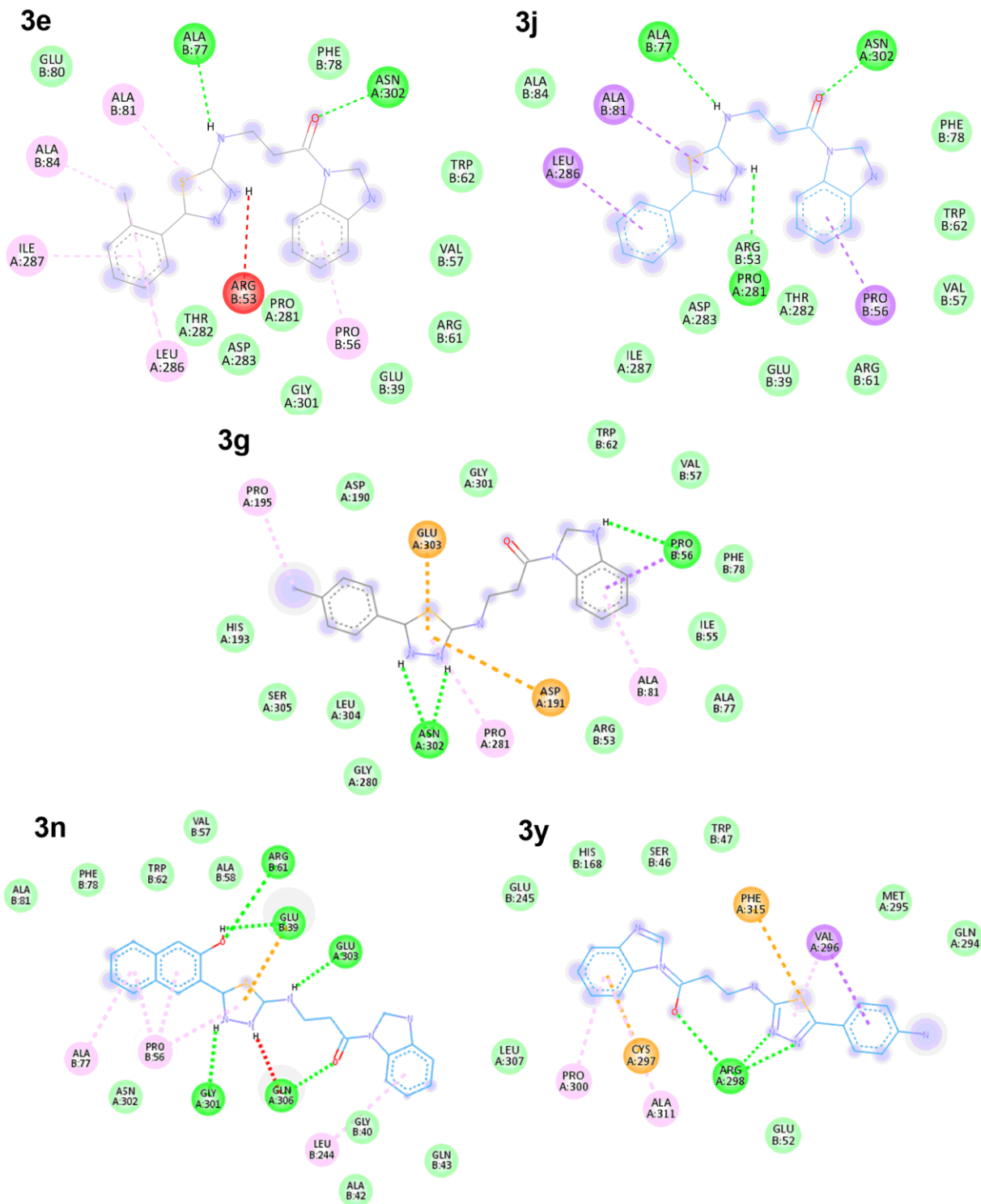


Figure 14.2D interactions of compounds 3e, 3g, 3j, 3n and 3y.

6.5. SYNTHESIS

The schematic representation for the synthesis of Mannich bases is represented in **Figure 5-scheme 1**. Mannich bases were synthesized by reaction of different thiadiazoles containing amines (2a-2ai) with active hydrogen compound (1-acetyl benzimidazole) in formaldehyde at ambient temperature and at microwave yielded the desired compounds. The yield of the synthesized compounds ranges from 70-85%.

6.6. CHARACTERISATION

All the compounds were characterized by IR, ¹H and ¹³C NMR, MS, and elemental analysis. The IR spectra of synthesized compounds showed absorption bands due to stretching vibrations of N-H, C=O and C-N at 3209-3315 cm⁻¹, 1734-1750 cm⁻¹ and 1265-1272 cm⁻¹ respectively. The strong absorption peak at 1396 cm⁻¹ is due the presence of CH₂ group. The mass spectrum showed molecular ion peak which was in agreement with molecular mass of compound while the base peak was observed at 145 (100%).

Synthesis of 1-(1H-benzo[d]imidazol-1-yl)-3-((5-(2-chlorophenyl)-1,3,4-thiadiazol-2-yl)amino)propan-1-one (3e):

In a solution of 1-acetyl benzimidazole (0.01 mol, 1.6g,) in ethanol (10mL), were added formaldehyde (0.11 mole, 1 ml) and appropriate amines **2e** (0.11 mol). The mixture was heated in microwave at the power of 300 watts for 10 min. The mixture was kept overnight in refrigeration. The product thus obtained was filtered and recrystallized using aqueous ethanol to yield pure products.

Orange solid; Yield: 79.3%; mp: 180-183°C FT-IRFT-IR(KBr, cm⁻¹): 3095.23(Ar C-H str), 3315.21(NH), 1432.59(Ar C-C str), 1686.58(C=N),646.70 (C-S str), 1527.82(C=C), 1759.54(C=O str),1275.56(C-N thiadiazole), 757.41(CH oop), 2920.25 (aliphatic CH str), 854.25(C-Cl),M+ calcd for C₁₈H₁₄ClN₅O₂S is 383.85 found: 382.34. Anal. Calcd. for C₁₈H₁₄ClN₅O₂S (%): C, 56.27; H, 3.64; N, 18.24 ; O, 4.17; S, 8.34; Cl, 9.24 found: C, 56.50; H, 3.66; N, 18.31, O, 4.18; S, 8.37; Cl, 9.27.

Synthesis of 1-(1H-benzo[d]imidazol-1-yl)-3-((5-(4-chlorophenyl)-1, 3, 4-thiadiazol-2-yl) amino) propan-1-one (3g):

In a solution of 1-acetyl benzimidazole (0.01 mol, 1.6g,) in ethanol (10mL), were added formaldehyde (0.11 mole, 1 ml) and appropriate amines **2g** (0.11 mol). The mixture was heated in microwave at the power of 300 watts for 10 min. The mixture was

kept overnight in refrigeration. The product thus obtained was filtered and recrystallized using aqueous ethanol to yield pure products.

Orange solid; Yield: 85.3%; mp: 181-185°C, FT-IR(Kerr, cm⁻¹): 3123 (Ar C-H str), 3209.61(NH), 1480, 1595(Ar C-C str), 1672.72(C=N),688.19 (C-S str), 1527.67(C=C), 1734.33(C=O str),1266.88(C-N thiadiazole), 737.18(CH oop), 2922.79 (aliphatic CH str), 828.93 (C-Cl),¹H NMR: δ 2.508 (2H, t, *J* = 6.5 Hz), 4.215 (2H, t, *J* = 6.5 Hz), 7.28-7.88, 8.42 (1H, t, *J* = 0.5 Hz), M⁺ calcd for C₁₈H₁₄ClN₅O₂S is 383.85 found: 382.34. Anal. Calcd. For C₁₈H₁₄ClN₅O₂S (%): C, 56.27; H, 3.64; N, 18.24 ; O, 4.17; S, 8.34; Cl, 9.24 found: C, 56.50; H, 3.66; N, 18.31, O, 4.18; S, 8.37; Cl, 9.27.

Synthesis of 1-(1H-benzo[d]imidazol-1-yl)-3-((5-(4-bromophenyl)-1,3,4-thiadiazol-2-yl)amino)propan-1-one (3j):

In a solution of 1-acetyl benzimidazole (0.01 mol, 1.6g,) in ethanol (10mL), were added formaldehyde (0.11 mole, 1 ml) and appropriate amines **2j** (0.11 mol). The mixture was heated in microwave at the power of 300 watts for 10 min. The mixture was kept overnight in refrigeration. The product thus obtained was filtered and recrystallized using aqueous ethanol to yield pure products.

Yellowish white solid; Yield: 75.1%; mp:183-186°C, FT-IR(KBr, cm⁻¹): 3090.63(Ar C-H str), 3209.61(NH), 1583.58(Ar C-C str), 1671.31(C=N),685.69(C-S str), 1583.58(C=C), 1734.33(C=O str),1276.55(C-N thiadiazole),848.83(CH oop), 2970.38 (aliphatic CH str), 543.49 (C-Br),

Synthesis of 1-(1H-benzo[d]imidazol-1-yl)-3-((5-(3-hydroxynaphthalen-2-yl)-1, 3, 4-thiadiazol-2-yl) amino) propan-1-one (3n):

In a solution of 1-acetyl benzimidazole (0.01 mol, 1.6g,) in ethanol (10mL), were added formaldehyde (0.11 mole, 1 ml) and appropriate amines **2n** (0.11 mol). The mixture was heated in microwave at the power of 300 watts for 10 min. The mixture was

kept overnight in refrigeration. The product thus obtained was filtered and recrystallized using aqueous ethanol to yield pure products.

Pale yellow solid; Yield: 70.4%; mp: 178-183°C, FT-IR(KBr, cm⁻¹): 3058.61(Ar C-H str), 3323.41(NH), 1450.01(Ar C-C str), 1647.77(C=N),688.24(C-S str), 1510.88(C=C), 1769.26(C=O str),1203.57(C-N thiadiazole),741.56(CH oop), 3540.23 (OH),

Synthesis of 3-((5-(4-aminophenyl)-1, 3, 4-thiadiazol-2-yl) amino)-1-(1H-benzo[d]imidazol-1-yl) propan-1-one (3y):

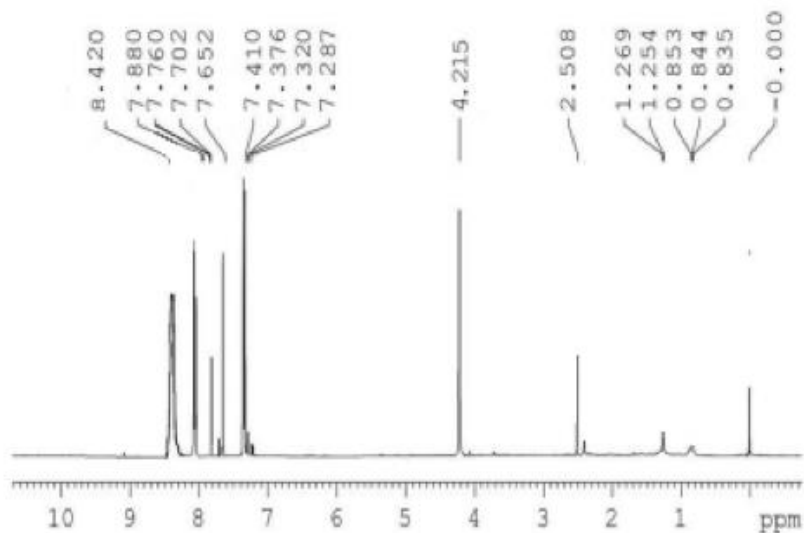
In a solution of 1-acetyl benzimidazole (0.01 mol, 1.6g,) in ethanol (10mL), were added formaldehyde (0.11 mole, 1 ml) and appropriate amines **2y** (0.11 mol). The mixture was heated in microwave at the power of 300 watts for 10 min. The mixture was kept overnight in refrigeration. The product thus obtained was filtered and recrystallized using aqueous ethanol to yield pure products.

Yellowish green solid; Yield: 70.4%; mp: 185-187°C, FT-IR(KBr, cm⁻¹): 3105.63 (Ar C-H str), 3271(NH), 1602.57(Ar C-C str), 1655.18(C=N),678.07(C-S str), 1504.87(C=C), 1750.03(C=O str),1248.84(C-N thiadiazole),830.99(CH oop), 2915.27(aliphatic CH str), 3442,3360 (primary amine stretch),M⁺ calcd for C₁₈H₁₆N₆O₂S is 364.42 found: 363.34. Anal. Calcd. for C₁₈H₁₆N₆O₂S (%): C, 59.27; H, 4.39; N,23.09; O, 4.39; S, 8.78; found: C, 59.45; H, 4.40; N, 23.11; O, 4.40; S, 8.81.

¹H NMR data:

3g

Signature SIF VIT VELLORE
3G



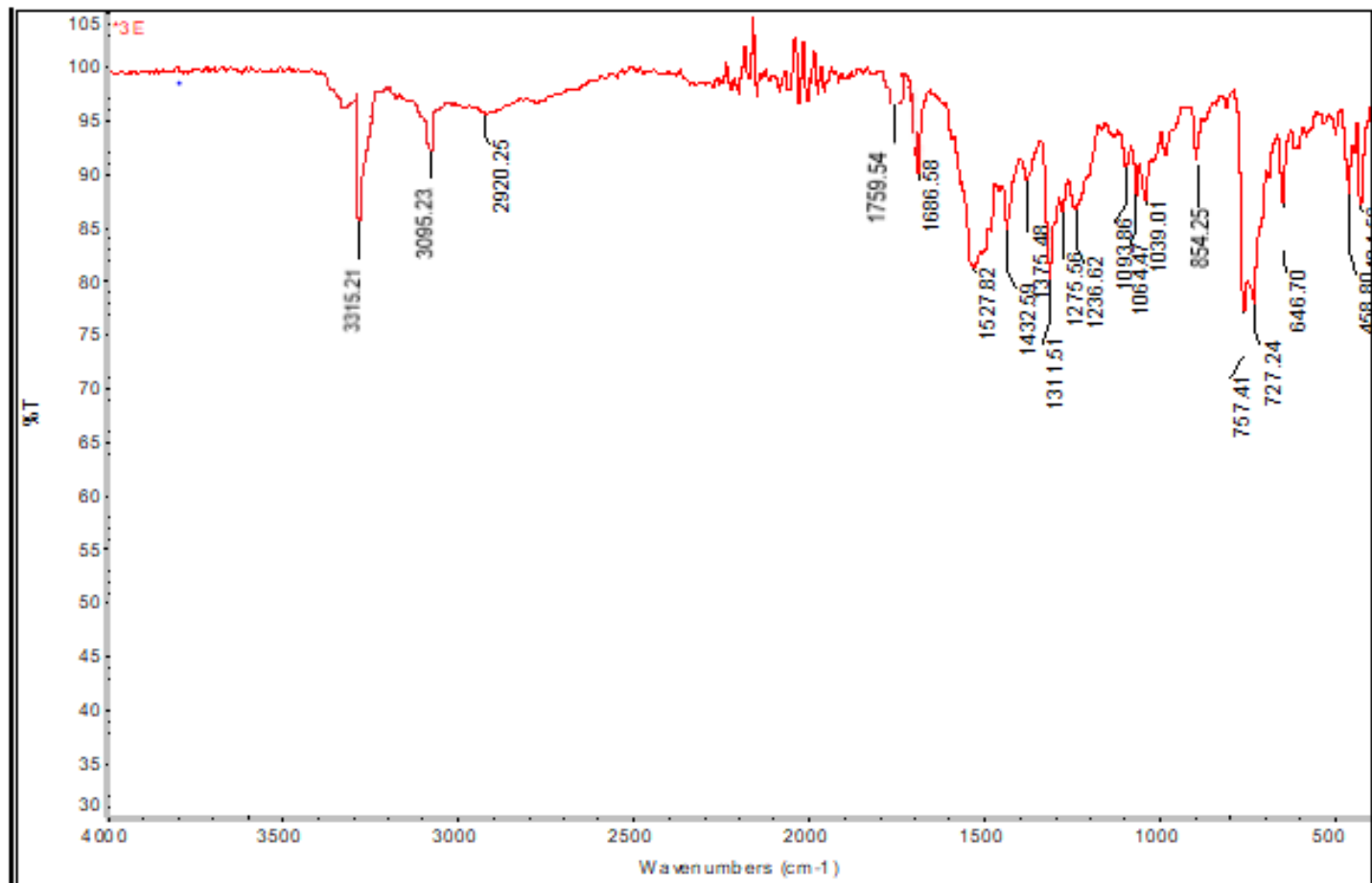
Current Data Parameters
NAME EXT40322
EXPNO 30
PROCNO 1

F2 - Acquisition Parameters
Date_ 20220303
Time 18.22 h
INSTRUM spect
PROBHD Z108618_0505 (
PULPROG zg30
TD 65536
SOLVENT DMSO
NS 32
DS 2
INH 8012.820 Hz
FIDRES 0.244532 Hz
AQ 4.0894465 sec
RG 199.6
DW 62.400 usec
DE 6.50 usec
TE 297.0 K
D1 1.00000000 sec
TDO 1
SFO1 400.2604716 MHz
NUC1 1H
P1 14.07 usec
PLW1 16.00000000 W

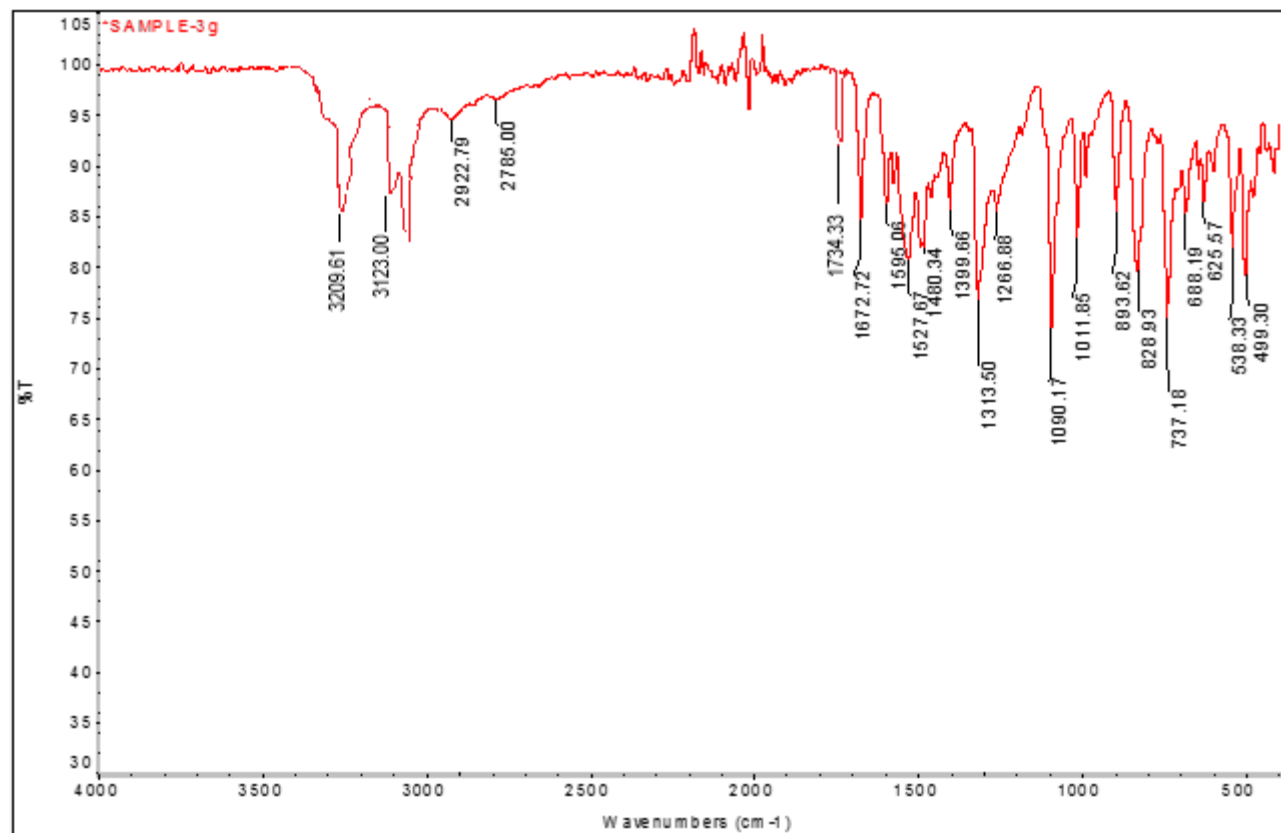
F2 - Processing parameters
SI 65536
SF 400.2580000 MHz
WDW EM
SSB 0
LB 0.30 Hz
GB 0
PC 1.00

IR Spectra data:

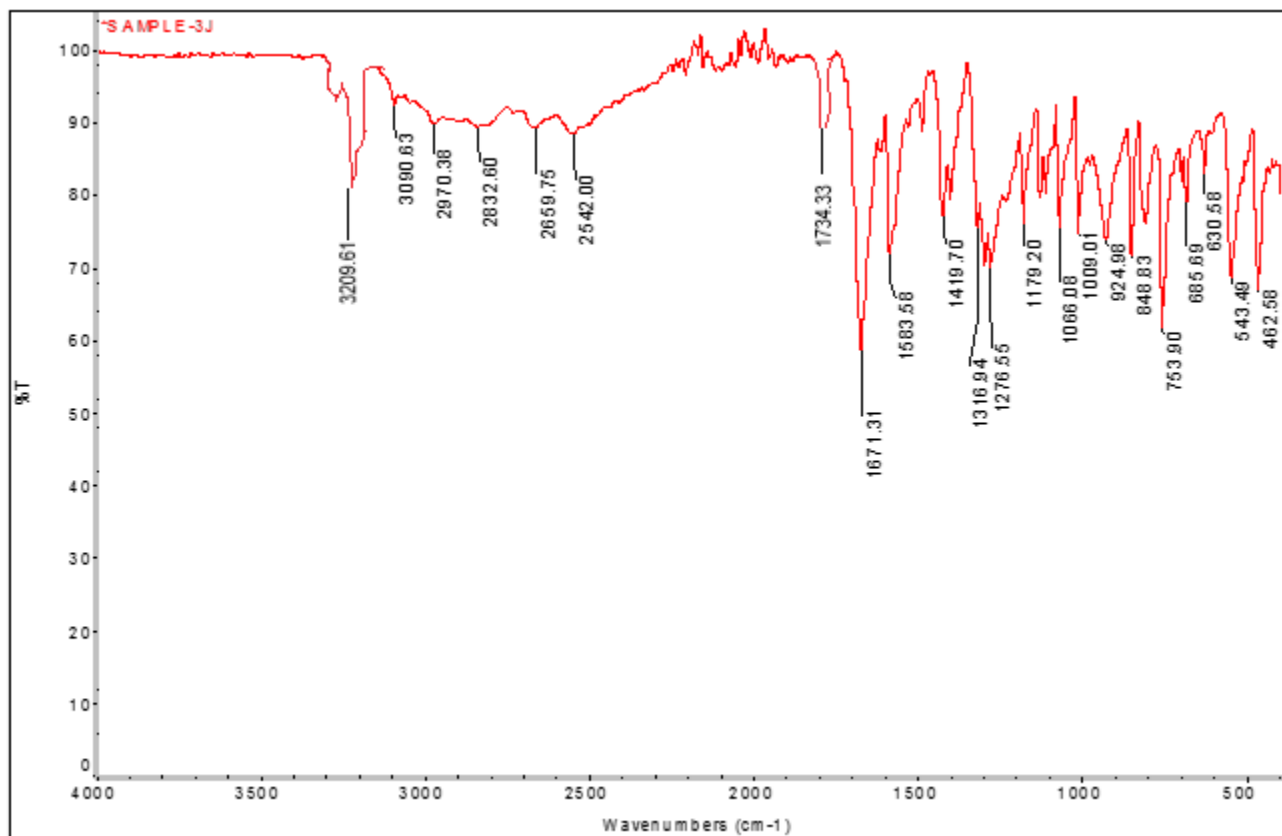
3e



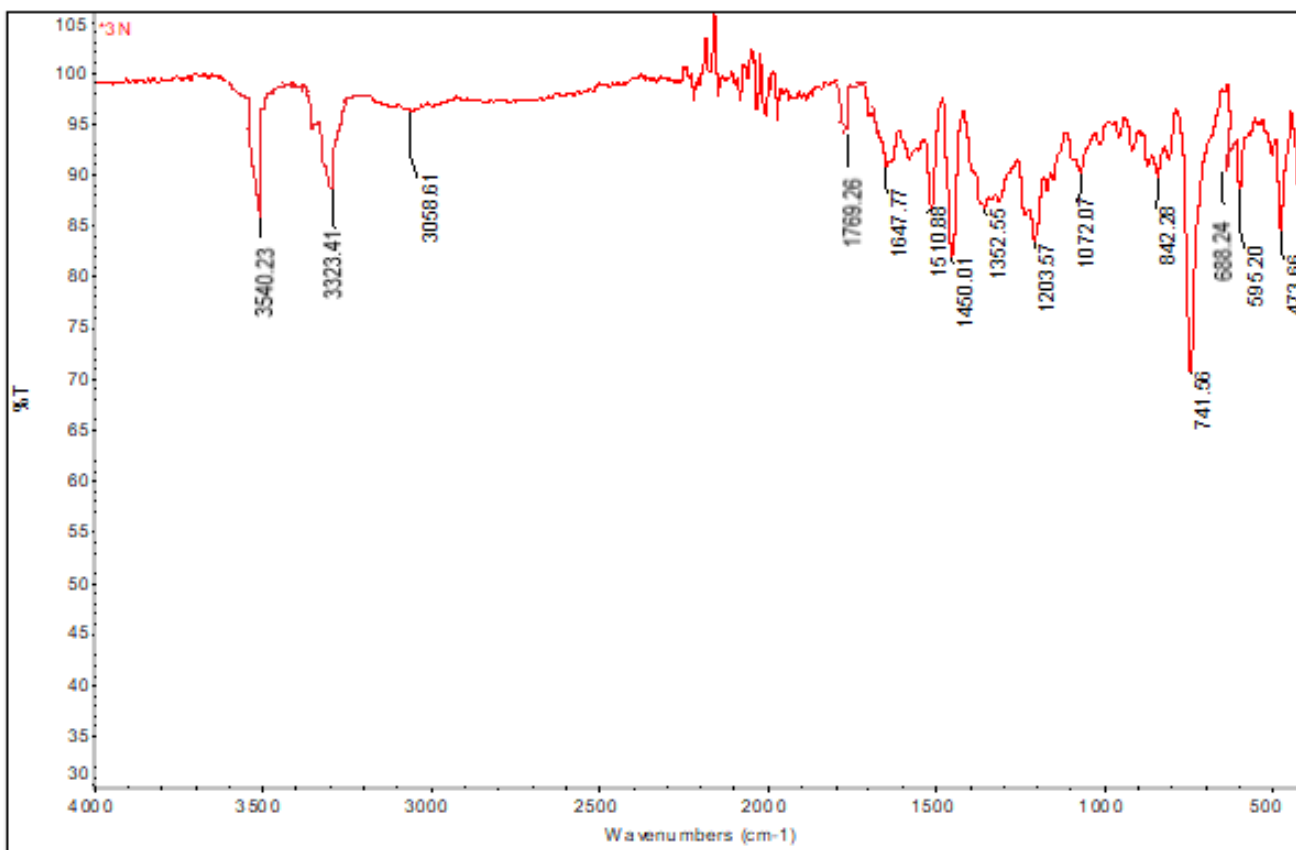
3g



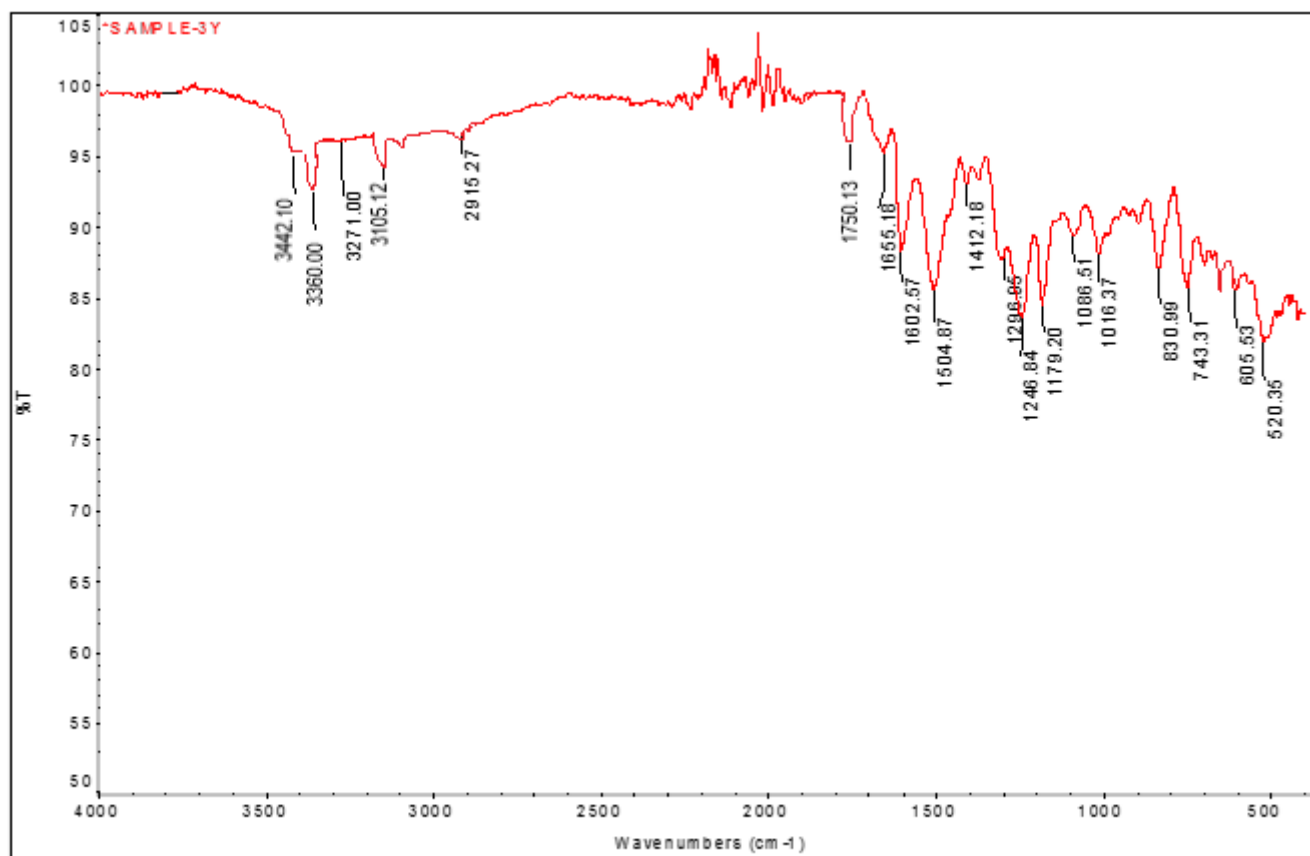
3j



3n

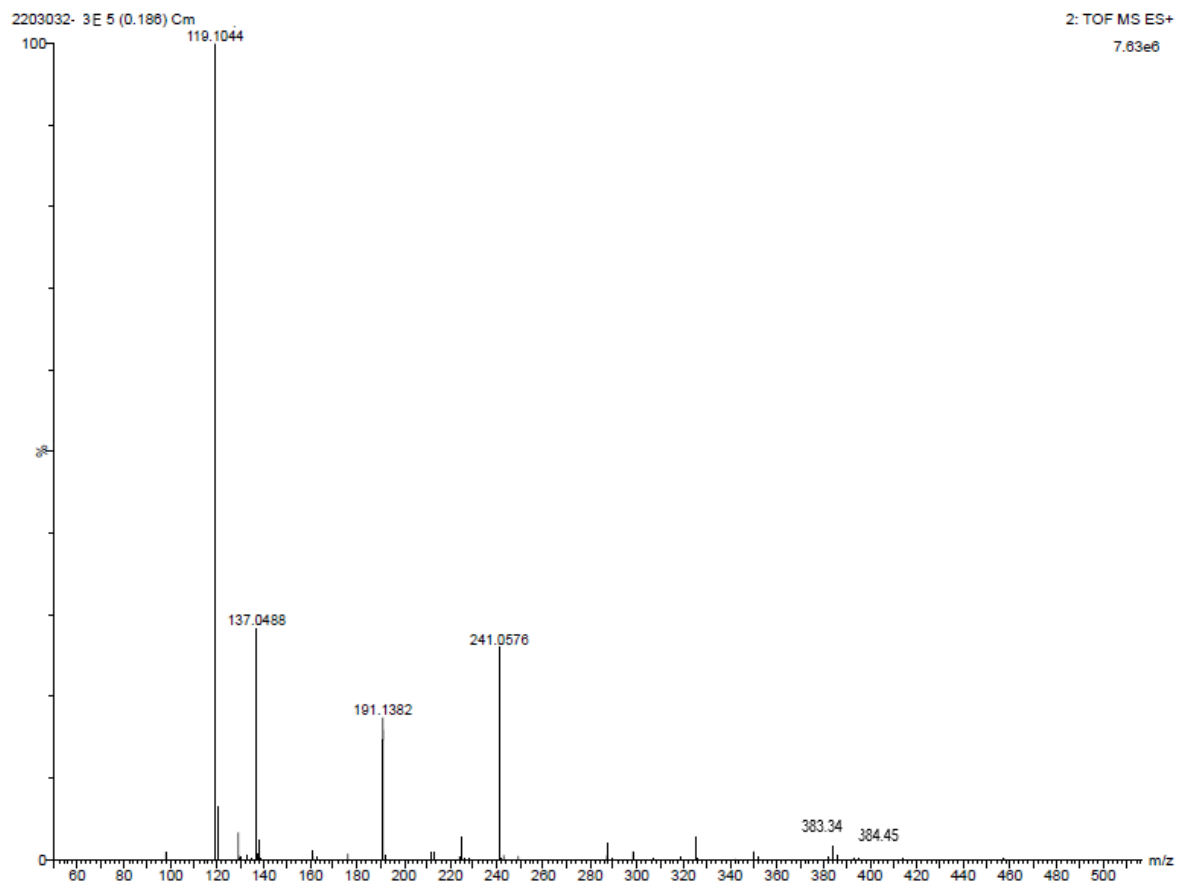


3y

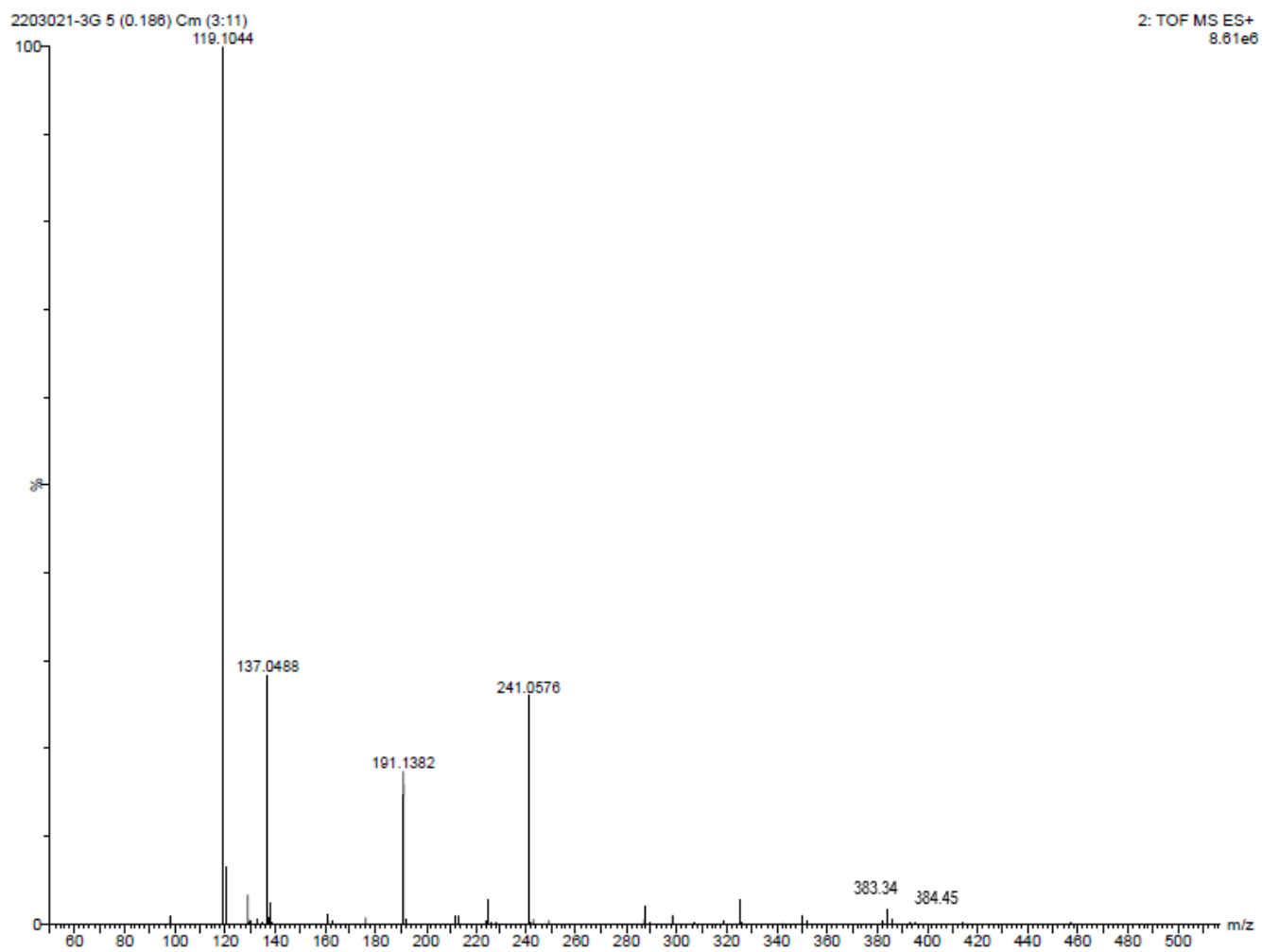


Mass Spectra:

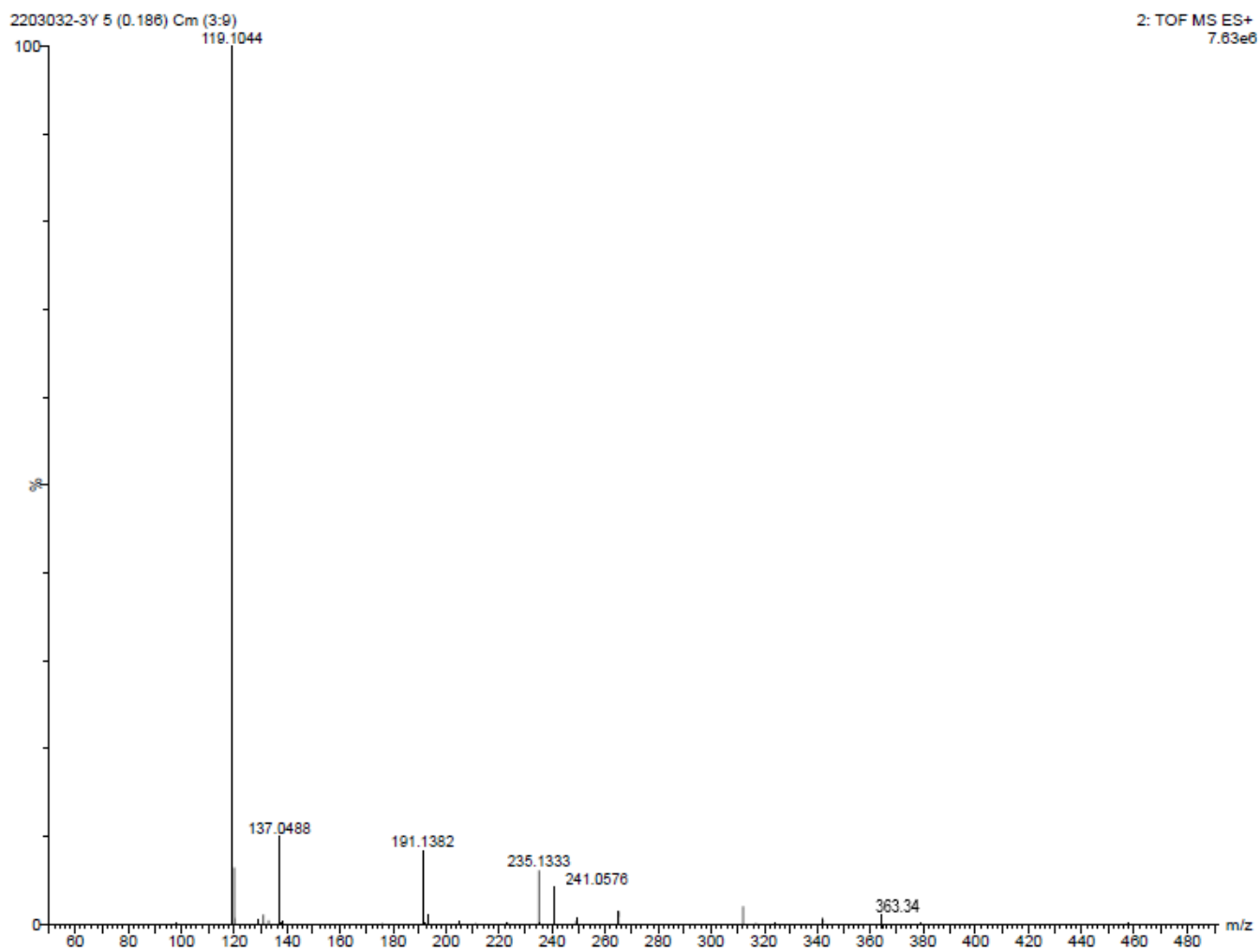
3e



3g



3y



6.7. Biological Studies:

The synthesized compounds have been subjected to antibacterial activity through Agar well diffusion method (zone of inhibition) using gentamycin as positive control for *E.coli*-443 strain.

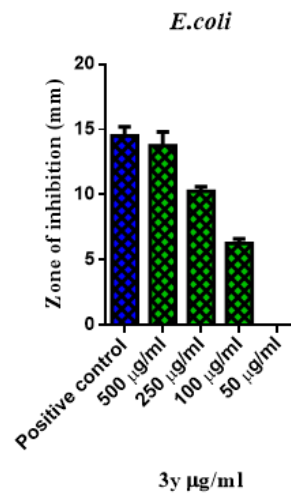
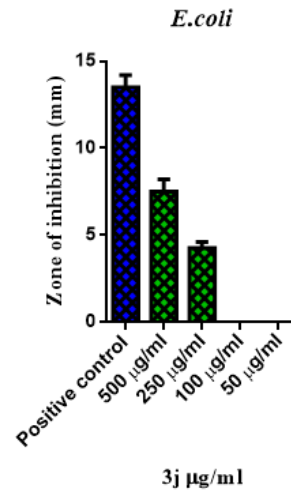
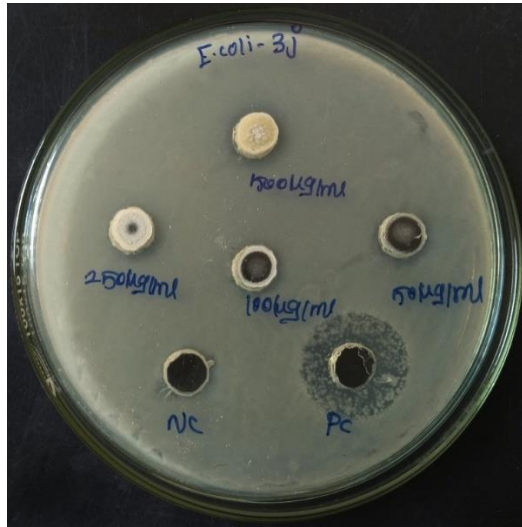
Among tested compounds, p-amino substituted compound **3y** showed potent activity of 13.75 ± 1.06 (500 $\mu\text{g/ml}$) compared to standard gentamycin against *E.coli*. The two compounds **3e** (2-Cl) and **3n** (3-OH-2-naphthyl) produced moderate potency of 11.25 ± 0.35 and 11.5 ± 0.7 in 500 $\mu\text{g/ml}$ respectively. Other compounds exhibited lesser activity than gentamycin against *E.coli*. The electron donating group substituted compounds (-OH, -NH₂) showed good cytotoxic activity compared to electron withdrawing group substituted compounds except ortho-chloro substituted compound. Only compound 3n showed bacterial inhibition in all the four concentrations against *E.coli*. The antibacterial activity results are given in **Table 13**. The effects of results were depicted in following **figures**. The results of *in vitro* antibacterial activity were in agreement with *in silico*docking studies.

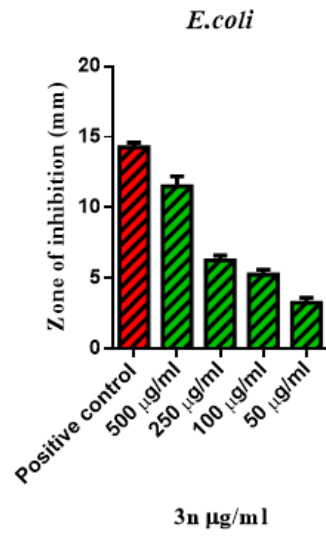
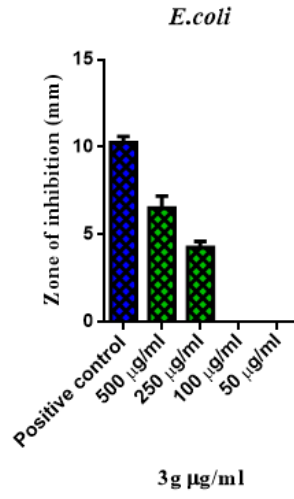
The results of compound 3y against quinolone-resistant *E.coli* strain showed an average bacterial inhibition of 10.25 ± 0.35 at 500 $\mu\text{g/ml}$.

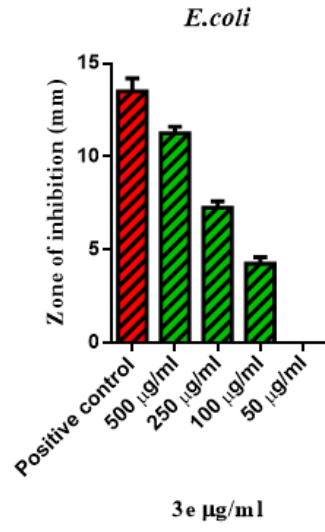
Table 13. SD± Means of zone of inhibition obtained by sample 3j, 3g and 3y against *E.coli*.

S. No	Name of the test organism	Name of the test sample	Zone of inhibition (mm) SD ± Mean				
			500 µg/ml	250 µg/ml	100 µg/ml	50 µg/ml	PC
1.	<i>E.coli</i>	3j	7.5±0.7	4.25±0.35	0	0	13.5±0.7
2.		3y	13.75±1.06	10.25±0.35	6.25±0.35	0	14.5±0.7
3.		3g	6.5±0.7	4.25±0.35	0	0	10.25±0.35
4.		3e	11.25±0.35	7.25±0.35	4.25±0.35	0	13.5±0.7
5.		3n	11.5±0.7	6.25±0.35	5.25±0.35	3.25±0.35	14.25±0.35
6.	Quinolone-resistant <i>E.coli</i>	3y	10.25±0.35	7.25±0.35	4.25±0.35	0	13.5±0.7

Figure 15. Effect of samples against *E.coli*.







7. CONCLUSION:

A quantitative analysis of the structure activity relationship (QSAR) was performed on a data set of 33 compounds of substituted benzimidazole as antibacterial agents against *E.coli*. The 2D-QSAR model for a series was established using multiple linear regression (MLR) methods that yielded a regression model with good predictive power. The predictability of the proposed models was demonstrated by various methods, including cross-validation, external evaluation, the root-mean-square error (RMSE) and Williams plot. All of these results showed the good statistical parameters of models to predict the activity for developing new compounds as antibacterial agents.

The developed 2D-QSAR model expressed by equation 2 was used to predict the biological activity (pMIC) of newly designed Benzimidazole-1, 3, 4-thiadiazole derivatives as antibacterial agent's against *E.coli*. From the results, three designed compounds 3y, 3e, 3n, can act as potential antibacterial agents against *E.coli*. The results were acceptable giving significance to model equation descriptors supporting QSAR studies. Thus, computer aided drug design is required to design new compounds before synthesis, thus reducing the cost by filtering the compounds. From the docking results, compounds with good docking score has been synthesized, characterized and subjected to antibacterial activity. The results of antibacterial study explain that the synthesized active compound could serve as intermediate for generating good biological agents.

8. BIBLIOGRAPHY

1. Serban G, Stanasel O, Serban E, Bota S. 2-Amino-1, 3, 4-thiadiazole as a potential scaffold for promising antimicrobial agents. *Drug design, development and therapy*. 2018;12:1545.
2. Pandey A, Rajavel R, Chandraker S, Dash D. Synthesis of Schiff bases of 2-amino-5-aryl-1, 3, 4-thiadiazole and its analgesic, anti-inflammatory and anti-bacterial activity. *E-Journal of Chemistry*. 2012 Jan 1; 9(4):2524-31.
3. Fascio ML, Sepúlveda CS, Damonte EB, D'Accorso NB. Synthesis and antiviral activity of some imidazo [1, 2-b] [1, 3, 4] thiadiazole carbohydrate derivatives. *Carbohydrate research*. 2019 Jul 1; 480:61-6.
4. Sharma R, Misra GP, Sainy J, Chaturvedi SC. Synthesis and biological evaluation of 2-amino-5-sulfanyl-1, 3, 4-thiadiazole derivatives as antidepressant, anxiolytics and anticonvulsant agents. *Medicinal chemistry research*. 2011 Mar; 20(2):245-53.
5. Kaur G, Silakari O. Benzimidazole scaffold based hybrid molecules for various inflammatory targets: Synthesis and evaluation. *Bioorganic chemistry*. 2018 Oct 1; 80:24-35.
6. Cozza G, Girardi C, Ranchio A, Lolli G, Sarno S, Orzeszko A, Kazimierczuk Z, Battistutta R, Ruzzene M, Pinna LA. Cell-permeable dual inhibitors of protein kinases CK2 and PIM-1: structural features and pharmacological potential. *Cellular and Molecular Life Sciences*. 2014 Aug; 71(16):3173-85.
7. Lavrador-Erb K, Ravula SB, Yu J, Zamani-Kord S, Moree WJ, Petroski RE, Wen J, Malany S, Hoare SR, Madan A, Crowe PD. The discovery and structure–activity relationships of 2-(piperidin-3-yl)-1H-benzimidazoles as selective, CNS penetrating H1-antihistamines for insomnia. *Bioorganic & medicinal chemistry letters*. 2010 May 1; 20(9):2916-9.
8. Seenaiyah D, Reddy PR, Reddy GM, Padmaja A, Padmavathi V. Synthesis, antimicrobial and cytotoxic activities of pyrimidinylbenzoxazole, benzothiazole

- and benzimidazole. *European Journal of Medicinal Chemistry*. 2014 Apr 22; 77:1-7.
9. Muñoz-Patiño N, Sánchez-Eguía BN, Araiza-Olivera D, Flores-Alamo M, Hernández-Ortega S, Martínez-Otero D, Castillo I. Synthesis, structure, and biological activity of bis (benzimidazole) amino thio-and selenoether nickel complexes. *Journal of Inorganic Biochemistry*. 2020 Oct 1; 211:111198.
 10. Anastassova NO, Mavrova AT, Yancheva DY, Kondeva-Burdina MS, Tzankova VI, Stoyanov SS, Shivachev BL, Nikolova RP. Hepatotoxicity and antioxidant activity of some new N, N'-disubstituted benzimidazole-2-thiones, radical scavenging mechanism and structure-activity relationship. *Arabian Journal of Chemistry*. 2018 Mar 1; 11(3):353-69.
 11. Bistrović A, Krstulović L, Stolić I, Drenjančević D, Talapko J, Taylor MC, Kelly JM, Bajić M, Raić-Malić S. Synthesis, anti-bacterial and anti-protozoal activities of amidinobenzimidazole derivatives and their interactions with DNA and RNA. *Journal of enzyme inhibition and medicinal chemistry*. 2018 Jan 1; 33(1):1323-34.
 12. Singh A, Yadav D, Yadav M, Dhamanage A, Kulkarni S, Singh RK. Molecular Modeling, Synthesis and Biological Evaluation of N-Heteroaryl Compounds as Reverse Transcriptase Inhibitors against HIV-1. *Chemical biology & drug design*. 2015 Mar; 85(3):336-47.
 13. Kumar JR, Jawahar L J, Pathak DP. Synthesis of benzimidazole derivatives: as anti-hypertensive agents. *E-Journal of chemistry*. 2006 Oct;3(4):278-85.
 14. Sadaf H, Fettouhi M, Fazal A, Ahmad S, Farooqi BA, Nadeem S, Ahmad W. Synthesis, crystal structures and biological activities of palladium (II) complexes of benzimidazole and 2-methylbenzimidazole. *Polyhedron*. 2019 Sep 15; 170:537-43.
 15. Richards ML, Lio SC, Sinha A, Tieu KK, Sircar JC. Novel 2-(substituted phenyl) benzimidazole derivatives with potent activity against IgE, cytokines, and CD23

- for the treatment of allergy and asthma. *Journal of medicinal chemistry*. 2004 Dec 16; 47(26):6451-4.
16. *Advanced Organic Chemistry: Reactions, Mechanisms, and Structure*, John Wiley & Sons, New York, NY, USA, 3rd edition, 1985.
17. Ruggiero SG, Rodrigues BL, Fernandes NG, Stefani GM, Veloso DP. 6 α , 7 β -Dihydroxyvouacapan-17 β -oic Acid. *Acta Crystallographica Section C: Crystal Structure Communications*. 1997 Jul 15; 53(7):982-4.
18. Joshi S, Khosla N, Tiwari P. In vitro study of some medicinally important Mannich bases derived from antitubercular agent. *Bioorganic & medicinal chemistry*. 2004 Feb 1; 12(3):571-6.
19. Bala S, Sharma N, Kajal A, Kamboj S, Saini V. Mannich bases: an important pharmacophore in present scenario. *International journal of medicinal chemistry*. 2014; 2014. Wieduwilt MJ, Moasser MM.
20. Bettelheim KA. Biochemical characteristics of *Escherichia coli*.
21. Edwards PR, Ewing WH. Identification of enterobacteriaceae. Identification of Enterobacteriaceae.. 1972(Third edition).
22. Russo TA, Johnson JR. Medical and economic impact of extraintestinal infections due to *Escherichia coli*: focus on an increasingly important endemic problem. *Microbes and infection*. 2003 Apr 1; 5(5):449-56.
23. Guerrant RL, Thielman NM. Types of *Escherichia coli* enteropathogens. *Infections of the Gastrointestinal Tract*. MJ Blaser, PD Smith, JI Ravdin, HB Greenberg, and RL Guerrant (eds.). Raven Press, New York. 1995:687-90.
24. Schito GC, Naber KG, Botto H, Palou J, Mazzei T, Gualco L, Marchese A. The ARESC study: an international survey on the antimicrobial resistance of pathogens involved in uncomplicated urinary tract infections. *International journal of antimicrobial agents*. 2009 Nov 1; 34(5):407-13

25. Allocati N, Masulli M, Alexeyev MF, Di Ilio C. *Escherichia coli* in Europe: an overview. *International journal of environmental research and public health*. 2013 Dec;10(12):6235-54.
26. Struyf T, Mertens K. European Antimicrobial Resistance Surveillance Network (EARS-Net Belgium) Report 2017.
27. Glasner C, Albiger B, Buist G, Andrašević AT, Canton R, Carmeli Y, Friedrich AW, Giske CG, Glupczynski Y, Gniadkowski M, Livermore DM. Carbapenemase-producing Enterobacteriaceae in Europe: a survey among national experts from 39 countries, February 2013. *Eurosurveillance*. 2013 Jul 11;18(28):20525.
28. Lee JH. Perspectives towards antibiotic resistance: from molecules to population. *Journal of Microbiology*. 2019 Mar;57(3):181-4.
29. Webber M, Piddock LJ. Quinolone resistance in *Escherichia coli*. *Veterinary research*. 2001 May 1;32(3-4):275-84.
30. Yılmaz Ç, Özcengiz G. Antibiotics: Pharmacokinetics, toxicity, resistance and multidrug efflux pumps. *Biochemical pharmacology*. 2017 Jun 1; 133:43-62.
31. Nikaido H. Molecular basis of bacterial outer membrane permeability revisited. *Microbiology and molecular biology reviews*. 2003 Dec; 67(4):593-656.
32. Ruiz N, Kahne D, Silhavy TJ. Advances in understanding bacterial outer-membrane biogenesis. *Nature Reviews Microbiology*. 2006 Jan; 4(1):57-66.
33. Gronow S, Brade H. Invited review: Lipopolysaccharide biosynthesis: which steps do bacteria need to survive? *Journal of Endotoxin Research*. 2001 Feb; 7(1):3-23.
34. Whitfield C, Trent MS. Biosynthesis and export of bacterial lipopolysaccharides. *Annual review of biochemistry*. 2014 Jun 2; 83:99-128.
35. Raetz CR, Whitfield C. Lipopolysaccharide endotoxins. *Annual review of biochemistry*. 2002 Jul; 71(1):635-700.
36. Kneidinger B, Marolda C, Graninger M, Zamyatina A, McArthur F, Kosma P, Valvano MA, Messner P. Biosynthesis pathway of ADP-l-glycero- β -d-mannoheptose in *Escherichia coli*. *Journal of Bacteriology*. 2002 Jan 15; 184(2):363-9.
37. Piek S, Kahler CM. A comparison of the endotoxin biosynthesis and protein oxidation pathways in the biogenesis of the outer membrane of *Escherichia coli*

- and *Neisseria meningitidis*. *Frontiers in cellular and infection microbiology*. 2012 Dec 20; 2:162.
38. F.A.S. Alasmay, A.M. Snelling, M.E. Zain, A.M. Alafeefy, A.S. Awaad, N. Karodia, Synthesis and Evaluation of Selected Benzimidazole Derivatives as Potential Antimicrobial Agents, *Mol. .* 20 (2015). <https://doi.org/10.3390/molecules200815206>.
39. N.T. Chandrika, S.K. Shrestha, H.X. Ngo, S. Garneau-Tsodikova, Synthesis and investigation of novel benzimidazole derivatives as antifungal agents, *Bioorg. Med. Chem.* 24 (2016) 3680–3686. <https://doi.org/10.1016/j.bmc.2016.06.010>.
40. P. Jeyakkumar, L. Zhang, S.R. Avula, C.-H. Zhou, Design, synthesis and biological evaluation of berberine-benzimidazole hybrids as new type of potentially DNA-targeting antimicrobial agents, *Eur. J. Med. Chem.* 122 (2016) 205–215. <https://doi.org/10.1016/j.ejmech.2016.06.031>.
41. H.-Z. Zhang, S.-C. He, Y.-J. Peng, H.-J. Zhang, L. Gopala, V.K.R. Tangadanchu, L.-L. Gan, C.-H. Zhou, Design, synthesis and antimicrobial evaluation of novel benzimidazole-incorporated sulfonamide analogues, *Eur. J. Med. Chem.* 136 (2017) 165–183. <https://doi.org/10.1016/j.ejmech.2017.04.077>.
42. N.S. El-Gohary, M.I. Shaaban, Synthesis, antimicrobial, antiquorum-sensing and antitumor activities of new benzimidazole analogs, *Eur. J. Med. Chem.* 137 (2017) 439–449. <https://doi.org/10.1016/j.ejmech.2017.05.064>.
43. H.-B. Liu, W.-W. GAO, V.K.R. Tangadanchu, C.-H. Zhou, R.-X. Geng, Novel aminopyrimidinyl benzimidazoles as potentially antimicrobial agents: Design, synthesis and biological evaluation, *Eur. J. Med. Chem.* 143 (2018) 66–84. <https://doi.org/10.1016/j.ejmech.2017.11.027>.
44. C. Karthikeyan, V.R. Solomon, H. Lee, P. Trivedi, Synthesis and biological evaluation of 2-(phenyl)-3H-benzo[d]imidazole-5-carboxylic acids and its methyl esters as potent anti-breast cancer agents, *Arab. J. Chem.* 10 (2017) S1788–S1794. <https://doi.org/10.1016/j.arabjc.2013.07.003>.
45. I. Abdullah, C.F. Chee, Y.-K. Lee, S.S.R. Thunuguntla, K. Satish Reddy, K. Nellore, T. Antony, J. Verma, K.W. Mun, S. Othman, H. Subramanya, N.A.

- Rahman, Benzimidazole derivatives as potential dual inhibitors for PARP-1 and DHODH, *Bioorg. Med. Chem.* 23 (2015) 4669–4680. <https://doi.org/https://doi.org/10.1016/j.bmc.2015.05.051>.
46. E. Łukowska-Chojnacka, P. Wińska, M. Wielechowska, M. Poprzeczko, M. Bretner, Synthesis of novel polybrominated benzimidazole derivatives—potential CK2 inhibitors with anticancer and proapoptotic activity, *Bioorg. Med. Chem.* 24 (2016) 735–741. <https://doi.org/https://doi.org/10.1016/j.bmc.2015.12.041>.
47. Y.-T. Wang, Y.-J. Qin, N. Yang, Y.-L. Zhang, C.-H. Liu, H.-L. Zhu, Synthesis, biological evaluation, and molecular docking studies of novel 1-benzene acyl-2-(1-methylindol-3-yl)-benzimidazole derivatives as potential tubulin polymerization inhibitors, *Eur. J. Med. Chem.* 99 (2015) 125–137. <https://doi.org/https://doi.org/10.1016/j.ejmech.2015.05.021>.
48. L. Wu, Z. Jiang, J. Shen, H. Yi, Y. Zhan, M. Sha, Z. Wang, S. Xue, Z. Li, Design, synthesis and biological evaluation of novel benzimidazole-2-substituted phenyl or pyridine propyl ketene derivatives as antitumour agents, *Eur. J. Med. Chem.* 114 (2016) 328–336. <https://doi.org/https://doi.org/10.1016/j.ejmech.2016.03.029>.
49. M.J. Akhtar, A.A. Siddiqui, A.A. Khan, Z. Ali, R.P. Dewangan, S. Pasha, M.S. Yar, Design, synthesis, docking and QSAR study of substituted benzimidazole linked oxadiazole as cytotoxic agents, EGFR and erbB2 receptor inhibitors, *Eur. J. Med. Chem.* 126 (2017) 853–869. <https://doi.org/https://doi.org/10.1016/j.ejmech.2016.12.014>.
50. T. Ma, M. Huang, A. Li, F. Zhao, D. Li, D. Liu, L. Zhao, Design, synthesis and biological evaluation of benzimidazole derivatives as novel human Pin1 inhibitors, *Bioorg. Med. Chem. Lett.* 29 (2019) 1859–1863. <https://doi.org/https://doi.org/10.1016/j.bmcl.2018.11.045>.
51. J.E. Cheong, M. Zaffagni, I. Chung, Y. Xu, Y. Wang, F.E. Jernigan, B.R. Zetter, L. Sun, Synthesis and anticancer activity of novel water soluble benzimidazole carbamates, *Eur. J. Med. Chem.* 144 (2018) 372–385. <https://doi.org/https://doi.org/10.1016/j.ejmech.2017.11.037>.
52. K. Gobis, H. Foks, M. Serocki, E. Augustynowicz-Kopec, A. Napiórkowska, Synthesis and evaluation of *in vitro* antimycobacterial activity of novel 1H-

- benzo[d]imidazole derivatives and analogues, *Eur. J. Med. Chem.* 89 (2015) 13–20. <https://doi.org/https://doi.org/10.1016/j.ejmech.2014.10.031>.
53. Y.K. Yoon, M.A. Ali, A.C. Wei, T.S. Choon, R. Ismail, Synthesis and evaluation of antimycobacterial activity of new benzimidazole aminoesters, *Eur. J. Med. Chem.* 93 (2015) 614–624. <https://doi.org/https://doi.org/10.1016/j.ejmech.2013.06.025>.
54. Y. Luo, J.-P. Yao, L. Yang, C.-L. Feng, W. Tang, G.-F. Wang, J.-P. Zuo, W. Lu, Design and synthesis of novel benzimidazole derivatives as inhibitors of hepatitis B virus, *Bioorg. Med. Chem.* 18 (2010) 5048–5055. <https://doi.org/https://doi.org/10.1016/j.bmc.2010.05.076>.
55. R. Srivastava, S.K. Gupta, F. Naaz, P.S. Sen Gupta, M. Yadav, V.K. Singh, A. Singh, M.K. Rana, S.K. Gupta, D. Schols, R.K. Singh, Alkylated benzimidazoles: Design, synthesis, docking, DFT analysis, ADMET property, molecular dynamics and activity against HIV and YFV, *Comput. Biol. Chem.* 89 (2020) 107400. <https://doi.org/https://doi.org/10.1016/j.compbiolchem.2020.107400>.
56. Y. Li, C. Tan, C. Gao, C. Zhang, X. Luan, X. Chen, H. Liu, Y. Chen, Y. Jiang, Discovery of benzimidazole derivatives as novel multi-target EGFR, VEGFR-2 and PDGFR kinase inhibitors, *Bioorg. Med. Chem.* 19 (2011) 4529–4535. <https://doi.org/https://doi.org/10.1016/j.bmc.2011.06.022>.
57. A. Bistrović, L. Krstulović, A. Harej, P. Grbčić, M. Sedić, S. Koštrun, S.K. Pavelić, M. Bajić, S. Raić-Malić, Design, synthesis and biological evaluation of novel benzimidazole amidines as potent multi-target inhibitors for the treatment of non-small cell lung cancer, *Eur. J. Med. Chem.* 143 (2018) 1616–1634. <https://doi.org/https://doi.org/10.1016/j.ejmech.2017.10.061>.
58. P. Flores-Carrillo, J.M. Velázquez-López, R. Aguayo-Ortiz, A. Hernández-Campos, P.J. Trejo-Soto, L. Yépez-Mulia, R. Castillo, Synthesis, antiprotozoal activity, and chemoinformatic analysis of 2-(methylthio)-1H-benzimidazole-5-carboxamide derivatives: Identification of new selective giardicidal and trichomonocidal compounds, *Eur. J. Med. Chem.* 137 (2017) 211–220. <https://doi.org/https://doi.org/10.1016/j.ejmech.2017.05.058>
59. M. Tonelli, E. Gabriele, F. Piazza, N. Basilico, S. Parapini, B. Tasso, R. Loddo, F. Sparatore, A. Sparatore, Benzimidazole derivatives endowed with potent

- antileishmanial activity., *J. Enzyme Inhib. Med. Chem.* 33 (2018) 210–226.
<https://doi.org/10.1080/14756366.2017.1410480>.
60. N. Escala, E. Valderas-García, M.Á. Bardón, V.C. Gómez de Agüero, R. Escarcena, J.L. López-Pérez, F.A. Rojo-Vázquez, A. San Feliciano, R. Balaña-Fouce, M. Martínez-Valladares, E. del Olmo, *Synthesis*, bioevaluation and docking studies of some 2-phenyl-1H-benzimidazole derivatives as anthelmintic agents against the nematode *Teladorsagia circumcincta*, *Eur. J. Med. Chem.* 208 (2020) 112554. <https://doi.org/10.1016/j.ejmech.2020.112554>.
61. H. Aman, N. Rashid, Z. Ashraf, A. Bibi, H.-T. Chen, N. Sathishkumar, *Synthesis*, density functional theory (DFT) studies and urease inhibition activity of chiral benzimidazoles. *Heliyon.* 6 (2020) e05187. <https://doi.org/10.1016/j.heliyon.2020.e05187>.
62. Fonkui TY, Ikhile MI, Njobeh PB, Ndinteh DT. Benzimidazole Schiff base derivatives: synthesis, characterization and antimicrobial activity. *BMC chemistry.* 2019 Dec; 13(1):1-1.
63. Nandwana NK, Singh RP, Patel OP, Dhiman S, Saini HK, Jha PN, Kumar A. Design and synthesis of imidazo/benzimidazo [1, 2-c] quinazoline derivatives and evaluation of their antimicrobial activity. *ACS omega.* 2018 Nov 30; 3(11):16338-46.
64. Yadav S, Narasimhan B, Lim SM, Ramasamy K, Vasudevan M, Shah SA, Mathur A. Synthesis and evaluation of antimicrobial, antitubercular and anticancer activities of benzimidazole derivatives. *Egyptian Journal of Basic and Applied Sciences.* 2018 Mar 1; 5(1):100-9.
65. Chandrasekar K, Kumar B, Saravanan A, Victor A, Sivaraj S, Haridoss M, Hemalatha CN, Muthukumar VA. Evaluation and Molecular Docking of Benzimidazole and its Derivatives as a Potent Antibacterial Agent. *Biomedical and Pharmacology Journal.* 2019 Dec 1; 12(4):1835-48.
66. Gramatica P, Cassani S, Chirico N. QSARINS-chem: Insubria datasets and new QSAR/QSPR models for environmental pollutants in QSARINS.
67. Eriksson L, Jaworska J, Worth AP, Cronin MT, McDowell RM, Gramatica P. Methods for reliability and uncertainty assessment and for applicability

evaluations of classification-and regression-based QSARs. Environmental health perspectives. 2003 Aug; 111(10):1361-75.

68. Savjani KT, Gajjar AK, Savjani JK. Drug solubility: importance and enhancement techniques. International Scholarly Research Notices. 2012;2012.
69. Desai NC, Pandya DD, Jadeja DJ, Panda SK, Rana MK. Design, synthesis, biological evaluation and molecular docking study of novel hybrid of pyrazole and benzimidazoles. Chemical Data Collections. 2021 Jun 1; 33:100703.
70. Bauer, A. W., C. E. Roberts Jr, and W. M. Kirby. "Single disc versus multiple disc and plate dilution techniques for antibiotic sensitivity testing." *Antibiotics annual* 7 (1959): 574-580
71. Bauer, Alfred W., DAVID M. PERRY, and WILLIAM MM KIRBY. "Single-disk antibiotic-sensitivity testing of staphylococci: An analysis of technique and results." *AMA archives of internal medicine* 104, no. 2 (1959): 208-216.

CERTIFICATE OF PARTICIPATION

This is to certify that

Padma Kumar

Attended the E-Workshop on 'Structure Based and Ligand Based Drug Design'
held on 13th and 14th July 2020

Organized by

Department of Pharmaceutical Chemistry

JSS College of Pharmacy, Sri Shivarathreeshwara Nagara, Mysuru 570015



Dr. B.R. Prashantha Kumar
Organizing Secretary



Dr. G. V. Pujar
Convener



Dr. T. M. Pramod Kumar
Chairman



PANNAI COLLEGE OF PHARMACY

Dindigul, Tamil nadu, India

Approved by AICTE & PCI, New Delhi, India

Affiliated to The TN Dr. MGR Medical University, Tamil Nadu, India

www.pannaicp.org

86755 20000, 86755 30000

pannaipharma@gmail.com



*This
Certificate of Participation
awarded to*

K.PADMA

Mpharm student 2nd yr , C.L.Baid Metha College of Pharmacy, Chennai.

for actively participated in 3rd International pharma Webinar on

“COMBINATORIAL CHEMISTRY- Prompt Tool for Medicinal Chemistry”

held on 14th June 2020, Organized by Pannai College of Pharmacy, Tamil Nadu, India.

[Signature]
Chief Patron

CA Dr. PANNAI M.KARTHIKEYAN

Chairman, Pannai Group of Educational Institutions

[Signature]
Convener

Dr. A.THANGA THIRUPATHI

Principal, PCOP

[Signature]
Co-Convener

Dr. M.AMUDHA

Associate Professor, PCOP


[Signature]
Coordinator

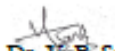
Mrs. R.REVATHI

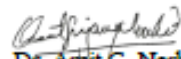
Associate Professor, PCOP

ATEOS FOUNDATION OF SCIENCE EDUCATION AND
RESEARCH, M.S., INDIA
IN ASSOCIATION WITH
E-CELL, INDIAN INSTITUTE OF TECHNOLOGY (IIT),
KHARAGPUR, INDIA

acknowledge that
Ms. Padma K.
Has earned the
Certificate of completion
In
Online Workshop on Basics of QA and QC
On
12th-14th March 2021


Prof. Dr. S. S. Chakravarthy,
Speaker, Professor and Head,
Dept. of QA and QC,
SES's R. C. Patel IPER,
Shirpur, Dhule, M.S., India


Dr. V. P. Sonar,
Speaker, Asst. Prof.,
Dept. of QA and QC,
SES's R. C. Patel IPER,
Shirpur, Dhule, M.S., India


Dr. Amit G. Nerkar,
Founder and Director,
AFSER, M.S., India

Certificate No. AFSEER/Workshop/2021/29